Report No. **267**

epaResearch
Climate - Water - Sustainability
*Identifying pressures • Informing policy • Developing solutions*

# High-resolution Gridded Datasets of Hydro-climate Indices for Ireland

Authors: Christopher Werner, Paul Nolan and Owen Naughton

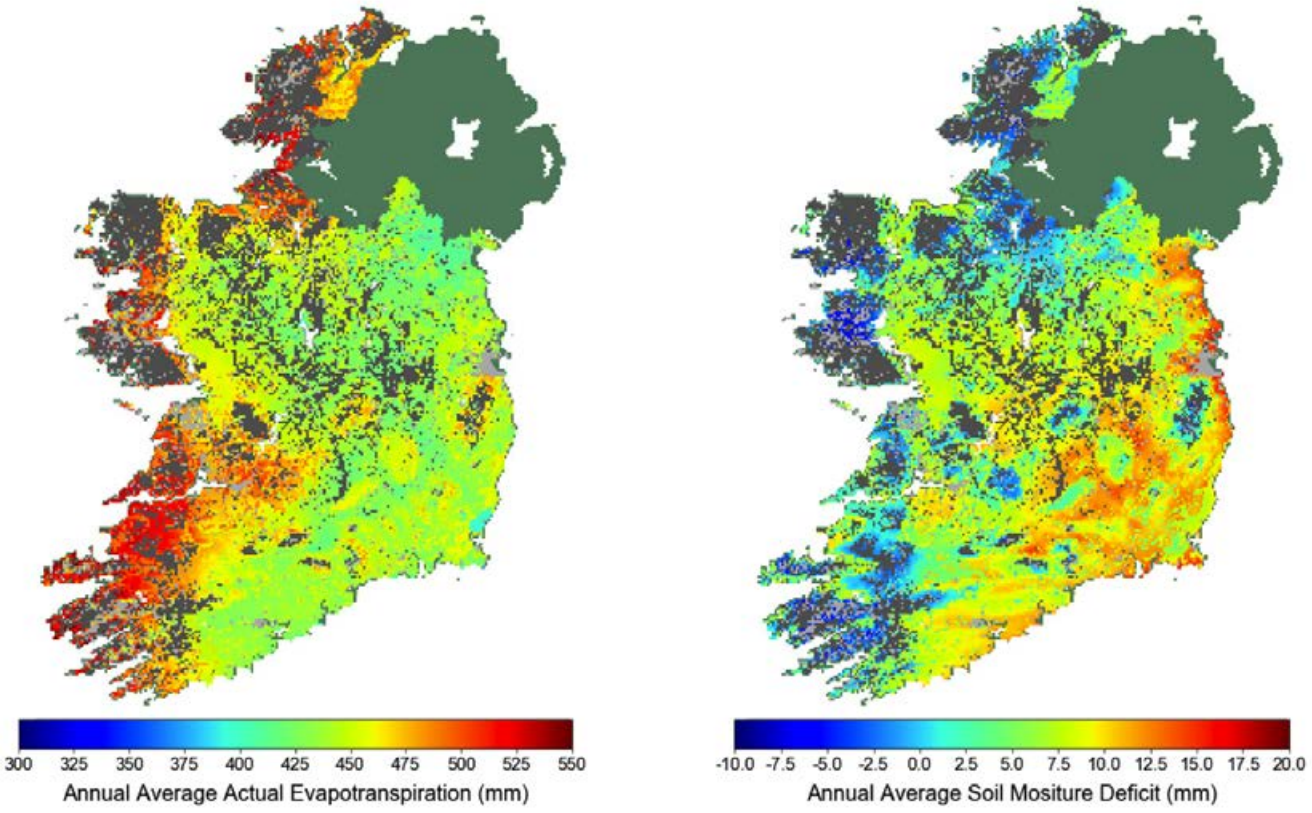


www.epa.ie

Geological Survey
Suirbhéireacht Gheolaíochta
Ireland | Éireann

Rialtas na hÉireann
Government of Ireland

**ENVIRONMENTAL PROTECTION AGENCY**

The Environmental Protection Agency (EPA) is responsible for protecting and improving the environment as a valuable asset for the people of Ireland. We are committed to protecting people and the environment from the harmful effects of radiation and pollution.

## The work of the EPA can be divided into three main areas:

**Regulation:** *We implement effective regulation and environmental compliance systems to deliver good environmental outcomes and target those who don't comply.*

**Knowledge:** *We provide high quality, targeted and timely environmental data, information and assessment to inform decision making at all levels.*

**Advocacy:** *We work with others to advocate for a clean, productive and well protected environment and for sustainable environmental behaviour.*

## Our Responsibilities

### Licensing

We regulate the following activities so that they do not endanger human health or harm the environment:

- waste facilities *(e.g. landfills, incinerators, waste transfer stations)*;
- large scale industrial activities (*e.g. pharmaceutical, cement manufacturing, power plants)*;
- intensive agriculture *(e.g. pigs, poultry)*;
- the contained use and controlled release of Genetically Modified Organisms *(GMOs)*;
- sources of ionising radiation *(e.g. x-ray and radiotherapy equipment, industrial sources)*;
- large petrol storage facilities;
- waste water discharges;
- dumping at sea activities.

### National Environmental Enforcement

- Conducting an annual programme of audits and inspections of EPA licensed facilities.
- Overseeing local authorities' environmental protection responsibilities.
- Supervising the supply of drinking water by public water suppliers.
- Working with local authorities and other agencies to tackle environmental crime by co-ordinating a national enforcement network, targeting offenders and overseeing remediation.
- Enforcing Regulations such as Waste Electrical and Electronic Equipment (WEEE), Restriction of Hazardous Substances (RoHS) and substances that deplete the ozone layer.
- Prosecuting those who flout environmental law and damage the environment.

### Water Management

- Monitoring and reporting on the quality of rivers, lakes, transitional and coastal waters of Ireland and groundwaters; measuring water levels and river flows.
- National coordination and oversight of the Water Framework Directive.
- Monitoring and reporting on Bathing Water Quality.

### Monitoring, Analysing and Reporting on the Environment

- Monitoring air quality and implementing the EU Clean Air for Europe (CAFÉ) Directive.
- Independent reporting to inform decision making by national and local government *(e.g. periodic reporting on the State of Ireland's Environment and Indicator Reports)*.

### Regulating Ireland's Greenhouse Gas Emissions

- Preparing Ireland's greenhouse gas inventories and projections.
- Implementing the Emissions Trading Directive, for over 100 of the largest producers of carbon dioxide in Ireland.

### Environmental Research and Development

- Funding environmental research to identify pressures, inform policy and provide solutions in the areas of climate, water and sustainability.

### Strategic Environmental Assessment

- Assessing the impact of proposed plans and programmes on the Irish environment *(e.g. major development plans)*.

### Radiological Protection

- Monitoring radiation levels, assessing exposure of people in Ireland to ionising radiation.
- Assisting in developing national plans for emergencies arising from nuclear accidents.
- Monitoring developments abroad relating to nuclear installations and radiological safety.
- Providing, or overseeing the provision of, specialist radiation protection services.

### Guidance, Accessible Information and Education

- Providing advice and guidance to industry and the public on environmental and radiological protection topics.
- Providing timely and easily accessible environmental information to encourage public participation in environmental decision-making *(e.g. My Local Environment, Radon Maps)*.
- Advising Government on matters relating to radiological safety and emergency response.
- Developing a National Hazardous Waste Management Plan to prevent and manage hazardous waste.

### Awareness Raising and Behavioural Change

- Generating greater environmental awareness and influencing positive behavioural change by supporting businesses, communities and householders to become more resource efficient.
- Promoting radon testing in homes and workplaces and encouraging remediation where necessary.

### Management and structure of the EPA

The EPA is managed by a full time Board, consisting of a Director General and five Directors. The work is carried out across five Offices:

- Office of Environmental Sustainability
- Office of Environmental Enforcement
- Office of Evidence and Assessment
- Office of Radiation Protection and Environmental Monitoring
- Office of Communications and Corporate Services

The EPA is assisted by an Advisory Committee of twelve members who meet regularly to discuss issues of concern and provide advice to the Board.

**EPA RESEARCH PROGRAMME 2014–2020**

# High-resolution Gridded Datasets of Hydro-climate Indices for Ireland

# (2016-W-DS-29)

# EPA Research Report

Prepared for the Environmental Protection Agency and Geological Survey of Ireland

by

Irish Centre for High-End Computing (ICHEC)

**Authors:**

**Christopher Werner, Paul Nolan and Owen Naughton**

**ENVIRONMENTAL PROTECTION AGENCY**
An Ghníomhaireacht um Chaomhnú Comhshaoil
PO Box 3000, Johnstown Castle, Co. Wexford, Ireland

Telephone: +353 53 916 0600 Fax: +353 53 916 0699
Email: info@epa.ie Website: www.epa.ie

## ACKNOWLEDGEMENTS

This report is published as part of the EPA Research Programme 2014–2020. The EPA Research Programme is a Government of Ireland initiative funded by the Department of Communications, Climate Action and Environment. It is administered by the Environmental Protection Agency, which has the statutory function of co-ordinating and promoting environmental research.

The project team would like to thank the project's co-funders, namely the Environmental Protection Agency and Geological Survey of Ireland, for contributing towards this project. The project team also wish to thank Eoin Whelan, Seamus Walsh and Emily Gleeson of Met Éireann for providing critical datasets for this project, and Raemonn Fealy of Teagasc for providing the Irish Indicative Soil Drainage dataset. The project team thank Alastair McKinstry of the Irish Centre for High-End Computing (ICHEC) for his assistance in uploading the datasets produced in this project to the ICHEC ERDDAP server. The authors would like to acknowledge the members of the project steering committee, namely Keith Lambkin (Met Éireann), Taly Hunter Williams (Geological Survey of Ireland), Conor Quinlan (Environmental Protection Agency), Ian Holman (Cranfield University) and Edward Tully (Irish Water). The research was carried out at ICHEC.



**EPA RESEARCH PROGRAMME 2014–2020**
Published by the Environmental Protection Agency, Ireland

ISBN: 978-1-84095-810-2 January 2019

Price: Free Online version

# Project Partners

**Christopher Werner**
Irish Centre for High-End Computing
Trinity Technology and Enterprise Campus
Grand Canal Quay
Dublin 2
Ireland
Tel.: +353 1 524 1608
Email: christopher.werner@ichec.ie

**Paul Nolan**
Irish Centre for High-End Computing
Trinity Technology and Enterprise Campus
Grand Canal Quay
Dublin 2
Ireland
Tel.: +353 1 524 1608
Email: paul.nolan@ichec.ie

**Owen Naughton**
Department of Built Environment
Institute of Technology, Carlow
Carlow
Ireland
Email: Owen.Naughton@itcarlow.ie

# Contents

# List of Figures

# List of Tables

# Executive Summary

This report describes the application of numerical weather prediction (NWP) simulations to develop high-quality, long-term, gridded climate datasets of hydro-climate variables for Ireland, covering the period 1981–2016. There is constant demand for such datasets from industry, research and governmental agencies for use in fields such as agriculture, water resource estimation and management, hydrology and hydrogeology, public health, energy and planning and studies on observed climate change trends and vulnerability. Variables such as evapotranspiration and soil moisture conditions are crucial factors in estimating water sustainability, understanding groundwater recharge, agronomic management and the management of flood and drought risk. However, with the exception of temperature and precipitation, spatially and temporally homogeneous, multi-decadal, gridded observational climate datasets are not readily available for hydro-climatic research applications in Ireland.

One approach to generating the requisite gridded datasets is through the use of NWP downscaled simulations. NWP models use mathematical models of the atmosphere to forecast weather based on current weather conditions. NWPs can also be used to “reanalyse” historical weather conditions, whereby past weather observations such as satellite, surface and upper-air conditions are used as model inputs. This report describes the application of downscaled NWP models to produce gridded climate datasets of key hydro-climate variables for Ireland.

In this research the performances of three NWP models (COSMO-CLM, WRF and MÉRA) are compared and analysed to assess their ability to accurately represent hydro-climate variables, focusing on reference evapotranspiration ($ET_0$) as calculated using the Food and Agriculture Organization of the United Nations (FAO) Penman–Monteith equation. Two of the NWP datasets assessed were produced by researchers at the Irish Centre for High-End Computing (ICHEC) using the COSMO-CLM5 and WRF v3.7.1 models. The third dataset (MÉRA) is derived from a 36-year (1981–2016) regional reanalysis of the Irish climate carried out by Met Éireann using the HARMONIE model and the ALADIN-HIRLAM NWP system. The MÉRA simulation included a data assimilation component. All NWP models of the current study downscaled the European Centre for Medium-Range Weather Forecasts (ECMWF) ERA-Interim global reanalyses dataset.

Modelled $ET_0$ data are analysed and validated against $ET_0$ data calculated from meteorological observations at 22 Met Éireann synoptic stations across Ireland. Least squared estimator monthly correction factors were applied to all three raw datasets to improve the output. Using these $ET_0$ datasets, actual evapotranspiration ($ET_a$) and soil moisture deficits (SMDs) have been derived using the hybrid soil moisture deficit (HSMD) model, created by Teagasc and in use in Ireland since 2006. The current project employed a more up-to-date model with five drainage classes. The following datasets were derived using MÉRA input variables containing daily, monthly, seasonal and yearly time steps:

- $ET_0$;
- $ET_a$ (five drainage classes);
- SMDs (five drainage classes).

The datasets described above are also available for the COSMO-CLM and WRF models with 1.5-km and 2-km grid spacing, respectively. Additionally, the Teagasc Indicative Soil Drainage Map has been implemented to capture the actual soil conditions throughout the country. All datasets are available for download through the ICHEC ERDDAP server, which can be found at https://erddap.ichec.ie/erddap/files/EPA_Hydroclimate.

Across all three models, the MÉRA model is the best performer for $ET_0$. Using a weighted average across 22 synoptic stations, root mean square errors equated to 0.337 mm/day for the MÉRA model compared with 0.402 mm/day and 0.442 mm/day for the WRF and COSMO-CLM models, respectively. The MÉRA model also performs best for the $ET_a$ and SMD variables and therefore the MÉRA datasets are the recommended datasets to be used as indicative maps for Ireland.

An additional project output was to facilitate an update to the *Agroclimatic Atlas for Ireland*. Met Éireann high-resolution (1-km) daily gridded datasets of temperature and precipitation were used to derive agro-climate variables such as the Standardised Precipitation Index (SPI) and growing season. Gridded datasets of the SPI for intervals of 1, 2, 3, 6, 12, 24 and 48 months have been derived for 1981–2016 using both the observational datasets and the NWP models specified above.

# 1 Introduction

There is constant demand from industry and research and governmental agencies for high-quality, long-term, gridded datasets with high spatial and temporal resolution for conducting climate research. These data have the potential to be used in a wide variety of fields such as agriculture (Collins and Cummins, 1996; Perry and Hollis, 2005; Olesen *et al*., 2007; Abatzoglou, 2013; Jones and Thornton, 2013), hydrology and hydrogeology (Hay *et al*., 2002; Analitis *et al*., 2008; Rajeevan and Bhate, 2009; Keshta and Elshorbagy, 2011; Di Luca *et al*., 2012; Duethmann *et al*., 2013; Williams *et al*., 2013; Merz *et al*., 2014; Schamm *et al*., 2014; Seyyedi *et al*., 2014), public health (Kunkel *et al*., 1999; D'Ippoliti *et al*., 2010; Vautard *et al*., 2013), energy (Troen and Petersen, 1989; SEAI, 2016; Gallagher *et al.,* 2014; Gallagher *et al*., 2016; Slater, 2016) and planning (Holman *et al*., 2005; Bouwer, 2011) and in studies on observed climate change trends and vulnerability (IPCC, 2014; Bollmeyer, 2015). The need for spatially represented hydro-climate variables is a prerequisite for many aspects of hydrological and ecological assessment. Variables such as evapotranspiration and soil moisture conditions are crucial factors in estimating water sustainability, understanding groundwater recharge, agronomic management and the management of flood and drought risk. However, at present gridded observational climate datasets are not readily available in Ireland, except for temperature and precipitation (Walsh, 2012).

In order to characterise groundwater and surface water systems, and to facilitate climate adaptation, a greater understanding of the primary processes driving energy and water exchanges within the hydrological cycle is required. It is therefore necessary to provide the evidence needed to inform policymakers, planners and stakeholders of potential climate change-related issues in Ireland. Such studies also support the development of pre-emptive mitigation strategies necessary to contribute towards developing a climate-resilient Ireland. To fully comprehend future climate change, a thorough analysis of the observational past is required.

As mentioned above, the only readily available gridded climate datasets available in Ireland are those for precipitation and temperature (Bollmeyer *et al*., 2015) and these variables alone are insufficient to enable scientists and policymakers across all sectors to make well-informed decisions. The lack of up-to-date gridded hydrological datasets, particularly for evapotranspiration, represents a serious information gap in Irish meteorology and agro-climate studies. This gap was outlined in the 2012 Catchment Flood Risk Assessment and Management (CFRAM) *National Preliminary Flood Risk Assessment* (PFRA) (CFRAM, 2012), which stated that "the information required to undertake a predictive analysis of the potential flood risk impacts of climate change is not currently available, but is under development and once available will be used to review the PFRA outcomes". The gap was also highlighted in the context of groundwater recharge assessment and the Water Framework Directive quantitative status characterisation (Williams *et al*., 2013). The datasets produced as part of the current project will allow scientists, engineers and policymakers to study observed changes and patterns in hydrological/hydrogeological datasets to an extent not covered before in Ireland and mitigate against the projected adverse effects in the coming decades. The performances of (1) the COSMO-CLM5 model, developed by Consortium for Small-scale Modelling and Climate Limited-area Modelling Community, (2) the Weather Research and Forecasting (WRF) model and (3) the Met Éireann Re-Analysis (MÉRA) datasets are compared and analysed to assess their ability to accurately represent hydro-climate variables. The overall goal of this project was to produce definitive gridded datasets of hydro-climate variables including reference ($ET_0$) and actual ($ET_a$) evapotranspiration, soil moisture deficits (SMDs), rainfall intensity and the Standardised Precipitation Index (SPI) for the period 1981–2016 for use by industry, policymakers, the general public and researchers.

# 2 Literature Review

## 2.1 Use of Regional Climate Models for Gridded Data Generation

One approach to generating homogeneous, long-term gridded datasets is using numerical weather prediction (NWP) hindcast simulations. NWP models use mathematical models of the atmosphere to forecast weather based on current weather conditions. NWPs can also be used to reanalyse historical weather conditions, whereby past weather observations such as satellite, surface and upper-air conditions are used as model inputs. Using data assimilation methods, a complete estimate of the atmospheric state is computed that is both dynamically consistent and close to observations. The primary advantage of using reanalysis data is that they provide the best estimate of the four-dimensional atmospheric state, for both observed variables and essential climate variables, which are not often measured (Dee *et al*., 2014; Bollmeyer *et al*., 2015). Such examples of global reanalysis datasets include ERA-Interim (Dee *et al*., 2011) from the European Centre for Medium-Range Weather Forecasts (ECMWF) and the National Center for Atmospheric Research (NCEP) Climate Forecasting Systems Reanalysis. However, these global reanalysis datasets have resolutions of the order of 80 km, which is too coarse to be of use in regional studies.

To address this problem, a regional climate NWP model (RCM) is typically employed to dynamically downscale the coarse global reanalysis datasets at a higher resolution over the area of interest. This downscaling can also include the assimilation of local observations, known as a regional reanalysis. If these local observations are not available a more general RCM approach is implemented. The constraints imposed by local observations should yield a more accurate analysis than the general RCM approach, which lacks these local observations. However, the data assimilation systems of the NWP model do not exactly follow observations because of a broader constraint requiring physical and dynamical consistency over the three-dimensional volume of the atmosphere. Both approaches have value, particularly when multiple NWP models are employed.

The overall basis of the RCM method is to dynamically downscale the coarse information provided by the global reanalysis data and provide high-resolution information on a sub-domain of interest. All models from global down to regional scale have errors, however, and more errors are introduced from the boundaries of the regional models. Numerous studies have demonstrated that high-resolution RCMs improve the simulation of precipitation (Rajeevan and Bhate, 2009; Saha *et al*., 2010; Di Luca *et al*., 2012; Lucas-Picher *et al*., 2012; Duethmann *et al*., 2013; Kendon *et al*., 2012; Kendon *et al*., 2014; Bieniek *et al*., 2016; McGrath and Nolan, 2016) and topography-influenced phenomena and extremes with relatively small spatial or short temporal character (Feser *et al*., 2011; Feser and Barcikowska, 2012; Shkol'nik *et al*., 2012; Flato *et al*., 2013). An additional advantage is that the physically based RCMs explicitly resolve more small-scale atmospheric features and provide a better representation of convective precipitation (Rauscher *et al*., 2010) and extreme precipitation (Kanada *et al*., 2008). Other examples of the added value of RCMs include improved simulation of near-surface temperature (Feser, 2006; Di Luca *et al*., 2016). The latest Intergovernmental Panel on Climate Change (IPCC) report has concluded that there is "high confidence that downscaling adds value to the simulation of spatial climate detail in regions with highly variable topography and for mesoscale phenomena and extremes" (Stocker *et al*., 2013).

## 2.2 Regional Climate Model Data for Ireland

Researchers at the Irish Centre for High-End Computing (ICHEC) completed two high-resolution historical simulations of the Irish climate, by downscaling ERA-Interim data for the period 1980 to present using the COSMO-CLM5 (Rockel *et al*., 2008) and WRF v3.7.1 (Skamarock *et al*., 2008) RCMs, with maximum spatial resolutions of 1.5 km and 2 km, respectively. The WRF nested model domains have 18-km, 6-km and 2-km grid spacings and are shown in Figure 2.1. The COSMO-CLM domains have the same resolution apart from the innermost domain (1.5 km)

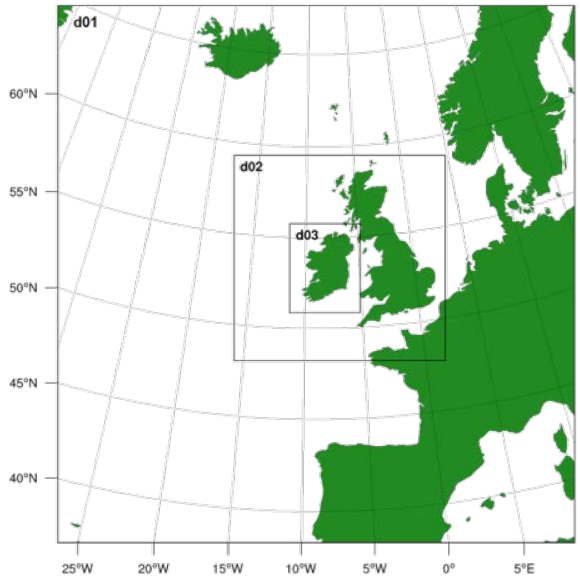


**Figure 2.1. WRF domains of 18 km, 6 km and 2 km.**

and are slightly larger than the corresponding WRF domains.

In 2017, Met Éireann completed a 36-year (1981–2016) regional reanalysis of the Irish climate using the HARMONIE model and the ALADIN-HIRLAM NWP system, called MÉRA (Whelan *et al*., 2016; Gleeson *et al*., 2017). In contrast to the COSMO-CLM and WRF simulations, MÉRA includes data assimilation, utilising time series of surface observations (Whelan *et al*., 2015), and has a different projection. MÉRA has performed with high accuracy, with small biases in temperatures, pressure and 10-m wind speeds, and outperformed "ERA-Interim reanalysis particularly in terms of standard deviations in screen-level temperatures and surface winds" (Gleeson *et al*., 2017) and compares well with surface observations. Because of the data assimilation component, the MÉRA model exhibits better skill than the WRF and COSMO-CLM models despite the lower resolution. However, the WRF and COSMO-CLM models add value given their finer spatial resolutions. The comparison of these different models provides information on the relative skill of the RCM methodologies.

In the current study, the COSMO-CLM, WRF and MÉRA datasets are compared and analysed to assess their ability to accurately represent hydro-climate variables. The overall goal of this project was to produce definitive gridded climate datasets of hydro-climate variables such as $ET_0$ and $ET_a$, SMDs, rainfall intensity and the SPI for the period 1981–2016 for use by industry, policymakers, the general public and researchers. Data for 2017 are made available for COSMO-CLM and WRF.

## 2.3 Hydroclimate Indices

### *2.3.1 $ET_0$*

Evapotranspiration is the transfer of water from the land to the atmosphere through a combination of two separate processes, evaporation from the land surface and transpiration from vegetation. Although evapotranspiration can be measured directly, meteorological agencies generally use calculation methods to determine a "reference" evapotranspiration ($ET_0$), which is evapotranspiration from a reference surface that is not water limited. The reference crop is typically taken as grass with an assumed height of 0.12 m, a fixed surface resistance of 70 s/m and an albedo of 0.23 (Allen *et al*., 1998). The potential evapotranspiration of any crop can be calculated by multiplying this value by a crop coefficient, *K*c, which depends on the crop type and time of growth.

There have been many developments and improvements in the calculation of evapotranspiration over time as it plays an important role in the field of agro- and hydro-meteorology. It is a crucial factor in estimating water sustainability and understanding agronomic management, is of more importance in a changing climate and is important in the management of flood and drought risk. Numerous methods of calculating evapotranspiration exist, including pan-based coefficient methods, such as described in Allen *et al*. (1998), and the Pereira models (Pereira *et al*., 1995). These methods will not be considered for this study, as $ET_0$ in Ireland is typically calculated from observed meteorological data recorded at synoptic stations.

There are numerous approaches for estimating $ET_0$, based on empirical, mass transfer, temperature, radiation and combination and direct measurement methods (Blaney and Criddle, 1950; Makkink, 1957; WMO, 1966; Mahringer, 1970; Priestley and Taylor, 1972; Szász, 1973; Doorenbos and Pruitt, 1977; Burman and Pochop, 1994). Direct measurements of $ET_0$ are severely limited in Ireland and so these were not considered in this study; they are recommended

more over monthly or longer time periods. Prior to 2006, Met Éireann employed the radiation-based Makkink methodology for estimating $ET_0$ (Keith Lambkin, Met Éireann, 2017, personal communication; https://www.met.ie/climate/services). Subsequently, the combination method of the Food and Agriculture Organization of the United Nations (FAO) Penman–Monteith equation has been used for $ET_0$ estimation. The Penman-Monteith method is recommended by the World Meteorological Organization as the sole standard method for estimating $ET_0$, as it has been shown to have a strong likelihood of correctly predicting $ET_0$ in a wide range of locations and climates. Studies such as that by Rácz *et al*. (2013), which compared 10 different $ET_0$ methodologies, found that the Penman–Monteith equation provided the best estimates.

Penman (1948) developed a method of calculating $ET_0$ by combining the energy balance with the mass transfer method and derived the equation to compute open source evaporation from standard climatological records of sunshine, temperature, humidity and wind speed. The method has been further developed, resulting in the Penman–Monteith $ET_0$ formula, given as:

$$ET_0 = \frac{0.408\,\Delta\left(R_n - G\right) + \gamma \frac{900}{T_{av} + 273} u_2 \left(e_s - e_a\right)}{\Delta + \gamma\left(1 + 0.34 u_2\right)} \quad (2.1)$$

where $ET_0$ is the measure in mm/day, $R_n$ is the net surface radiation (MJ/m$^2$/day), $G$ is the soil heat flux (MJ/m$^2$/day), $T_{av}$ is the mean daily 2-m temperature (°C), $u_2$ is the mean daily 2-m wind speed (m/s), $e_s$ is the daily saturation vapour pressure (kPa), $e_a$ is the daily actual vapour pressure (kPa), Δ is the slope of the vapour pressure curve (kPa/°C) and $\gamma$ is the psychometric constant (kPa/°C).

In line with international best practice and current practices at Met Éireann, the FAO Penman–Monteith equation has been used for calculating $ET_0$ in this study.

Other notable methodologies for estimating $ET_0$, including the Thornthwaite (1948), Hargreaves and Samani (1985) and Penman (1948) methods, can be used in place of the Penman–Monteith equation when all required input variables are not available (Hargreaves and Allen, 2003; Chen *et al*., 2005). Methods such as these have significant advantages over the Penman–Monteith equation when data are limited as they require fewer input parameters and are relatively easy to calculate. The quantity of input variables in the Penman–Monteith equation has its issues as many locations worldwide do not record all of the required meteorological variables. Appropriate documentation is available (Allen *et al*., 1998) for when this occurs.

Following the estimation of evapotranspiration for the grass reference crop outlined in Allen *et al*. (1998) and Zotarelli *et al*. (2010), to obtain evapotranspiration for a certain crop, a crop coefficient, $K_c$, must be applied:

$$ET_c = K_c \cdot ET_0 \quad (2.2)$$

where $ET_c$ is the evapotranspiration from disease-free, well-fertilised crops, grown in large fields under optimum soil water conditions and achieving full production under the given climatic conditions. Depending on the crop and time of year, different $K_c$ values are applied, and are typically employed for areas where irrigation is a prominent activity. A full list of the different $K_c$ values is outlined in Chapter 6 in Allen *et al*. (1998).

### *2.3.2 $ET_a$ and SMDs*

The calculation of $ET_0$ is determined by the available energy supply and is based on the assumption that the system is not water limited, i.e. an ample supply of water is available. However, the actual rate of water loss from a vegetated surface does not always proceed at the potential rate $ET_0$. When vegetation is unable to extract water from the soil column, $ET_a$ falls below the potential rate $ET_0$. This difference between potential and actual rates is dependent on the soil moisture content.

When a soil is saturated it will not hold any more water, and any further rainfall is drained via run-off or percolation to groundwater. When rainfall ceases, the soil becomes unsaturated until it reaches “field capacity”, the water that the soil can hold against the force of gravity. When the soil moisture is at or above field capacity, evapotranspiration can occur at the potential rate ($ET_a = ET_0$). In the absence of further rainfall, soil moisture gradually becomes depleted to produce a SMD, defined as the amount of water required to restore the soil to field capacity. As the SMD increases, water becomes more difficult for vegetation to access and $ET_a$ becomes progressively less than $ET_0$.

Actual evapotranspiration is of particular interest to agriculturalists and hydrologists for groundwater research for the purposes of monitoring decreases in crop productivity and producing groundwater recharge maps, respectively (Burke, 1962; Brereton and Keane, 1982; Williams *et al*., 2013). In Ireland, $ET_a$ and SMD are typically not directly measured but are instead estimated from measurements of $ET_0$ and precipitation. In a broadly similar climate to Ireland, the UK Meteorological Office has established a regular procedure for evaluating agricultural water shortage in Britain using the water budget approach. The UK's Meteorological Office Rainfall and Evaporation Calculation System (MORECS; Thompson *et al*., 1981) (discussed further in section 2.4.) is applied to grid cells of size 40 × 40 km and employs regularly collected meteorological data to estimate $ET_a$ using a modified Penman equation that accounts for both meteorological conditions and vegetation characteristics.

Several studies have used remote sensing (RS) to estimate $ET_a$ rather than physical observations (Soer, 1980; Carlson *et al*., 1995; Timmermans and Meijerink, 1999; Wu *et al*., 2006; Senay *et al*., 2007; Gao *et al*., 2008; Teixeira, 2010; Elhag *et al*., 2011; Glenn *et al*., 2011a,b). There are some advantages to this as $ET_a$ can be determined on a large scale rather than by point measurement analysis. However, each captured image is still a snapshot and the temporal resolutions can vary between satellites. Field data are usually required in interpreting and calibrating RS imagery, and validating models for large areas, but extensive fieldwork in such cases is not necessarily required (Kite and Droogers, 2000). RS is mostly prominent in areas where irrigation is a key activity.

No single method of measuring or calculating evapotranspiration is without fault as some point analysis methods are difficult to apply spatially (Wu *et al*., 2006), and traditionally $ET_a$ has been computed as a residual in water balance equations. Estimates of $ET_0$ are derived by means of a ratio or indirectly from field measurements at meteorological stations (Kite and Droogers, 2000).

In Ireland, $ET_a$ and SMD are not widely monitored directly (Mills, 2000) but are instead calculated using the hybrid soil moisture deficit (HSMD) model implemented by Met Éireann in 2006 (Schulte *et al*., 2005; Keith Lambkin, Met Éireann, 2017, personal communication; https://www.met.ie/climate/services), with a newer version described in Schulte *et al*. (2015). In this model $ET_a$ is assumed to reduce linearly to zero as SMD approaches a theoretical maximum value, beyond which $ET_a$ is assumed to be zero. In the Met Éireann model $ET_a$ is given by:

$$ET_a = ET_0 \frac{SMD_{max} - SMD_{t-1}}{SMD_{max} - SMD_c} \quad (2.3)$$

where $SMD_{max}$ is a theoretical maximum SMD value, $SMD_{t-1}$ is the SMD at time $t$–1 and $SMD_c$ is a critical value above which moisture availability is no longer a limiting factor (Aslyng, 1965). When SMD is less than $SMD_c$, moisture is not limiting respiration and is assumed to equal $ET_0$. For SMD values below this critical level, it is assumed that $ET_0$ decreases linearly to zero as the SMD approaches the critical maximum value.

Soil moisture conditions are an important interface between agriculture and the environment because of their impact on the length of the grazing season, grass growth conditions and nutrient uptake. The balance exchange is driven by the hydrological cycle, one of the most fundamental cycles in the earth–atmosphere system. The hydrological cycle refers to the passage of water in gaseous, liquid and solid forms between the oceans, atmosphere, lithosphere and biosphere. It can easily be expressed as a water budget, accounting for precipitation (P), evapotranspiration (E), run-off (R) and the fluctuations in the water stored in the soil (DS) as:

$$P - E - R = \Delta S \quad (2.4)$$

The difference between evapotranspiration and precipitation represents differences in water stored within the soil. For a saturated soil, run-off will be generated, and the saturation of the soil is often represented by the "field capacity", the depth of water that can be held in the soil against the force of gravity. When a soil is at field capacity, any excess water runs off overland or percolates downwards through the soil. Measures for countrywide SMDs and soil moisture content are not common; however, the European Space Agency (ESA) has been monitoring global soil moisture using active and passive microwave instruments (Silvestrin *et al*., 2001; Mecklenburg *et al*., 2012). A number of studies have also derived soil moisture datasets from radar and satellite imagery (Ulaby, 1974; Huisman *et al*., 2003; Wagner *et al*., 2007). A number of international studies have

attempted to estimate SMDs using meteorological models (Lockwood *et al*., 1989). In Ireland, attempts have been made to evaluate the soil moisture and deficit in the context of the water budget and soil associations (Gardiner and Radford, 1980). Some of the most notable attempts involved the implementation of a 5 × 5 km grid superimposed onto Ireland using measured meteorological variables (precipitation, temperature, sunshine hours) to calculate each of the water budget terms (Mills, 2000) and to calculate $ET_0$ and SMDs for North County Dublin from 1950 to 1961 using the Penman method (Burke, 1962). However, with recent advances in climate modelling and observations, this can be improved on.

In Ireland, a method for estimating SMDs across the whole country, the HSMD model (Schulte *et al*., 2005), was derived by Teagasc, which has been used at Met Éireann since 2006. The preliminary calculations are described as:

$$SMD_t = SMD_{t-1} - Rain + ET_a + Drain \quad (2.5)$$

where $SMD_t$ and $SMD_{t-1}$ are the SMDs on day $t$ and day $t$–1 respectively, *Rain* is the daily incoming precipitation, $ET_a$ is the daily $ET_a$ and *Drain* is the amount of water drained daily by percolation and/or overland flow, which is dependent on the soil drainage capacity. There are three soil drainage classes, outlined in Table 2.1. As with the water budget equation, SMDs and surpluses are computed from differences between rainfall, $ET_a$ and drainage, with soil moisture surpluses assumed to be removed by drainage and surface run-off over time.

Since the implementation of this model, an updated and higher resolution version has been developed, the HSMD model version 2 (Hallett *et al*., 2014; Schulte *et al*., 2015). The new model includes two new soil drainage classes as well as an optional module to account for the topographic wetness index at any location (Lewis and Holden, 2012; Schulte *et al*., 2015). The two new drainage classes included are "excessive" and "imperfect". The new classes follow the same characteristics as for the older corresponding classes, with the exception of the excessive class, for which the $SMD_{max}$ value is 50 mm. The imperfect class has a drainage of 3 mm, with other characteristics similar to those for the moderately and poorly drained classes. The topographic wetness index is used in locations that receive water from both direct precipitation and adjacent areas via overland flow. The only difference in the equations is the topographic wetness index, from which a Y modifier is derived and put as a denominator to the drain term.

Other methods of calculating SMDs include methods from the FAO (Allen *et al*., 1998) and the Penman–Grindley model (Grindley, 1969). These models calculate $ET_a$ using alternative methods to represent the crop stress factor. For the standard Penman–Grindley approach, the potential evapotranspiration term (taken to be the same as $ET_0$) is reduced once the SMD reaches a so-called rooting constant, the value below which evapotranspiration may occur at its maximum rate. When this occurs, $ET_a$ is instantly reduced to 10% of potential evapotranspiration, during a period in which the crop is stressed. During this time, the SMD is less than the crop rooting constant, beyond which transpiration reduces. The point beyond which transpiration ceases is known as the wilting point. The FAO assumes that $ET_a$ decreases linearly from the rooting constant to the wilting point. The difference from the Schulte model is the inclusion of the rooting constant and wilting points. For practical reasons, the updated Schulte model will be implemented in this study. The primary reasoning is the inclusion of different soil drainage characteristics, which the Penman–Grindley model does not implement. Second, the Penman–Grindley method uses the Penman $ET_0$ method as an input instead of the Penman–Monteith

**Table 2.1. Overview of soil drainage classes in the HSMD model version 1 from Schulte *et al.* (2005)**

| Variable | Well drained | Moderately drained | Poorly drained |
|---|---|---|---|
| $SMD_{max}$ | 110 mm | 110 mm | 110 mm |
| $SMD_{min}$ | 0 mm | –10 mm | –10 mm |
| Drainage | – | 10 mm/day | 0.5 mm/day |
| Comments | Soil never saturates, remaining at field capacity even on very wet winter days | Soil may saturate on wet winter days, but returns to field capacity on first dry day | Soil saturates on wet winter days, with water surplus drained at very slow rates |

method, which is used by Met Éireann for calculating $ET_0$. Finally, the Penman–Grindley method is believed to not operate satisfactorily when the surface or the subsurface run-off is a significant part of the soil water balance (Mackenzie *et al*., 1991).

Soil moisture deficits are an effective way of monitoring the soil conditions and a measure of the difference between water in the soil and the amount that the soil can actually hold. As mentioned previously, this is known as the field capacity of the soil and can be considered as one of the most viable options for ascertaining soil moisture conditions. One study has gone further to develop a SMD index and evapotranspiration deficit index for agricultural drought monitoring, based on weekly values (Narasimhan and Srinivasan, 2005). They work in a similar way to the SPI (McKee *et al*., 1993) and represent conditions from extremely dry to extremely wet. The study by Narasimhan and Srinivasan (2005) includes the acknowledgement that the drought indices introduced needed to be aggregated at spatial and temporal scales for comparison with other drought indices. Droughts are rare in Ireland; however, the drought during the summer months of 2018 makes this a more viable option as the impacts of climate change become more apparent in Ireland. The applications of the SPI are further discussed in the following section.

### *2.3.3 Precipitation*

*Rainfall intensities*

Rainfall intensities are used primarily in run-off analysis and are of huge importance in agricultural and groundwater monitoring (Allen *et al*., 1998; Williams *et al*., 2013). When rain falls, the first drops of water are intercepted by the leaves and stems of the vegetation, usually referred to as the “interception storage”’. As the rain continues, water reaching the ground surface infiltrates into the soil until it reaches a stage where the rate of rainfall (the intensity) exceeds the infiltration capacity of the soil. After this time, surface ponding occurs and depression areas are filled, after which run-off is generated. The infiltration capacity of the soil is dependent on its structure and texture, as well as the soil moisture content as a result of previous rainfall or dry periods. The main factors that affect run-off are soil type, vegetation cover, the slope and the catchment size. The details of these factors are outside the scope of this project and are more applicable to end users of rainfall intensity datasets.

Additionally, rainfall intensities have been utilised in intensity–duration–frequency curves (Linsley, 1958; Jalee and Farawn, 2014; Liew *et al*., 2014), which are common tools used by insurance industries and in water resources engineering for the planning, design and operation of water resources projects. These curves typically go down to timescales of 15 minutes or less, which goes beyond the scope of the datasets being produced, which have a maximum temporal resolution of 1 hour.

*Standardised Precipitation Index*

The SPI has been accepted as the best practice standard for monitoring drought events since its inception in 1993 (McKee *et al*., 1993) and it has replaced the Palmer Drought Severity Index (PDSI) (Palmer, 1965; WAMIS, 2012). The SPI allows an analyst to determine the rarity of a drought at a given timescale of interest for any rainfall station with long-term historical datasets. The SPI is typically used over timescales ranging from months to years but can be updated daily to provide a moving window approach. Timescales of less than 3 months can be used to assess drought severity.

Advantages of the SPI include its simplicity, its being based solely on rainfall, its ability to describe drought at different timescales and its comparability across different climatic regimes, and its probabilistic nature provides a historical context that is well suited for decision making (Bussay *et al*., 1999). Its simplicity is also a disadvantage, as calculation is based solely on precipitation; there is no soil–water balance component and no ability to calculate evapotranspiration ratios. An updated version, developed in 2010 (Vicente-Serrano *et al*., 2010), attempts to address this latter issue of evapotranspiration and will be covered later in this section. Studies of the SPI’s usage have been carried out in Hungary (Edwards, 1997; Szalai and Szinell, 2000) and Greece (Karavatis *et al*., 2011), with streamflow best described with 2- to 6-month timescales. At 5–24 months there were good relationships to groundwater levels and agricultural drought was well represented at scales of 2–3 months in the Hungary examples. In Greece, where drought is becoming more of a concern, the SPI described drought conditions very well, establishing the onset,

ending and severity levels of exceptional drought events.

Mathematically, the SPI is based on the cumulative probability of a given rainfall event occurring at a location. The historical rainfall data are fitted to a gamma distribution, through a process of maximum likelihood estimation of the gamma distribution parameters *α* and *β*. The probability density function is defined as:

$$g(x) = \frac{1}{\beta^{\alpha}\Gamma(\alpha)} x^{\alpha-1} e^{-x/\beta} \tag{2.6}$$

where *α* and *β* are shape and scale parameters, respectively, and *x* is the amount of precipitation. The gamma function Γ(*α*) is defined as:

$$\Gamma(\alpha) = \lim_{n\to\infty} \prod_{v=0}^{n-1} \frac{n! n^{y-1}}{y+v} \equiv \int_0^{\infty} y^{\alpha-1} e^{-y}\, dy \tag{2.7}$$

Simplified approximations for the *α* and *β* parameters are given by:

$$\alpha = \frac{1}{4A}\left(1+\sqrt{1+\frac{4A}{3}}\right) \tag{2.8}$$

$$\beta = \frac{\overline{x}}{\alpha} \tag{2.9}$$

where:

$$A = \ln(\overline{x}) - \frac{\sum \ln(x)}{n} \tag{2.10}$$

and *n* is the number of observations (Lana *et al*., 2001). There are a number of other approximations to calculate these parameters, which depend on practicality and size of dataset.

The SPI is measured on a scale of –3 to +3, with zero representing normal conditions, values less than –2 representing severe drought and values greater than +2 representing severe wet conditions.

Despite SPI being typically used as a drought index, recent studies have demonstrated its use in flood risk management. One such study focused on recurrent floods in the southern Cordoba Province in Argentina (Seiler *et al*., 2002). The results showed that the SPI was able to satisfactorily explain the development of conditions leading up to three major flood events in the region from 1979 to 1998. The results indicated the potential for SPI as a tool for monitoring hydrological conditions and flood risk and the potential of incorporating SPI analysis into a regional system for climate risk monitoring as part of a comprehensive flood mitigation programme.

The different time periods over which the SPI is calculated enhances the analysis capacity, as it allows the estimation of different antecedent conditions in the soils. Shorter scales of 3–6 months quantify superficial soil water, which bears significance for agriculture. In contrast, longer accumulation scales indicate the state of subsurface moisture, as well as other surface and subsurface water resources.

The lack of consideration in the SPI of other variables such as evapotranspiration was addressed by Vicente-Serrano *et al*. (2010), with the Standardised Precipitation Evapotranspiration Index (SPEI). The SPEI is based on both precipitation and temperature data and has the advantage of combining multi-scalar character with the capacity to include the effects of temperature variability on drought assessment. The SPEI differs from the SPI as it includes a climatic water balance, the accumulation of water deficit and surpluses at different timescales and the adjustment to a log-log logistic probability distribution. The SPEI performed well under global warming conditions and identified an increase in drought severity associated with higher water demand as a result of evapotranspiration. The SPEI study (Vicente-Serrano *et al*., 2010) used the Thornthwaite (1948) method of calculating evapotranspiration because of its simplicity, which is given as:

$$ET = 16\left(\frac{N}{12}\right)\left(\frac{NDM}{30}\right)\left(\frac{10T}{I}\right)^{m} \tag{2.11}$$

where *T* is the monthly mean temperature in °C; *m* is a cubic equation coefficient based on the value *I* (see Vicente-Serrano *et al*., 2010); *NDM* is the number of days in a month; *N* is the maximum number of sun hours calculated from the hourly angle of sun rising, the latitude and solar declination; and *I* is a heat index. This heat index is calculated as the sum of 12 monthly index values, *i*, which is derived from:

$$i = \left(\frac{T}{5}\right)^{1.514} \tag{2.12}$$

Both the SPI and the SPEI have great potential for application in Ireland, for example in the analysis of droughts and winter floods. These indexes have not been applied in Ireland or many places worldwide and can be used to establish Ireland's place in a warming world.

## 2.4 International Methodologies

As evapotranspiration and soil moisture contents are critical hydroclimate variables, many nations have derived methodologies for spatially observing and modelling these variables. This section will focus on relevant methodologies, which include systems implemented in the UK, USA, Australia and New Zealand.

### *2.4.1 UK*

The UK Meteorological Office Rainfall and Evaporation Calculation System was implemented in the UK in 1978 as a replacement for the estimated soil moisture deficit (ESMD) and was updated in 1995 (Hough and Jones, 1997). Compared with methods currently in use in Ireland, the availability of digitalized soil databases across the UK allowed MORECS access to the soil data for calculations of actual soil moisture rather than soil drainage type. This highlights the need for actual soil moisture measurements across the different soil types in Ireland. MORECS is produced in a grid square format of 40 × 40 km and uses daily synoptic weather data to provide estimates of weekly and monthly evaporation and SMD in the form of averages. The potential evapotranspiration is calculated for each grid square for a range of surface covers from bare soil to forest, using a modified form of the Penman–Monteith equation (Monteith and Unsworth, 1990). Estimates of potential evapotranspiration are converted to estimates of $ET_a$ by progressively reducing the rate of water loss from the potential value to zero as the available water decreases from a fraction of its maximum value to zero.

Crop models are also used in MORECS, but it should be noted that they are idealised representations of crop growth. The models describe aspects such as plant development through the growth stages, the leaf area index, crop height, variation of crop canopy resistance with weather and crop age. The water in the soil available for plant growth has been the subject of wide-ranging research over the last 40+ years in the UK. Difficulties arise in estimating the amount of water available for plant growth because of variables such as rooting depths and in simulating the process by which roots extract water from the soil. MORECS is based on suctions (measured in kPa); the lower limit of ≈5 kPa approximates to field capacity and the higher value of ≈1500 kPa indicates the wilting point. The system outlines two classes of water availability based on these values. For values between 5 and 200 kPa, the retention is termed “easily available water” (EAW). For suctions between 200 and 1500 kPa, it is termed “restricted available water” (RAW). The summation of these two terms provides the total available water (TAW) or available water capacity.

Soil available water data are extracted from the Land Information System, which contains unique soil and related environmental data for England and Wales, the UK’s National Soil Map and a National Catalogue of Soils that cover a wide range of properties from water retention to density measurements (Ragg and Proctor, 1983; Hallett *et al*., 1996). The data are taken from large samples and have an overall resolution of 100 m × 100 m and overall available water content (AWC) values for grid squares of 1 km × 1 km. Systems such as MORECS show the complicated overall structure of an evapotranspiration and soil moisture network required to yield a more sophisticated network.

Other UK datasets are CHESS (Climate, Hydrological and Ecological research Support System), JULES (Joint UK Land Environment Simulator) and COSMO-UK. The first of these draws mainly on MORECS data (temperature, humidity, wind speeds, sunshine hours) downscaled to 1-km resolution. The CHESS datasets can be used with rainfall datasets to drive the JULES model, a land surface model that includes soil moisture, soil temperature and evaporation. Finally, the COSMOS-UK dataset is a network of soil monitoring stations for the UK that provides near-real-time soil moisture data for use in a variety of applications including farming, water resources, flood forecasting and land surface modelling. Networks and datasets such as these, which have real-time applications, should be seen as a matter of high importance for Ireland in the near future.

### *2.4.2 USA*

In the USA, the evapotranspiration network is estimated using a regression with climate and land cover data (Sanford and Selnick, 2013). Precipitation and streamflow records were compiled for 838 watersheds for the period 1971–2000 to obtain long-term estimates of $ET_a$. Precipitation and temperatures were used from the PRISM datasets and land cover from the US Geological Survey

(USGS) National Land Cover Dataset. The system has been developed since its inception and at present ArcGIS actual evapotranspiration layers are available at 1-km cell size, derived from the MOD16 Global Evapotranspiration Product and MODIS satellite imagery. However, despite using the Penman–Monteith equation, the methodology uses satellite RS data rather than physical observations and at present the data cover only the period 2000–2010 (Mu *et al*. 2013 ). Additionally, the USGS has evapotranspiration networks on a state-by-state basis rather than across the whole country. Soil moisture estimates in the USA are surprisingly limited at present but new measures are being put in place to monitor droughts. Puerto Rico obtains excellent evapotranspiration and countrywide soil moisture monitoring from the GOES-PRWEB satellite, which provides near-real-time maps of $ET_0$, $ET_a$, soil moisture content and radiation (PRAGWATER).

### *2.4.3 New Zealand*

In New Zealand, the National Institute of Water and Atmospheric Research (NIWA) employs a virtual climate station network that produces daily datasets based on the spatial interpolation of actual data observations made at climate stations across the country. These observations include rainfall, potential evapotranspiration and soil moisture and are interpolated using a spline model (Tait *et al*., 2006; Tait and Woods, 2007). In addition to evapotranspiration, SMDs, soil moisture anomalies and the SPI over 30- and 60-day timescales are updated daily, with comparisons made from averages and the previous year. The evapotranspiration values in New Zealand are calculated using the Penman method (Penman, 1963; Westerhoff, 2015).

### *2.4.4 Australia*

In Australia, the Bureau of Meteorology and the Cooperative Research Centre for Catchment Hydrology released a set of evapotranspiration maps for Australia in 2001 as part of the Bureau's Climatic Atlas series (Australia Bureau of Meteorology and Wang, 2001; Chiew *et al*., 2002). These maps provide average monthly and annual values of three evapotranspiration variables: point and areal evapotranspiration and areal actual evapotranspiration. The evapotranspiration estimates are based on the Morton relationship (Morton, 1983). However, these maps are not used day to day by the Bureau of Meteorology. Instead, a map of point values is provided showing 7-day $ET_0$ sums, with monthly data also available, which is similar to the approach employed in Ireland.

# 3 Methodology

## 3.1 Study Area and Data

The study area was taken over the island of Ireland, using three downscaled NWP models, at three different spatial resolutions (1.5, 2 and 2.5 km). Two of the datasets were produced by researchers at the ICHEC, with nested domains, using the COSMO-CLM5 and WRF v3.7.1 models, and the third dataset, MÉRA, was produced by Met Éireann. MÉRA includes a data assimilation component, utilising time series of surface observations. An overview of the variables that are produced by each of these models is available in Appendix 1. Validation data for hydro-climate indices ($ET_0$, $ET_a$, SMD and SPI) were obtained from the Met Éireann network of synoptic stations (22 in total).

## 3.2 Methods and Bias Corrections

### *3.2.1 $ET_0$*

Reference evapotranspiration was calculated from the following RCM input variables: 2-m temperature, humidity/dew point temperature, 10-m wind speed, surface pressure and surface short-wave and long-wave radiation. As long-wave radiation was not available in the WRF model variables, it was calculated using the Julian day and solar declination methodology.

### *3.2.2 $ET_0$ bias correction*

In their raw format, the variables produced from the NWP models have biases. Two approaches to correcting these biases were considered: bias correction of the constituent time series used in the estimation of $ET_0$ and an overall bias correction of the calculated $ET_0$ series.

A sensitivity analysis was undertaken to establish the sensitivity of the component variables of $ET_0$. It was found that the most sensitive variables were humidity and radiation. Additionally, it was found that the errors in $ET_0$ using previously corrected input variables showed very little difference compared with raw input variables, with root mean square error (RMSE) differences of only ±0.01 mm. Therefore, $ET_0$ was calculated using raw model data and a correction factor was then applied to $ET_0$.

Two correction methodologies were tested: bias correction and least squared estimator methods. The bias correction technique, developed by Hawkins *et al*. (2013), is given as:

$$M_{BC} = \overline{O_{REF}} + \left( \frac{\sigma_{O\_REF}}{\sigma_{M\_REF}} \right) \left( M_{REF}(t) - \overline{M_{REF}} \right) \tag{3.1}$$

where $M_{BC}$ is the bias-corrected model, $O_{REF}$ are the observations taken over a reference period and $Ml_{REF}$ are the model data taken over the same reference period.

The advantages of this technique are its simplicity and the inclusion of standard deviations of both model and reference period. The second method, least squared estimator, is given as:

$$\hat{a} = \frac{\sum_{n=1}^{N} x_n y_n - N\overline{xy}}{\sum_{n=1}^{N} x_n^2 - N\overline{x}^2} \tag{3.2}$$

$$\hat{b} = y - \hat{a}x \tag{3.3}$$

$$\hat{y} = \hat{a}x + \hat{b} \tag{3.4}$$

The variables $x$ and $y$ are the input model data and observational datasets, respectively, and $\hat{y}$ is the corrected data or “line of best fit”. Of the two methods tested, it was determined that the least squared estimator method produced the lowest errors. As $ET_0$ varies considerably throughout the year, a best line fit for each month was derived. The regression analysis was carried out at all stations where $ET_0$ is calculated from meteorological observations (22 in total) and so a more complete countrywide profile was achieved. The locations of these stations are shown in Figure 3.1, with blue stations referring to those stations where data are available from 1981. The corrections were calculated for all stations for the period 2006 to present.

Once the regression coefficients ($a$, $b$) were calculated at all stations, the values were interpolated onto the corresponding model grids. These gridded datasets were then used to correct the corresponding gridded $ET_0$ datasets. This method was repeated for each

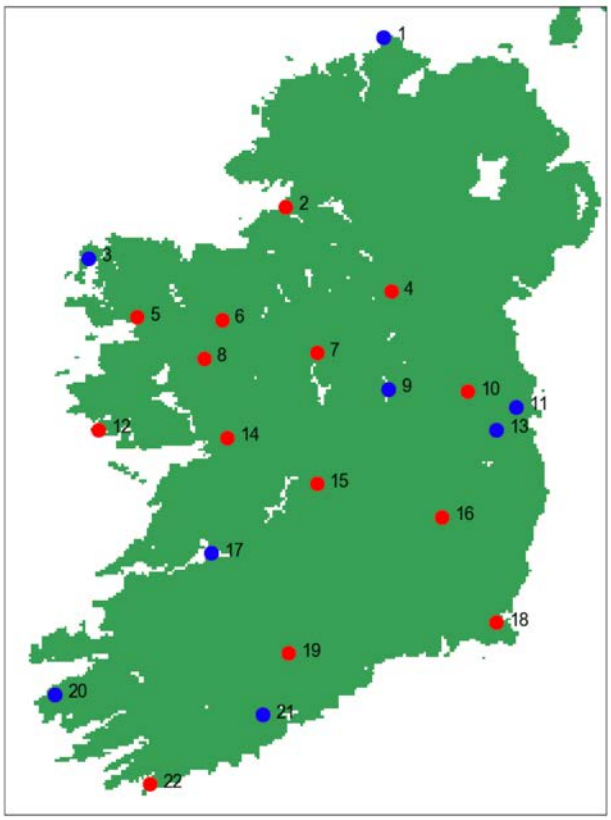


1 - Malin Head
2 - Finner
3 - Belmullet
4 - Ballyhaise
5 - Newport
6 - Knock Airport
7 - Mt Dillon
8 - Claremorris
9 - Mullingar
10 - Dunsany
11 - Dublin Airport
12 - Mace Head
13 - Casement
14 - Athenry
15 - Gurteen Agri-College
16 - Oak Park
17 - Shannon Airport
18 - Johnstown
19 - Moore Park
20 - Valentia Observatory
21 - Cork Airport
22 - Sherkin Island

**Figure 3.1. Locations of synoptic stations used in hydro-climate model calibration and validation.**

month and applied to the full dataset (1981–2016). Figure 3.2, which presents yearly $ET_0$ sums for Dublin Airport and Valentia Observatory, shows the improvement of the corrected data compared with the raw output. For the raw WRF data, in particular, there was shown to be a consistent overestimation of $ET_0$ over the whole country, of between 50 and 100 mm depending on the station. Figure 3.3 shows the difference between the raw output and corrected $ET_0$ for Dublin Airport and Valentia.

### *3.2.3 $ET_a$ and SMDs*

Time series of $ET_a$ and SMD were generated using the HSMD model. Inputs to the model were the bias-corrected $ET_0$ data and gridded observational precipitation datasets provided by Met Éireann. Observed rather than modelled precipitation data were used because of the uncertainties in precipitation in all three RCM models, and observed data were considered to provide a better representation of historical precipitation patterns. These data extended only to 2016 and so $ET_a$ and SMD series are limited to this date.

In order to start a HSMD model run, an initial value is required for SMD. Uncertainty in the initial model outputs can be reduced by initialising the model at a time when soils are at field capacity. In December 1980, there was a major rainfall event that caused all eight long-term synoptic stations in operation to be at field capacity. It was assumed that soils were at field capacity on this date across the country and so December 1980 was taken as the start time for the SMD model.

National datasets for $ET_a$ and SMD were derived for the five separate drainage classes described in the HSMD model. A single combined dataset was also produced, which used the Teagasc Indicative Soil Drainage Map for Ireland (Creamer *et al.*, 2016) to assign a drainage type and corresponding $ET_a$ and SMD series to each grid square.

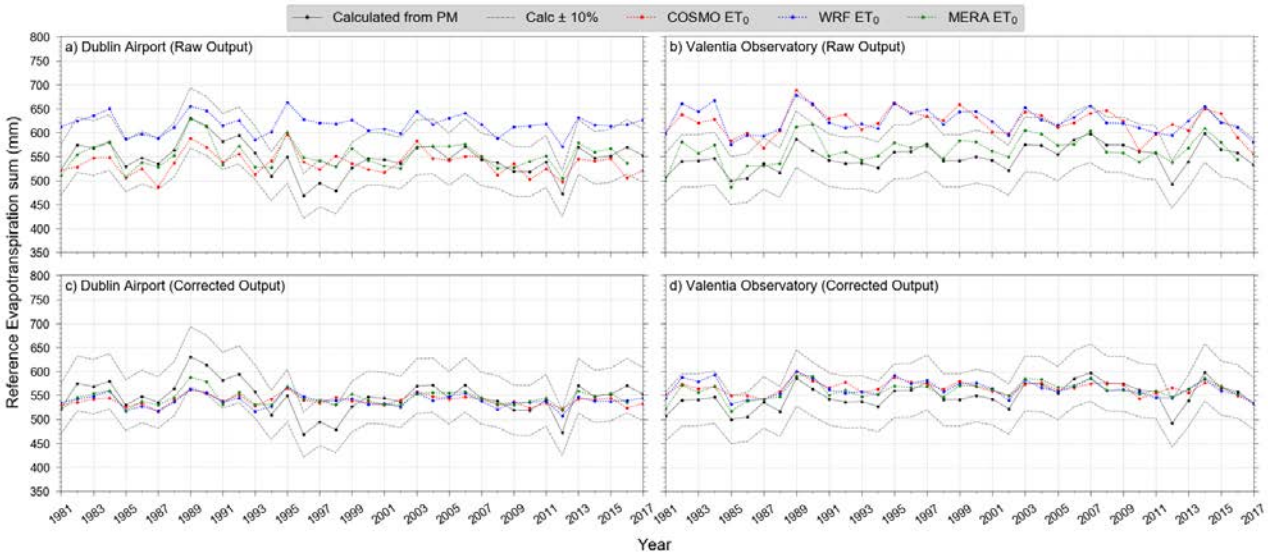


**Figure 3.2. Raw output and corrected output for annual $ET_0$ sums at Dublin Airport and Valentia Observatory.**

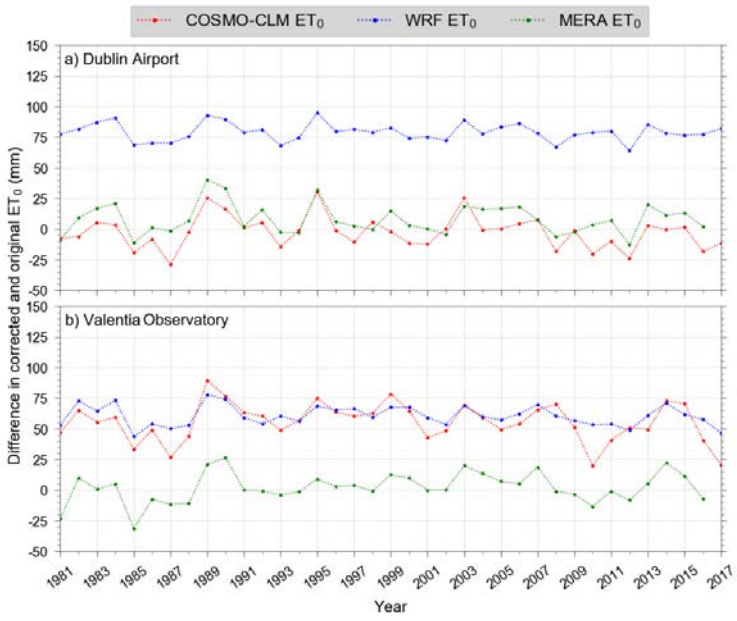


**Figure 3.3. Difference in $ET_0$ yearly sums between corrected and original $ET_0$ values for Dublin Airport and Valentia Observatory.**

# 4 Results and Validations

## 4.1 Reference Evapotranspiration

The primary variable analysed, $ET_0$, was calculated over multiple time periods. These include annual, seasonal, monthly and daily time periods, with both sums and averages calculated for the three models. The following sections will investigate the performance of all three models, which underwent correction using the methods described in Chapter 3. Following bias corrections, all models were found to perform with a high degree of accuracy and were in good agreement with observations. Prior to validation, it was expected that MÉRA would outperform both the WRF dataset and the COSMO-CLM dataset because of the advantage of data assimilation. The COSMO-CLM and WRF datasets were expected to add value because of the higher resolutions (1.5 km and 2 km, respectively) than in the MÉRA dataset (2.5 km).

### *4.1.1 Daily and annual analysis*

The models were validated over a 37-year period (1981–2017) for COSMO-CLM and WRF and over a 36-year period for MÉRA (1981–2016) at 22 stations. As a result of the corrections, bias values were minimised. Table 4.1 shows the errors associated with daily $ET_0$ values for all three models. The MÉRA model outperformed both the WRF and the COSMO-CLM models for RMSE and correlation coefficients but was outperformed by the COSMO-CLM model for standard deviation. This is of less importance because of the variability of $ET_0$ throughout the course of the year. Analysis in the following sections investigates the variability in monthly values. Figure 4.1 shows scatter plots at Dublin Airport and Valentia Observatory.

As shown in Figure 4.1, the MÉRA data show the best fit, with the majority of values within 1 mm of the calculated values. The WRF and COSMO-CLM data are slightly more varied as shown in both Figure 4.1 and Table 4.1.

Among the more important tests is the performance of $ET_0$ on an annual basis and whether modelled values can pick up more abrupt changes. Figure 4.2 shows yearly sums of $ET_0$ at Dublin Airport and Valentia Observatory dating back to 1981. As mentioned previously, the corrections factors were generated using data from 2006 to 2017, with the resulting best line fits being applied back to 1981.

As shown in Figure 4.2, there is a good match between synoptic values and each of the models. For some stations, however, sudden drops or increases in $ET_0$ highlight an issue of the least squared

**Table 4.1. Errors in daily $ET_0$ values for selected stations from 1981 to 2017 and using an overall weighted average across 22 stations**

| Station | RMSE (mm) | | | Standard deviation (mm) | | | Correlation coefficient | | |
|---|---|---|---|---|---|---|---|---|---|
| | COSMO-CLM | WRF | MÉRA | COSMO-CLM | WRF | MÉRA | COSMO-CLM | WRF | MÉRA |
| Belmullet | 0.42 | 0.389 | 0.32 | 0.838 | 0.917 | 0.869 | 0.884 | 0.908 | 0.934 |
| Casement | 0.46 | 0.417 | 0.343 | 0.928 | 0.958 | 0.954 | 0.889 | 0.910 | 0.939 |
| Cork Airport | 0.495 | 0.432 | 0.395 | 0.934 | 0.964 | 0.98 | 0.884 | 0.913 | 0.928 |
| Dublin Airport | 0.451 | 0.418 | 0.343 | 0.912 | 0.927 | 0.949 | 0.893 | 0.909 | 0.939 |
| Malin Head | 0.422 | 0.398 | 0.321 | 0.719 | 0.826 | 0.775 | 0.861 | 0.884 | 0.922 |
| Mullingar | 0.426 | 0.390 | 0.330 | 0.941 | 0.959 | 0.967 | 0.911 | 0.926 | 0.948 |
| Shannon Airport | 0.455 | 0.430 | 0.362 | 0.959 | 1.057 | 0.989 | 0.904 | 0.918 | 0.941 |
| Valentia | 0.451 | 0.401 | 0.339 | 0.832 | 0.888 | 0.876 | 0.877 | 0.905 | 0.933 |
| All | 0.442 | 0.402 | 0.337 | 0.882 | 0.937 | 0.924 | 0.892 | 0.913 | 0.939 |

**The best and worst performers are colour coded green and red, respectively.**

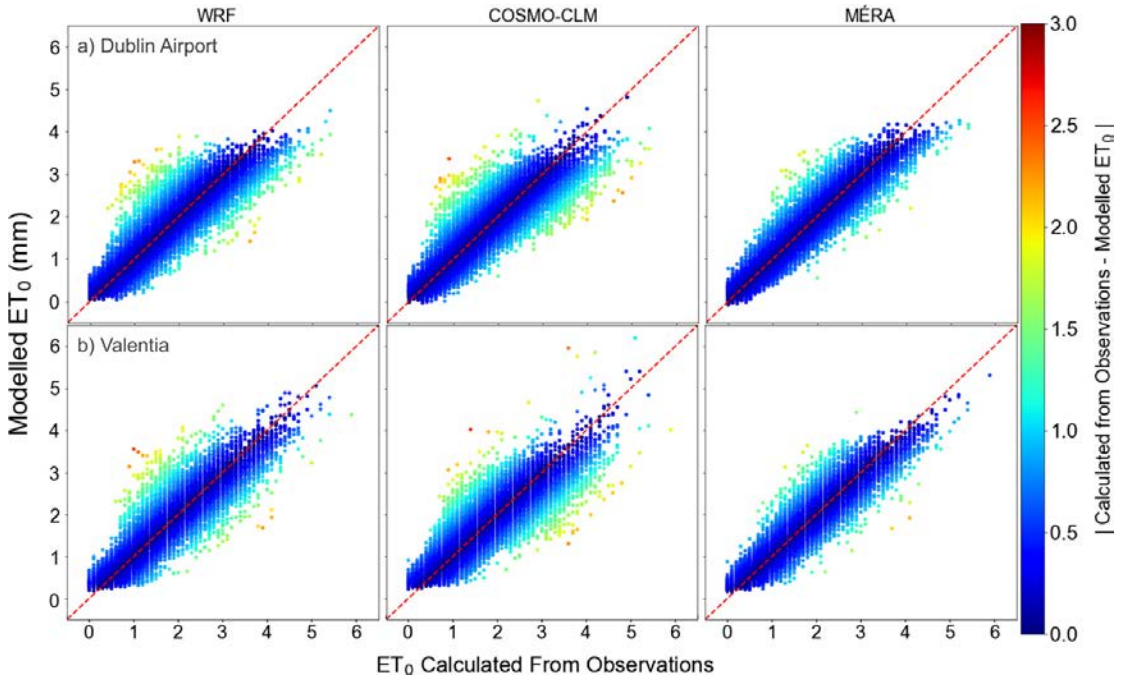


**Figure 4.1. Scatter plots of daily $ET_0$ values for each model at Dublin Airport and Valentia Observatory. The colour coding represents deviation from a one-to-one relationship.**

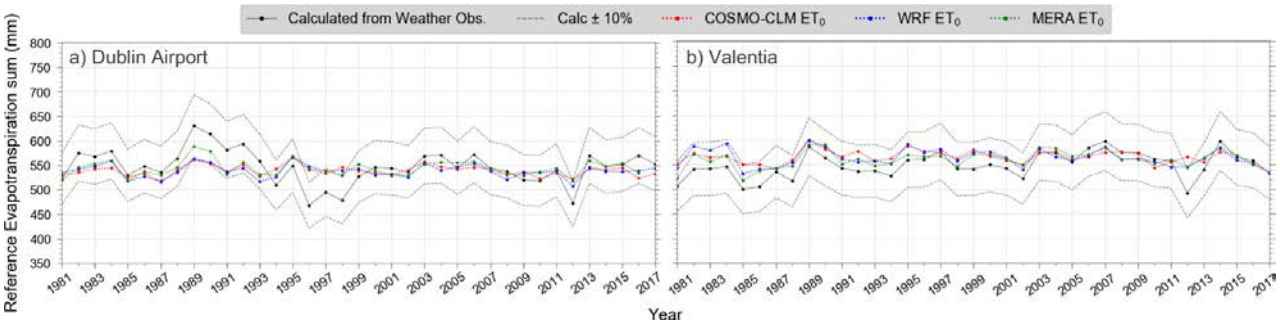


**Figure 4.2. Annual $ET_0$ sums for Dublin Airport and Valentia Observatory from 1981 to 2017. The solid black line shows the Met Éireann-calculated values from observations, with a ±10% interval shown by the dashed black line.**

estimator method being unable to correct distinct outliers. Nevertheless, all models are able to capture $ET_0$ to within 10% of values calculated from station measurements for all stations analysed. Table 4.2 shows associated errors in $ET_0$ for annual summed values for each station analysed above. The pattern is similar to the daily values presented in Table 4.1 However, the difference in $ET_0$ between the nested models (WRF, COSMO-CLM) and data-assimilated model (MÉRA) is small.

Figure 4.3 shows corrected maps of $ET_0$ for all three models and is one of the datasets provided for download. A breakdown of individual year sums for each model has also been produced. All three models show high values around coastlines, urban areas and the mouth of the Shannon River. The WRF model better resolves the urban centres because of the enhanced dynamics of its urban model. The MÉRA model shows a better fit to the calculated observations than the higher resolution models of COSMO-CLM and WRF.

### *4.1.2 Monthly and seasonal analysis*

Analysis of monthly evapotranspiration values is of importance because of the variability of evapotranspiration throughout the year. Figures 4.4 and 4.5 show the average monthly sums of $ET_0$ at synoptic stations and countrywide, respectively.

**Table 4.2. Errors in yearly summed values of $ET_0$ at selected stations from 1981 to 2017 using an overall weighted average across 22 stations**

| Station | RMSE (mm) | | | Standard deviation (mm) | | | Correlation coefficient | | |
|---|---|---|---|---|---|---|---|---|---|
| | COSMO-CLM | WRF | MÉRA | COSMO-CLM | WRF | MÉRA | COSMO-CLM | WRF | MÉRA |
| Belmullet | 23.646 | 23.565 | 20.479 | 11.492 | 14.600 | 15.532 | 0.554 | 0.555 | 0.679 |
| Casement | 20.844 | 17.937 | 15.279 | 12.391 | 14.642 | 17.044 | 0.715 | 0.798 | 0.877 |
| Cork Airport | 36.967 | 31.98 | 33.576 | 14.554 | 18.54 | 21.516 | 0.667 | 0.805 | 0.769 |
| Dublin Airport | 32.156 | 31.514 | 27.048 | 10.72 | 13.065 | 15.741 | 0.458 | 0.489 | 0.681 |
| Malin Head | 19.698 | 21.543 | 18.733 | 9.198 | 13.94 | 12.069 | 0.521 | 0.415 | 0.596 |
| Mullingar | 17.666 | 17.318 | 18.849 | 12.143 | 13.807 | 15.604 | 0.783 | 0.798 | 0.813 |
| Shannon Airport | 26.508 | 19.071 | 22.622 | 14.011 | 16.482 | 16.076 | 0.698 | 0.78 | 0.836 |
| Valentia | 26.868 | 24.485 | 19.757 | 13.423 | 17.644 | 16.853 | 0.545 | 0.655 | 0.801 |
| All | 24.164 | 21.293 | 20.402 | 12.301 | 14.035 | 14.813 | 0.561 | 0.678 | 0.755 |

**The best and worst performers are colour coded green and red, respectively.**

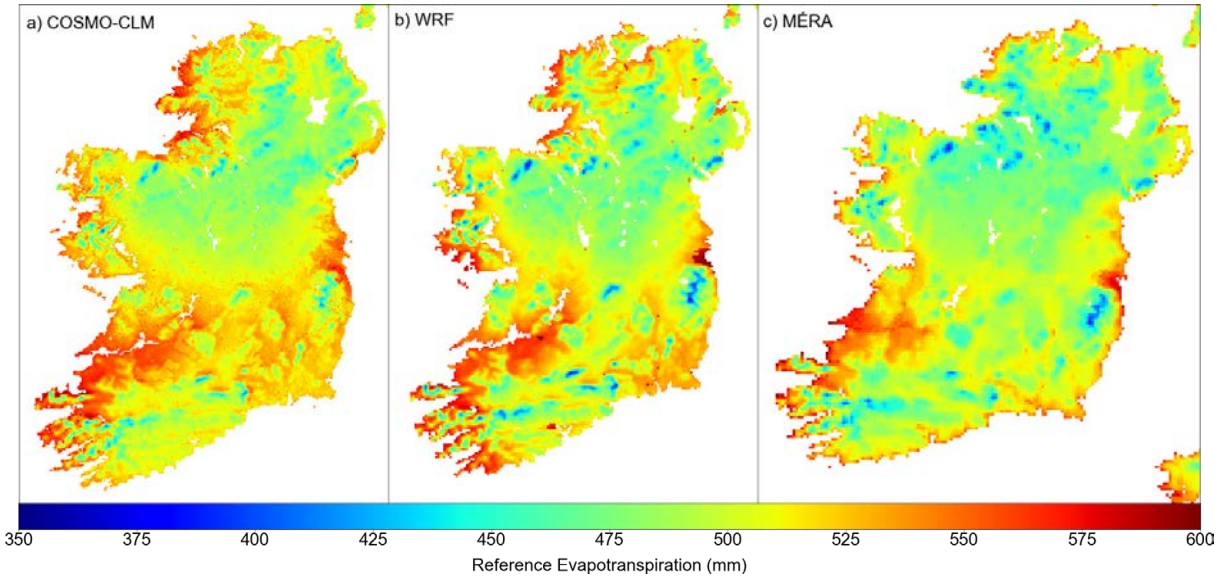


**Figure 4.3. Average annual $ET_0$ maps for the COSMO-CLM and WRF (1981–2017) and MÉRA (1981–2016) models. The MÉRA model shows the best fit to observations and the WRF model performs the best of the higher resolution models.**

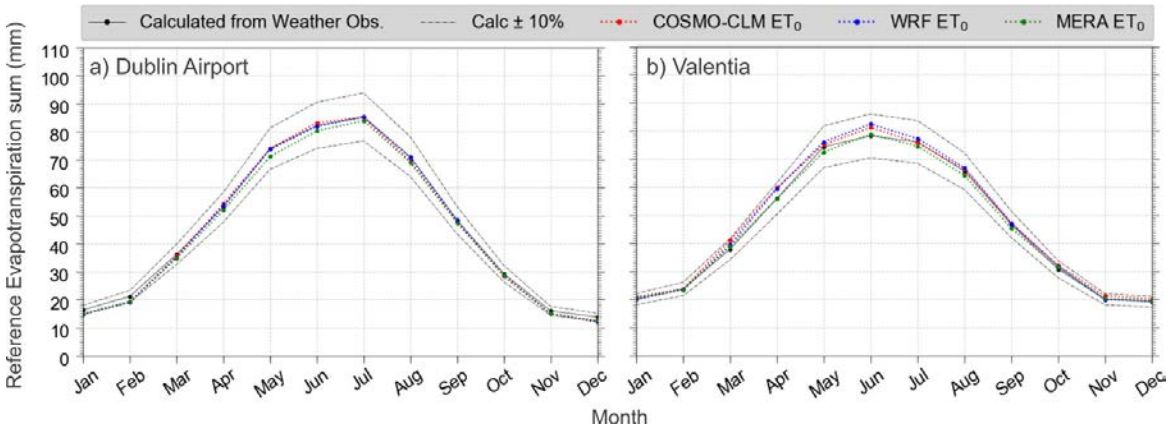


**Figure 4.4. Average monthly sums of $ET_0$ at selected stations for the WRF and COSMO-CLM (1981–2017) and MÉRA (1981–2016) models.**

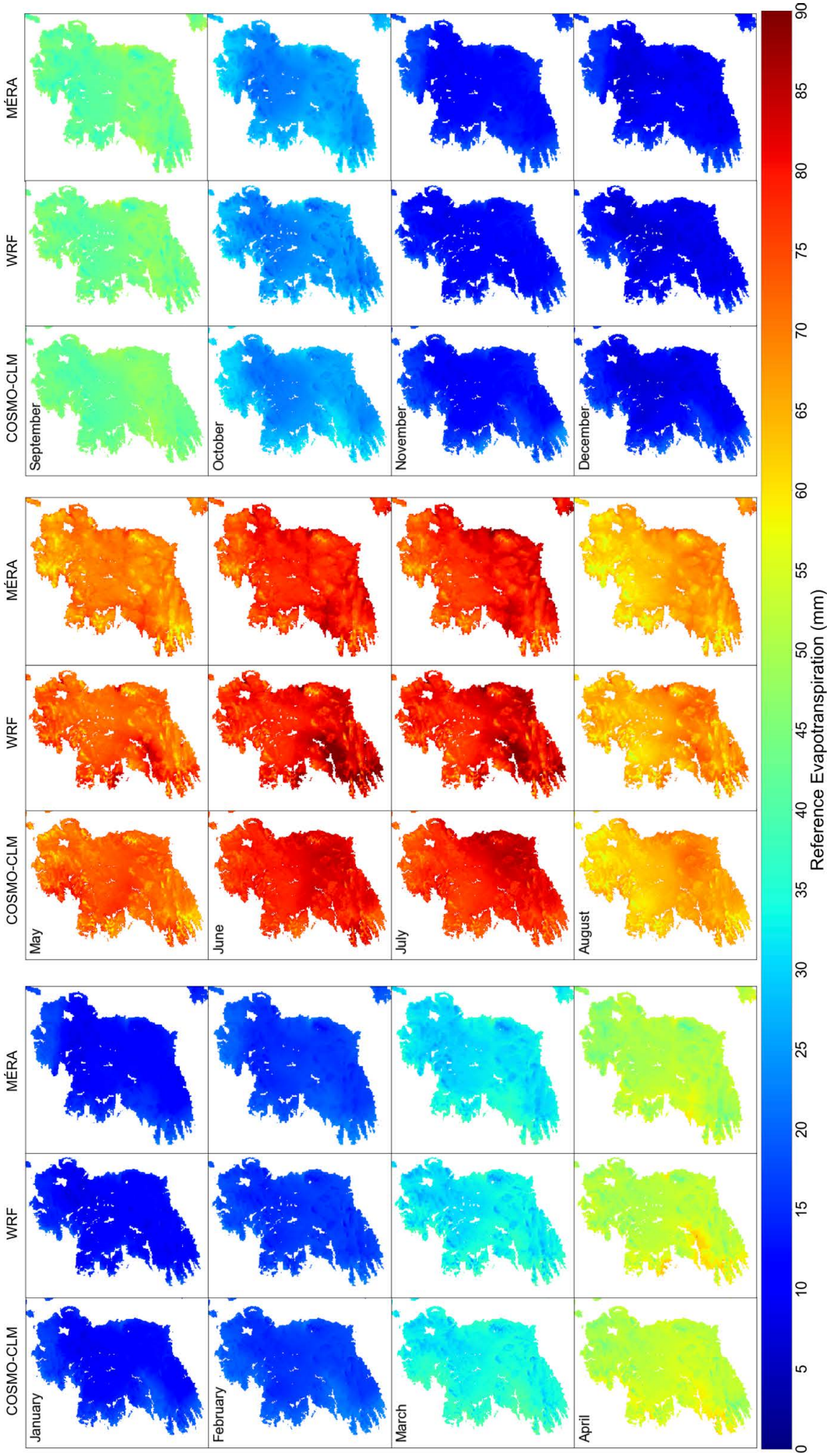


**Figure 4.5. Average monthly sums of $ET_0$ for the WRF and COSMO-CLM (1981–2017) and MÉRA (1981–2016) models.**

As shown in Figures 4.4 and 4.5, there is good agreement between models and calculated observations. The largest differences between models were noted around the Shannon region between April and July (see Figure 4.5). The WRF model produces the largest $ET_0$ value, with values approximately 10 mm greater than in the MÉRA model (see Figures 4.4 and 4.5). Averaging out the monthly sums and daily values for all stations gives the errors shown in Table 4.3. To quantify an overall view of the model performance, weighted averages are implemented, given by:

$$\bar{x} = \sum_{i=1}^{n} w_i x_i \qquad (4.1)$$

where $x$ is the error at a station and $w$ is the weight assigned to that station. Depending on the time period of the dataset at each station, a different weight is assigned. Those with data covering the full model time period (1981–2016) will have a higher weight and therefore exert more influence on the weighted average. With all stations considered, weighted averages show that MÉRA model outperforms the WRF model, which outperforms the COSMO-CLM model. For standard deviations, the COSMO-CLM model performs the best for 11 of the 12 months, and the MÉRA model is outperformed by both the WRF and the COSMO-CLM models for 10 months, reflecting the performance seen in the yearly sums of Table 4.2. For correlation coefficients, the MÉRA model performs best, followed by the WRF model.

## 4.2 Actual Evapotranspiration

Given the small error of the $ET_0$ series described in section 4.1, and the use of observational precipitation data, it follows that the corresponding $ET_a$ and SMD series would be a close match for observed records.

Actual evapotranspiration depends on the drainage of the soil, and at present there are five soil drainage types identified in Ireland, from excessively drained to poorly drained. A combined dataset for $ET_a$ was calculated using the Teagasc soil map to assign soil drainage classes to each grid square. However, the majority of datasets presented in the following sections show calculated soil moisture conditions using a single soil drainage type for each grid square.

The selection of synoptic stations used previously still applies for $ET_a$; however, only well-drained, moderately drained and poorly drained soil drainage types are calculated from $ET_0$ and precipitation using the HSMD model at synoptic stations. Because of the nature of the model, $ET_a$ for moderately drained and well-drained soils was found to be nearly identical, so only well-drained and poorly drained soils are described in the following sections. Moderately drained soils are analysed in more detail in section 4.3 for SMDs.

### *4.2.1 Well-drained soils*

For well-drained soils, $ET_a$ is equal to $ET_0$ when the SMD at time $t$–1 is equal to 0. In the HSMD model, well-drained soils never saturate and remain at field

**Table 4.3. RMSEs of monthly summed $ET_0$ values and daily $ET_0$ values for each month (1981–2017) using an overall weighted average across 22 stations**

| Model | Jan | Feb | Mar | Apr | May | Jun | Jul | Aug | Sep | Oct | Nov | Dec |
|---|---|---|---|---|---|---|---|---|---|---|---|---|
| **Monthly** | | | | | | | | | | | | |
| COSMO-CLM | 2.644 | 2.724 | 2.8 | 4.272 | 5.733 | 5.956 | 6.363 | 5.073 | 3.334 | 2.353 | 2.398 | 2.73 |
| WRF | 2.895 | 2.797 | 2.446 | 3.795 | 4.82 | 5.505 | 5.437 | 4.005 | 2.649 | 2.324 | 2.78 | 3.048 |
| MÉRA | 2.458 | 2.397 | 2.437 | 2.617 | 3.929 | 4.016 | 4.232 | 3.701 | 2.812 | 2.119 | 2.311 | 2.625 |
| **Daily** | | | | | | | | | | | | |
| COSMO-CLM | 0.22 | 0.232 | 0.324 | 0.465 | 0.605 | 0.7 | 0.65 | 0.532 | 0.405 | 0.264 | 0.217 | 0.224 |
| WRF | 0.217 | 0.218 | 0.277 | 0.402 | 0.559 | 0.642 | 0.603 | 0.484 | 0.337 | 0.227 | 0.215 | 0.226 |
| MÉRA | 0.197 | 0.202 | 0.265 | 0.338 | 0.433 | 0.499 | 0.489 | 0.419 | 0.318 | 0.221 | 0.197 | 0.199 |

**The best and worst performers are colour coded green and red, respectively.**

capacity even on very wet days in winter. For all times when SMD > 0 mm, $ET_a$ is less than $ET_0$, and this has a large effect on the actual values. The difference in the well-drained soil $ET_a$ value relative to the $ET_0$ value varies substantially across the country, with the largest differences in the central and south-eastern regions. To the west and north, where it is generally wetter and more mountainous, the difference is smaller, as soil saturation is high enough to result in $ET_a$ being equal to $ET_0$ more often. Differences such as these have large effects on the outputs of models that require evapotranspiration as an input. This is reflected in Figure 4.6, which presents $ET_0 - ET_a$ at Dublin Airport. Encouragingly, most of the data points for all three models lie within 0.5 mm of a one-to-one relationship. The precipitation data used in the HSMD model (used in turn to produce $ET_a$ values) extend to 2016 only. Figure 4.7 shows scatter plots of daily $ET_a$ values at Dublin Airport.

Table 4.4 shows errors in the $ET_a$ values for the eight long-term synoptic stations and overall weighted averages of all 22 stations. There is very little difference in the relative performance of the models, with the MÉRA model outperforming the WRF model, which in turn outperforms the COSMO-CLM model. As previously noted, the COSMO-CLM model performs best for standard deviations. Reflecting the decrease in $ET_a$ values relative to $ET_0$, RMSE and standard deviation values have also decreased. Figure 4.8 shows yearly sums from 1981 to 2016 for Dublin Airport and Valentia Observatory.

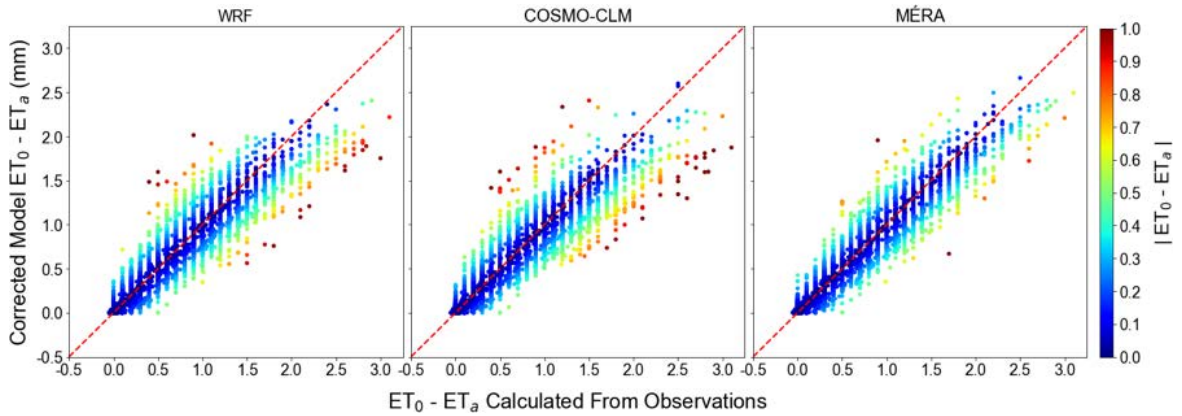


**Figure 4.6. Difference between $ET_0$ and $ET_a$ for Dublin Airport for the WRF, COSMO-CLM and MÉRA models (1981–2016).**

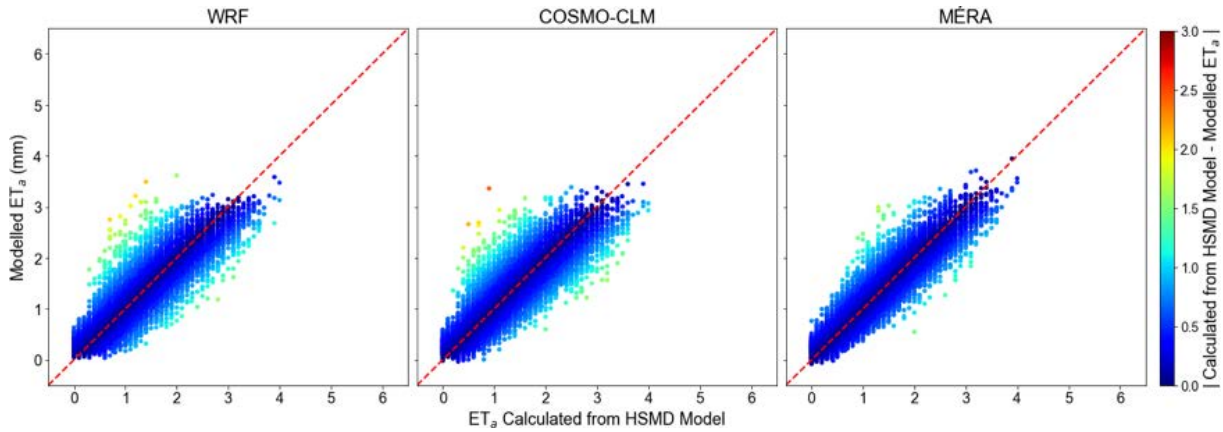


**Figure 4.7. Scatter plots of daily $ET_a$ values for well-drained soils for each model at Dublin Airport. The colour coding represents deviation from a one-to-one relationship.**

**Table 4.4. Errors in yearly summed values of $ET_a$ at selected stations and overall weighted averages for 22 stations from 1981 to 2016**

| Station | RMSE (mm) | | | Standard deviation (mm) | | | Correlation coefficient | | |
|---|---|---|---|---|---|---|---|---|---|
| | COSMO-CLM | WRF | MÉRA | COSMO-CLM | WRF | MÉRA | COSMO-CLM | WRF | MÉRA |
| Belmullet | 0.376 | 0.344 | 0.288 | 0.704 | 0.748 | 0.724 | 0.867 | 0.894 | 0.923 |
| Casement | 0.366 | 0.334 | 0.275 | 0.675 | 0.684 | 0.686 | 0.864 | 0.887 | 0.924 |
| Cork Airport | 0.418 | 0.38 | 0.334 | 0.763 | 0.773 | 0.78 | 0.868 | 0.892 | 0.918 |
| Dublin Airport | 0.363 | 0.341 | 0.279 | 0.673 | 0.677 | 0.686 | 0.867 | 0.883 | 0.923 |
| Malin Head | 0.376 | 0.356 | 0.291 | 0.599 | 0.669 | 0.638 | 0.836 | 0.861 | 0.906 |
| Mullingar | 0.357 | 0.33 | 0.276 | 0.762 | 0.766 | 0.771 | 0.9 | 0.915 | 0.942 |
| Shannon Airport | 0.375 | 0.358 | 0.298 | 0.733 | 0.787 | 0.751 | 0.884 | 0.899 | 0.928 |
| Valentia | 0.31 | 0.268 | 0.237 | 0.713 | 0.74 | 0.741 | 0.86 | 0.891 | 0.922 |
| All | 0.378 | 0.347 | 0.291 | 0.713 | 0.740 | 0.735 | 0.874 | 0.896 | 0.927 |

**The best and worst performers are colour coded green and red, respectively.**

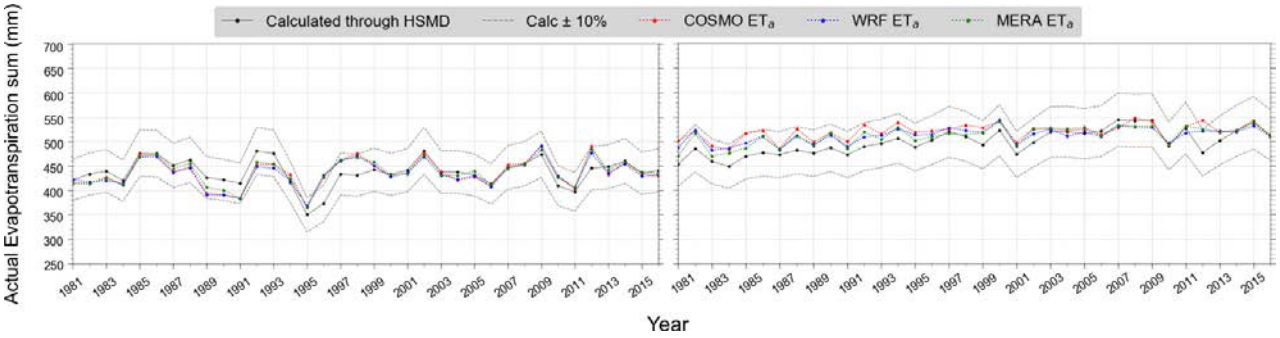


**Figure 4.8. Annual $ET_a$ sums for Dublin Airport and Valentia Observatory synoptic stations from 1981 to 2016. The solid black line shows the Met Éireann-calculated values from observations, with a ±10% interval shown by the dashed black line.**

Figure 4.8 shows a good match between all modelled $ET_a$ and calculated $ET_a$ values as derived through the HSMD model. Here, the errors are lower, with higher correlation coefficients also noted. Unlike for $ET_0$, where the models occasionally missed out on significant drops, for the most part modelled $ET_a$ values are better represented. For the eight long-term synoptic stations, there is a consistent small increase in annual sums of 0.73–0.83 mm/year from 1981 to 2016. Table 4.5 shows an increase in these annual $ET_a$ sums per year at each synoptic station, which estimated $ET_0$ back to 1981. This is particularly evident in stations such as Belmullet and Valentia in Figure 4.8.

As mentioned previously, there is an improvement in the performance of the models compared to the $ET_0$ equivalent, with a better fit and lower errors overall,

**Table 4.5. Increase in $ET_a$ (mm/year) for each station for each model (1981–2016)**

| Model | Belmullet | Casement | Cork Airport | Dublin Airport | Malin Head | Mullingar | Shannon Airport | Valentia | All |
|---|---|---|---|---|---|---|---|---|---|
| COSMO-CLM | 0.532 | 0.753 | 0.626 | 0.586 | 0.732 | 0.785 | 1.115 | 0.710 | 0.730 |
| WRF | 0.512 | 0.836 | 0.494 | 0.562 | 0.843 | 0.807 | 1.082 | 0.769 | 0.738 |
| MÉRA | 0.588 | 0.735 | 0.810 | 0.581 | 0.640 | 0.973 | 1.223 | 1.134 | 0.836 |

as shown in Table 4.6. Regarding the overall average annual sums, there are large differences between $ET_a$ and $ET_0$. This is further illustrated in Figure 4.9, with the highest values over to the west rather than the east as with $ET_0$. However, it must be noted throughout that these datasets are not necessarily representative of the soil type at each location. The indicative $ET_a$ datasets, which use the Teagasc soil drainage datasets, are discussed in section 4.2.4. Annual sums for the eight long-term synoptic stations are shown in Figure 4.10 and average monthly sums across the country are shown in Figure 4.11.

**Table 4.6. Errors in yearly summed values of $ET_a$ for well-drained soils at selected stations from 1981 to 2016 using an overall weighted average across 22 stations**

| Station | RMSE (mm) | | | Standard deviation (mm) | | | Correlation coefficient | | |
|---|---|---|---|---|---|---|---|---|---|
| | COSMO-CLM | WRF | MÉRA | COSMO-CLM | WRF | MÉRA | COSMO-CLM | WRF | MÉRA |
| Belmullet | 21.016 | 20.029 | 18.315 | 17.217 | 16.957 | 16.322 | 0.597 | 0.596 | 0.674 |
| Casement | 14.664 | 12.283 | 10.142 | 34.175 | 32.668 | 30.499 | 0.937 | 0.934 | 0.945 |
| Cork Airport | 25.403 | 24.385 | 25.59 | 22.299 | 20.093 | 21.075 | 0.555 | 0.642 | 0.626 |
| Dublin Airport | 20.423 | 20.496 | 18.182 | 28.935 | 26.848 | 26.927 | 0.867 | 0.883 | 0.923 |
| Malin Head | 18.137 | 17.918 | 17.225 | 18.601 | 19.785 | 16.038 | 0.706 | 0.623 | 0.677 |
| Mullingar | 10.429 | 10.018 | 10.856 | 23.891 | 22.37 | 21.596 | 0.906 | 0.917 | 0.921 |
| Shannon Airport | 17.514 | 15.667 | 14.781 | 34.744 | 34.262 | 35.677 | 0.745 | 0.785 | 0.805 |
| Valentia | 27.724 | 20.912 | 19.449 | 16.54 | 15.174 | 18.881 | 0.693 | 0.805 | 0.833 |
| All | 18.024 | 16.148 | 15.597 | 22.759 | 21.624 | 20.947 | 0.745 | 0.785 | 0.805 |

**The best and worst performers are colour coded green and red, respectively.**

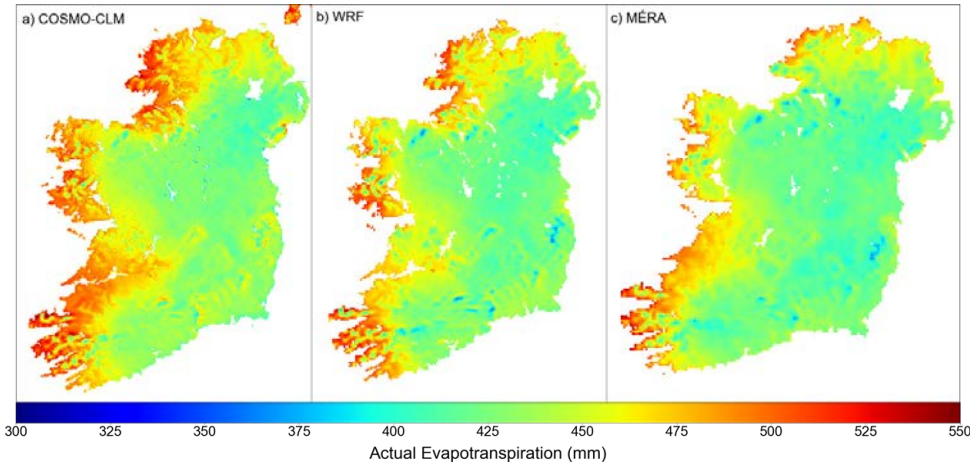


**Figure 4.9. Average annual $ET_a$ maps for well-drained soils for the COSMO-CLM, WRF and MÉRA models (1981–2016).**

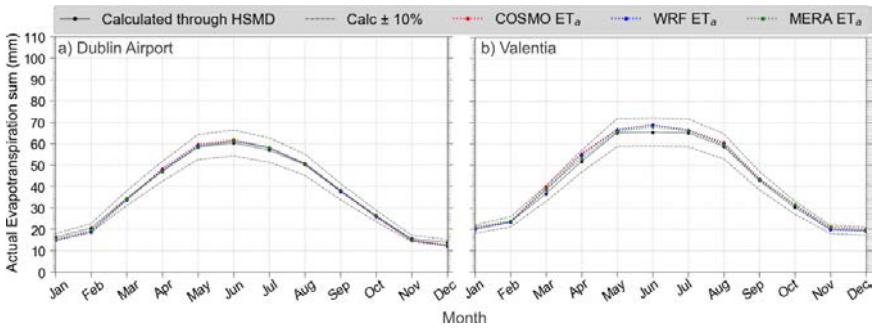


**Figure 4.10. Average monthly sums of $ET_a$ for well-drained soils at Dublin Airport and Valentia Observatory for the COSMO-CLM, WRF and MÉRA models (1981–2016).**

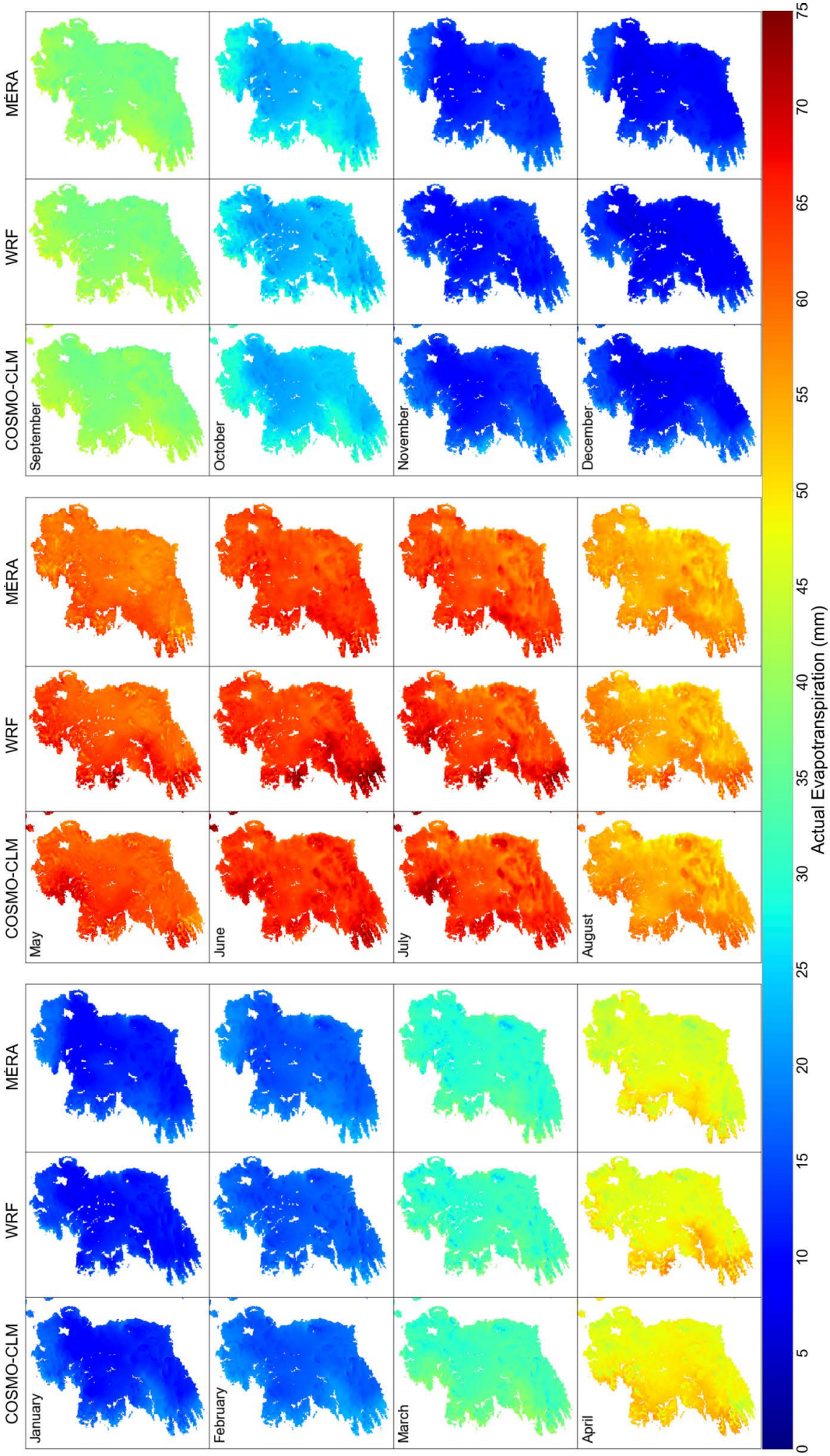


**Figure 4.11. Average monthly sums of $ET_a$ for well-drained soils using the COSMO-CLM, WRF and MÉRA models (1981–2016).**

As shown in Figures 4.10 and 4.11, there is a notable difference between $ET_a$ and $ET_0$ across the country because of the lack of moisture in the soils during the summer months. During the winter months, as expected, there is very little difference noted between the models. During the summer months, particularly June and July, there is a notable difference between the WRF model and the other two models, which show higher values, particularly in the south and western regions. Table 4.7, which presents the errors on a monthly basis, shows that, once again, the MÉRA model is the best performer. Errors have also decreased for most months compared with the $ET_0$ equivalent of this table (see Table 4.3). Errors in monthly sums have decreased by over 1 mm during the summer months for all models and daily value errors have decreased by up to 0.15 mm during the summer months. The errors for winter months have stayed consistent because of the low values of $ET_a$ during these months.

### 4.2.2 *Poorly drained soils*

The difference in evapotranspiration between well-drained and poorly drained soils varies across the country, from approximately 15 mm/year in mountainous regions in the north and west to 25 mm/year in the eastern and southern regions. As poorly drained soils hold more water than well-drained soils, yearly sums of $ET_a$ are greater in poorly drained soils than in well-drained soils.

Tables 4.8 and 4.9 shows the errors for daily and yearly summed $ET_a$ values for poorly drained soils, respectively. Validation results thus far have demonstrated that the MÉRA model consistently outperforms both the WRF model and the

**Table 4.7. RMSEs of monthly summed $ET_a$ and daily $ET_a$ values for each month (1981–2016) using an overall weighted average across 22 stations for well-drained soils**

| Model | Jan | Feb | Mar | Apr | May | Jun | Jul | Aug | Sep | Oct | Nov | Dec |
|---|---|---|---|---|---|---|---|---|---|---|---|---|
| **Monthly** | | | | | | | | | | | | |
| COSMO-CLM | 2.666 | 2.617 | 2.644 | 3.672 | 4.116 | 4.541 | 4.058 | 3.700 | 2.53 | 2.13 | 2.354 | 2.735 |
| WRF | 2.88 | 2.677 | 2.255 | 3.149 | 3.515 | 4.046 | 3.741 | 3.176 | 2.142 | 2.085 | 2.677 | 3.066 |
| MÉRA | 2.453 | 2.281 | 2.291 | 2.145 | 2.788 | 3.094 | 2.950 | 2.854 | 2.251 | 1.914 | 2.263 | 2.579 |
| **Daily** | | | | | | | | | | | | |
| COSMO-CLM | 0.217 | 0.227 | 0.306 | 0.426 | 0.514 | 0.567 | 0.510 | 0.446 | 0.353 | 0.249 | 0.212 | 0.224 |
| WRF | 0.215 | 0.213 | 0.266 | 0.367 | 0.478 | 0.523 | 0.479 | 0.410 | 0.299 | 0.216 | 0.210 | 0.226 |
| MÉRA | 0.195 | 0.198 | 0.255 | 0.307 | 0.368 | 0.402 | 0.386 | 0.350 | 0.277 | 0.210 | 0.195 | 0.197 |

**The best and worst performers are colour coded green and red, respectively.**

**Table 4.8. Errors in daily values of $ET_a$ at selected stations and using overall weighted averages for 22 stations (1981–2016) for poorly drained soils**

| Station | RMSE (mm) | | | Standard deviation (mm) | | | Correlation coefficient | | |
|---|---|---|---|---|---|---|---|---|---|
| | COSMO-CLM | WRF | MÉRA | COSMO-CLM | WRF | MÉRA | COSMO-CLM | WRF | MÉRA |
| Belmullet | 0.396 | 0.377 | 0.329 | 0.76 | 0.811 | 0.804 | 0.867 | 0.889 | 0.917 |
| Casement | 0.386 | 0.352 | 0.297 | 0.731 | 0.742 | 0.769 | 0.87 | 0.893 | 0.926 |
| Cork Airport | 0.444 | 0.404 | 0.357 | 0.829 | 0.843 | 0.872 | 0.874 | 0.897 | 0.921 |
| Dublin Airport | 0.383 | 0.359 | 0.299 | 0.728 | 0.734 | 0.765 | 0.873 | 0.890 | 0.926 |
| Malin Head | 0.396 | 0.374 | 0.309 | 0.650 | 0.730 | 0.714 | 0.846 | 0.870 | 0.912 |
| Mullingar | 0.377 | 0.349 | 0.295 | 0.822 | 0.829 | 0.855 | 0.905 | 0.919 | 0.943 |
| Shannon Airport | 0.397 | 0.38 | 0.321 | 0.794 | 0.851 | 0.836 | 0.889 | 0.902 | 0.929 |
| Valentia | 0.431 | 0.384 | 0.329 | 0.773 | 0.809 | 0.825 | 0.868 | 0.897 | 0.927 |
| **All** | 0.399 | 0.368 | 0.313 | 0.771 | 0.803 | 0.818 | 0.879 | 0.900 | 0.929 |

**The best and worst performers are colour coded green and red, respectively.**

**Table 4.9. Errors in yearly summed values of $ET_a$ at selected stations and using overall weighted averages for 22 stations (1981–2016) for poorly drained soils**

| Station | RMSE (mm) | | | Standard deviation (mm) | | | Correlation coefficient | | |
|---|---|---|---|---|---|---|---|---|---|
| | COSMO-CLM | WRF | MÉRA | COSMO-CLM | WRF | MÉRA | COSMO-CLM | WRF | MÉRA |
| Belmullet | 35.263 | 31.564 | 34.649 | 18.774 | 19.679 | 18.41 | 0.558 | 0.527 | 0.604 |
| Casement | 14.107 | 11.866 | 12.732 | 39.107 | 37.453 | 36.39 | 0.957 | 0.952 | 0.952 |
| Cork Airport | 27.381 | 26.351 | 25.339 | 24.549 | 22.469 | 24.719 | 0.578 | 0.659 | 0.649 |
| Dublin Airport | 21.302 | 21.569 | 20.502 | 33.542 | 31.385 | 32.768 | 0.79 | 0.773 | 0.819 |
| Malin Head | 18.419 | 18.817 | 21.157 | 20.719 | 22.504 | 19.197 | 0.746 | 0.672 | 0.736 |
| Mullingar | 10.982 | 10.658 | 10.382 | 26.065 | 24.581 | 24.982 | 0.912 | 0.923 | 0.919 |
| Shannon Airport | 19.209 | 17.627 | 15.363 | 34.744 | 34.262 | 35.677 | 0.873 | 0.900 | 0.905 |
| Valentia | 28.444 | 22.061 | 23.781 | 16.464 | 16.324 | 20.477 | 0.698 | 0.803 | 0.852 |
| All | 20.034 | 18.111 | 19.229 | 24.972 | 24.161 | 24.052 | 0.758 | 0.792 | 0.813 |

**The best and worst performers are colour coded green and red, respectively.**

COSMO-CLM model. However, for yearly sums, the average RMSE best performer is the WRF model (a possible explanation is provided in section 4.3.3). As mentioned previously, $ET_a$ for poorly drained soils is expected to be greater than for well-drained soils and this is confirmed by Figure 4.12. The high evapotranspiration regions observed in the yearly well-drained soil maps of Figure 4.10 remain similar. The main difference is in the centre of the country, with values in the region of 30 mm/year greater than for well-drained soils. However, it must be stressed that these maps assume that all soils in the country are of the same drainage class and do not necessarily reflect the actual evapotranspiration at that location, so dataset end users must be aware of the regional drainage qualities of soil before utilising them at a specific location. Figure 4.13 shows the average monthly sums of $ET_a$ for poorly drained soils at Dublin

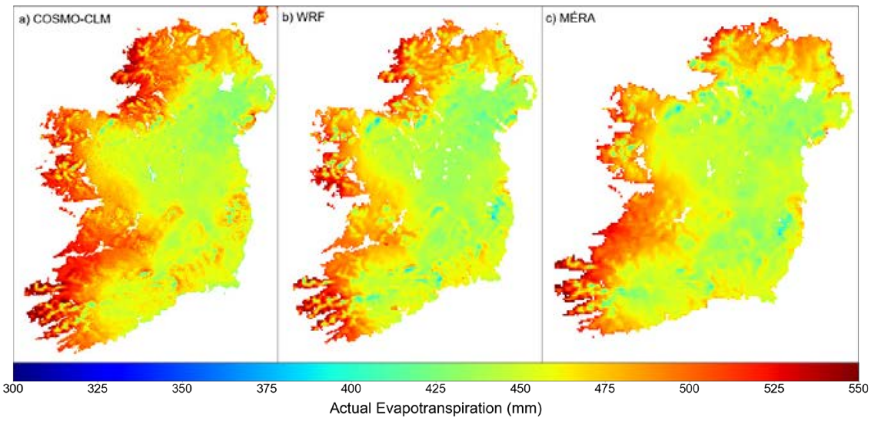


**Figure 4.12. Average annual $ET_a$ maps for poorly drained soils for the COSMO-CLM, WRF and MÉRA models (1981–2016).**

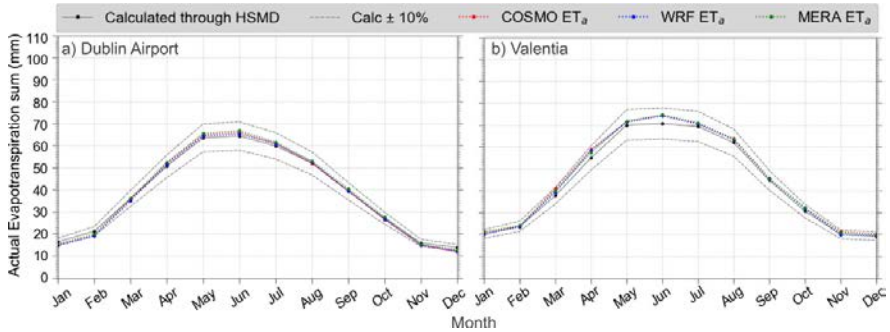


**Figure 4.13. Average monthly sums of $ET_a$ for poorly drained soils at Dublin Airport and Valentia Observatory stations from 1981 to 2016.**

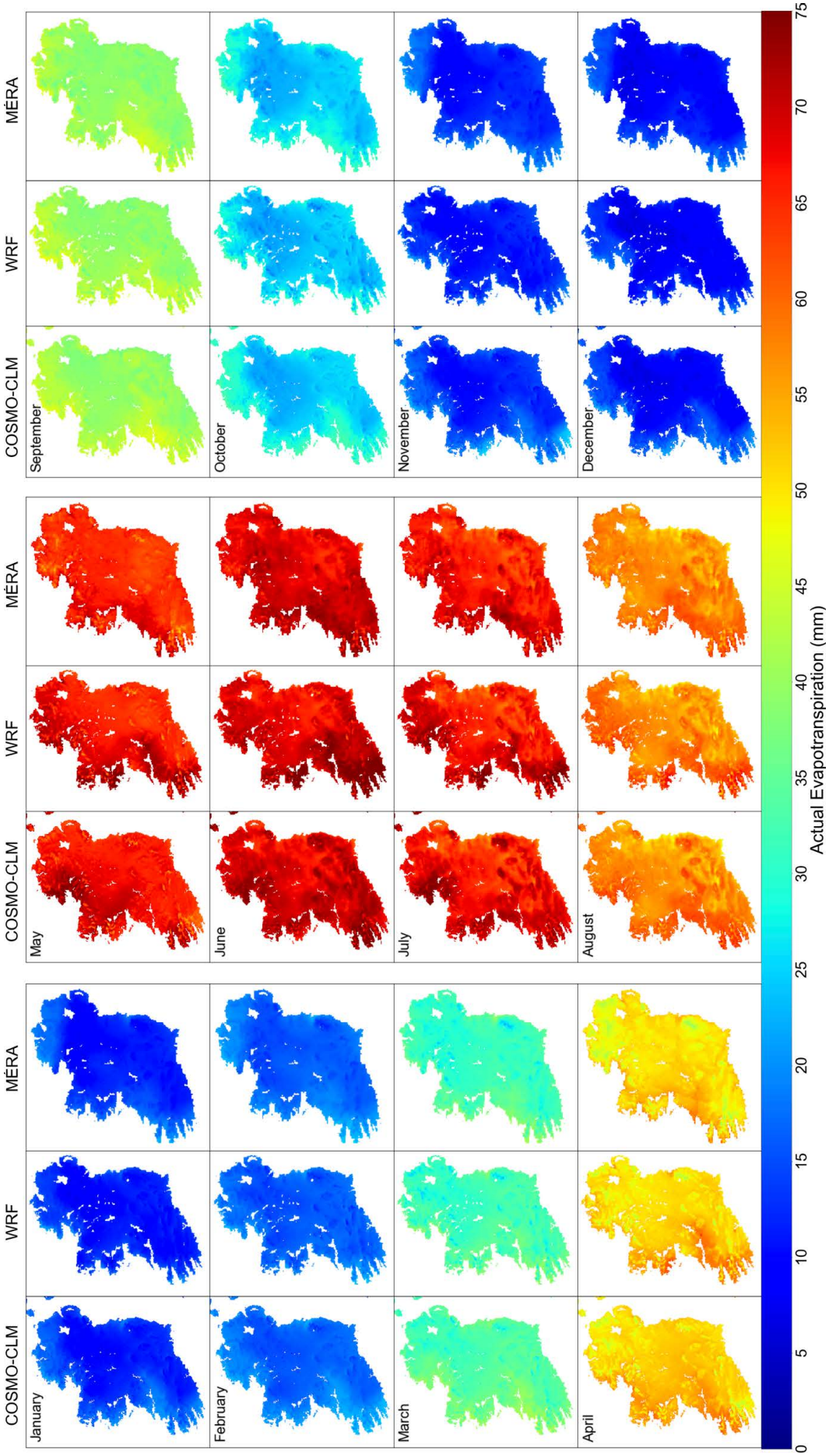


**Figure 4.14. Average monthly sums of $ET_a$ for poorly drained soils using the COSMO-CLM, WRF and MÉRA models (1981–2016).**

Airport and Valentia Observatory, Figure 4.14 shows the monthly sums countrywide for poorly drained soils and Table 4.10 shows RMSEs of monthly summed and daily $ET_a$ values for the same soil class for each month (1981–2016).

### *4.2.3 Excessively and imperfectly drained soils*

Excessively and imperfectly drained soils are the newest additions to the Irish soil drainage classes, but SMDs for these drainage classes are not calculated from observed weather parameters at present. Figures 4.15 and 4.16 show the excessively and imperfectly

**Table 4.10. RMSEs of monthly summed and daily $ET_a$ values for poorly drained soil for each month (1981–2016) using an overall weighted average across 22 stations**

| Model | Jan | Feb | Mar | Apr | May | Jun | Jul | Aug | Sep | Oct | Nov | Dec |
|---|---|---|---|---|---|---|---|---|---|---|---|---|
| **Monthly** | | | | | | | | | | | | |
| COSMO-CLM | 2.702 | 2.748 | 2.802 | 4.133 | 4.721 | 5.177 | 4.615 | 4.129 | 2.758 | 2.224 | 2.400 | 2.779 |
| WRF | 2.925 | 2.815 | 2.450 | 3.69 | 4.316 | 4.718 | 4.307 | 3.626 | 2.405 | 2.189 | 2.738 | 3.124 |
| MÉRA | 2.481 | 2.389 | 2.459 | 3.125 | 4.036 | 4.646 | 4.207 | 3.519 | 2.613 | 2.041 | 2.295 | 2.621 |
| **Daily** | | | | | | | | | | | | |
| COSMO-CLM | 0.219 | 0.232 | 0.317 | 0.455 | 0.554 | 0.608 | 0.541 | 0.467 | 0.37 | 0.256 | 0.214 | 0.226 |
| WRF | 0.217 | 0.218 | 0.276 | 0.395 | 0.521 | 0.563 | 0.509 | 0.432 | 0.313 | 0.221 | 0.212 | 0.229 |
| MÉRA | 0.197 | 0.202 | 0.265 | 0.338 | 0.401 | 0.449 | 0.423 | 0.373 | 0.293 | 0.215 | 0.197 | 0.199 |

**The best and worst performers are colour coded green and red, respectively.**

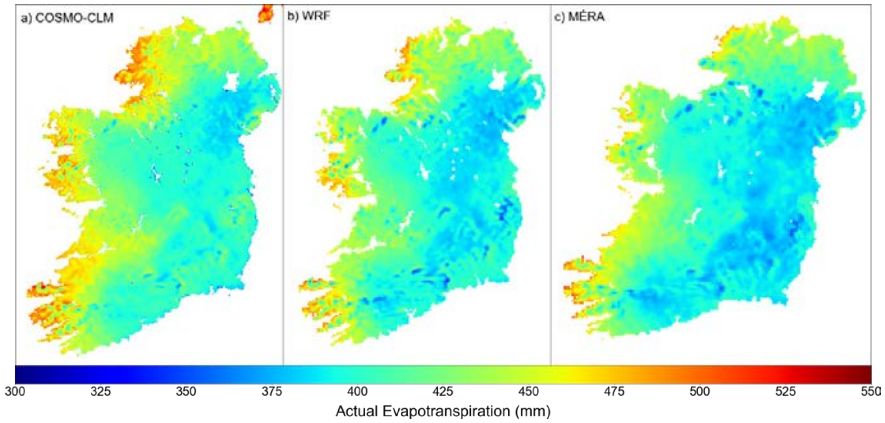


**Figure 4.15. Average annual $ET_a$ maps for excessively drained soils for the COSMO-CLM, WRF and MÉRA models (1981–2016).**

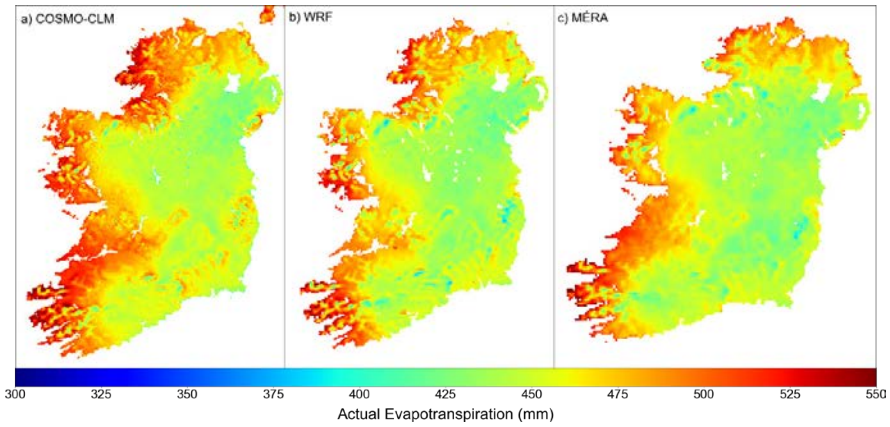


**Figure 4.16. Average annual $ET_a$ maps for imperfectly drained soils for the COSMO-CLM, WRF and MÉRA models (1981–2016).**

drained average annual $ET_a$ sums, respectively. The imperfectly drained datasets shown in Figure 4.16 are very similar to the poorly drained datasets shown in Figure 4.12. This is because the only significant difference between the soils is the drainage term, which assumes maximum drainage for poorly and imperfectly drained soils of 0.5 and 3 mm, respectively. This equates to a difference of 5 mm/year on average.

### *4.2.4 Indicative ETa maps*

Individual maps, prepared under the assumption that all areas are of the same drainage class, are useful if the user knows explicitly the type of soil at the specific location of interest. In a previous EPA project (Creamer *et al*., 2016), high-resolution soil property maps of Irish soils were prepared and sorted into their associated drainage classes. This dataset was acquired from Teagasc and scaled up to the resolution of the three models in the current study. The dataset contains all five soil drainage classes and also includes urban, bare rock and peat environments. These latter classes are not included in the current analysis as they are not classified under any drainage class. Figure 4.17 shows an indicative $ET_a$ map, which incorporates the spatially variable soil drainage classes. Although the enhanced spatial resolution of the WRF and COSMO-CLM models may have advantages for certain applications, based on the performance of the MÉRA model, we recommend that the $ET_a$ MÉRA dataset (as presented in Figure 4.17c) should be taken as an official national dataset for Ireland.

## 4.3 Soil Moisture Deficits

The following sections will investigate the performance of the HSMD model in the calculation of SMDs in well-drained, moderately drained and poorly drained soils. Because of the nature of the variable, summed values are not applicable, so monthly averages will be analysed. The number of field capacity days per year are also investigated and the results are presented in Appendix 2.

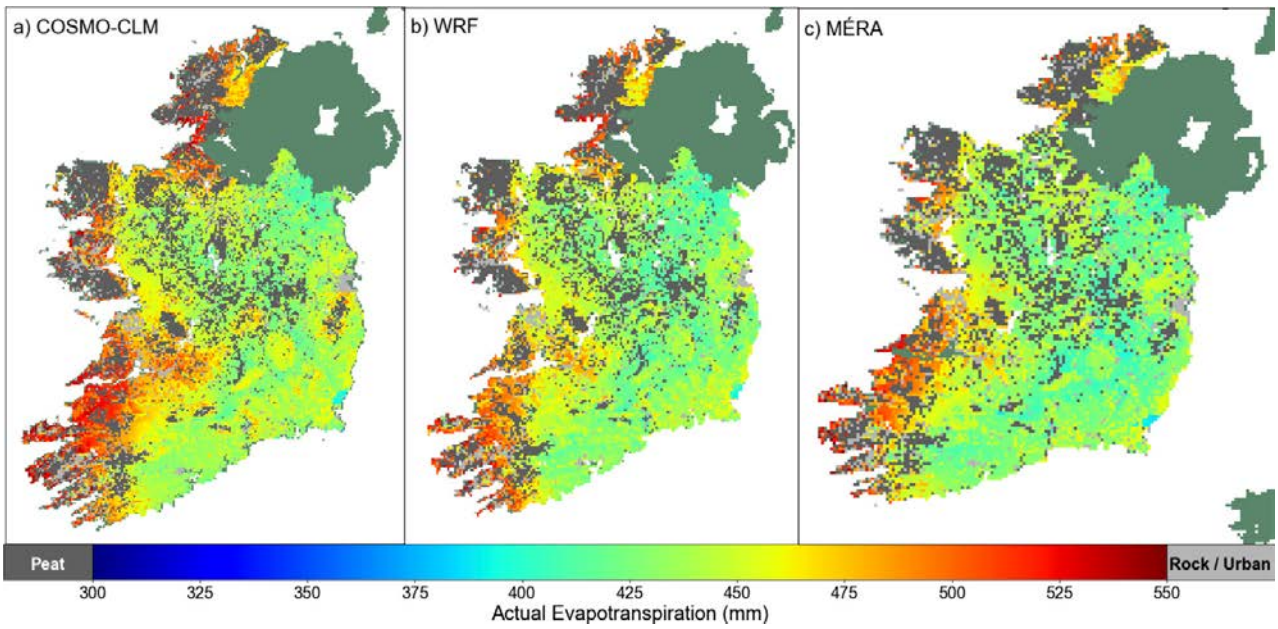


**Figure 4.17. Average annual $ET_a$ maps incorporating the Teagasc National Soil Map of soil drainage classes for the COSMO-CLM, WRF and MÉRA models (1981–2016).**

### *4.3.1 Well-drained SMD*

For well-drained soils, the maximum SMD possible is 110 mm, although this is rarely observed in Ireland. Looking at overall daily values, as shown in Figure 4.18 and Table 4.11, the SMDs are in very good agreement with the synoptic values for all models, with all showing very high correlation coefficients.

The MÉRA model is marginally the better performer. A preliminary calculation of uncorrected SMDs, using modelled precipitation data as the input, resulted in poor correlations and skill scores. Therefore, it was decided to use Met Éireann observational precipitation gridded datasets, which results in a reliable and usable SMD dataset.

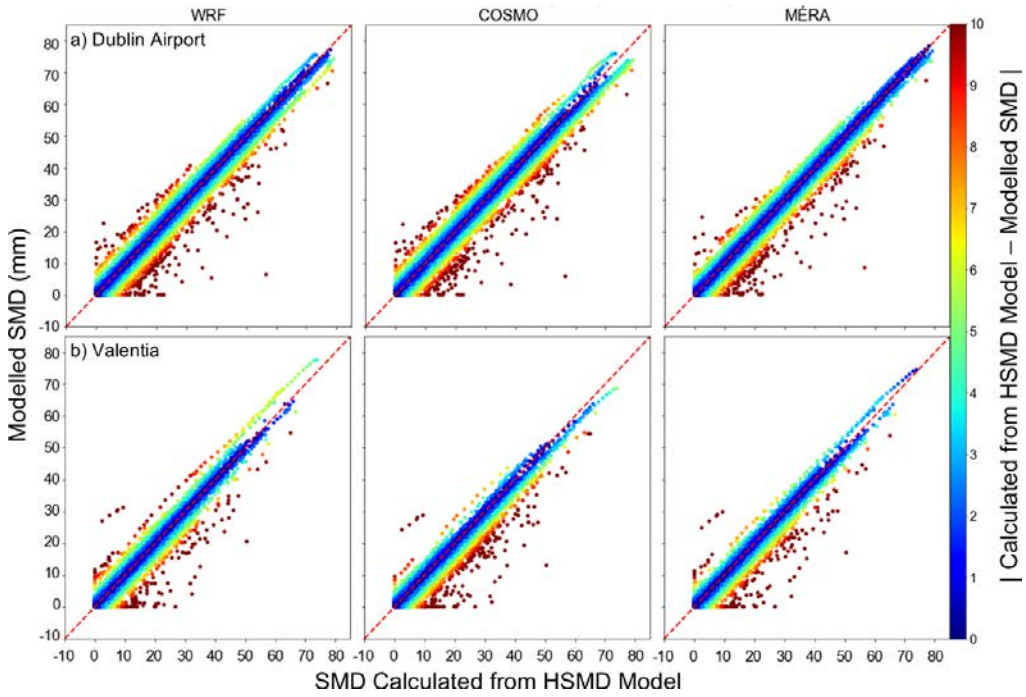


**Figure 4.18. Scatter plots of daily SMD values for well-drained soils for Dublin Airport and Valentia Observatory for all models (1981–2016).**

**Table 4.11. Errors in daily values of SMDs (mm) (well drained) at selected stations from 1981 to 2016 using an overall weighted average across 22 stations**

| Station | RMSE | | | Standard deviation | | | Correlation coefficient | | |
|---|---|---|---|---|---|---|---|---|---|
| | COSMO-CLM | WRF | MÉRA | COSMO-CLM | WRF | MÉRA | COSMO-CLM | WRF | MÉRA |
| Belmullet | 2.256 | 2.335 | 2.066 | 10.931 | 12.018 | 11.152 | 0.98 | 0.982 | 0.984 |
| Casement | 2.686 | 2.696 | 2.609 | 18.381 | 18.691 | 18.121 | 0.989 | 0.99 | 0.991 |
| Cork Airport | 2.998 | 2.48 | 2.361 | 14.096 | 14.874 | 14.776 | 0.986 | 0.988 | 0.989 |
| Dublin Airport | 3.057 | 2.694 | 2.839 | 17.401 | 17.536 | 17.705 | 0.987 | 0.988 | 0.990 |
| Malin Head | 2.441 | 2.124 | 2.124 | 10.909 | 11.942 | 11.449 | 0.982 | 0.984 | 0.985 |
| Mullingar | 2.454 | 2.252 | 2.274 | 13.938 | 14.161 | 14.035 | 0.989 | 0.99 | 0.991 |
| Shannon Airport | 2.949 | 2.844 | 2.642 | 16.252 | 17.176 | 16.448 | 0.986 | 0.986 | 0.989 |
| Valentia | 2.48 | 2.158 | 2.152 | 10.168 | 11.072 | 10.649 | 0.977 | 0.981 | 0.982 |
| All | 2.615 | 2.375 | 2.299 | 12.993 | 13.672 | 13.346 | 0.976 | 0.980 | 0.983 |

**The best and worst performers are colour coded green and red, respectively.**

Figures 4.19–4.21 show yearly averages, monthly averages at synoptic stations and a comparison of monthly averages for all models for the whole country, respectively. Although monthly analysis is more relevant, yearly average datasets can help determine the drier regions. Figure 4.21 shows the similarity of SMD across the country using all three models for each month. As differences between models are so small, the higher resolution models, WRF and COSMO-CLM, can be used as a secondary option to

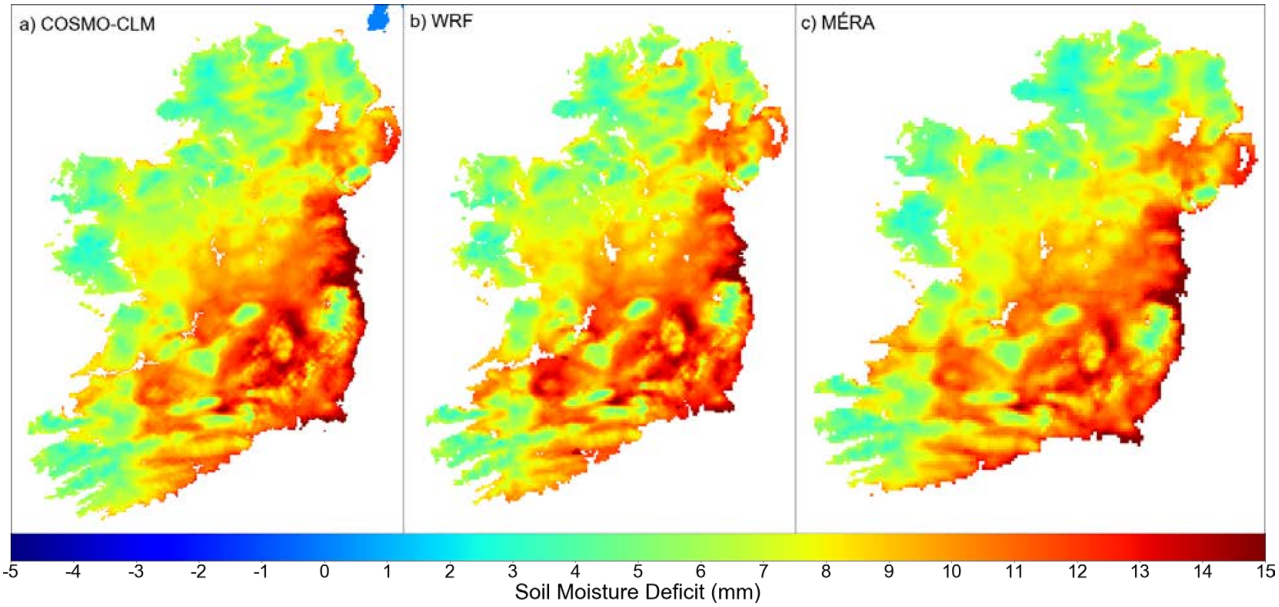


**Figure 4.19. Average annual mean SMD maps for well-drained soils for the COSMO-CLM, WRF and MÉRA models (1981–2016).**

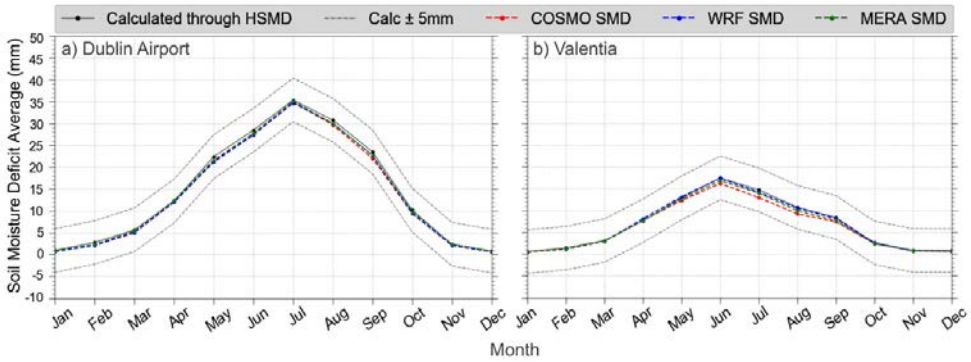


**Figure 4.20. SMD average monthly means for well-drained soils at Dublin Airport and Valentia Observatory (1981–2016).**

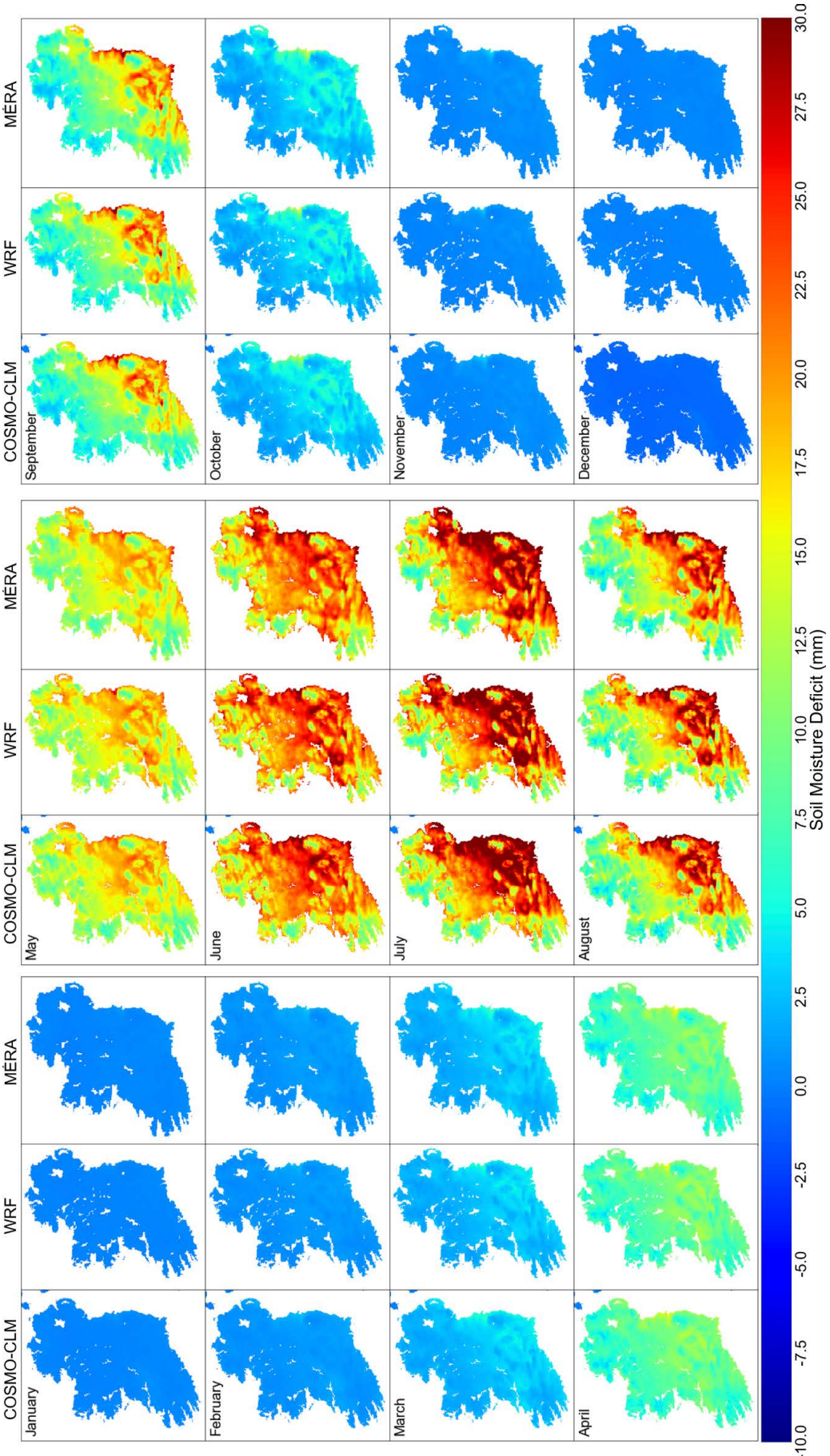


**Figure 4.21. Average monthly means of SMD for well-drained soils using the COSMO-CLM, WRF and MÉRA models (1981–2016).**

the MÉRA model. This is further shown in Table 4.12, which shows weighted RMSE averages for monthly and daily values.

### 4.3.2 *Moderately drained SMD*

Moderately drained soils are most commonly found in the centre of the country and extend to the northern counties of Dublin and Louth. For moderately drained soils, the minimum SMD is –10 mm; soils may saturate on wet winter days but return to field capacity on the first dry day. RMSE errors are subsequently greater for moderately drained soils than for well-drained soils, as shown in Table 4.13.

For moderately drained soils, a small variability in errors is noted between models, with the WRF model outperforming the MÉRA model on occasion. The COSMO-CLM model is consistently outperformed by the other models for RMSE and correlation coefficients. Table 4.14 and Figure 4.22 demonstrate

**Table 4.12. RMSEs of monthly average SMD (well drained) (mm) and daily values for each month (1981–2016) using an overall weighted average across 22 stations**

| Model | Jan | Feb | Mar | Apr | May | Jun | Jul | Aug | Sep | Oct | Nov | Dec |
|---|---|---|---|---|---|---|---|---|---|---|---|---|
| **Monthly** | | | | | | | | | | | | |
| COSMO-CLM | 0.374 | 0.754 | 0.893 | 1.434 | 2.219 | 2.998 | 2.912 | 2.875 | 2.457 | 1.166 | 0.389 | 0.377 |
| WRF | 0.411 | 0.81 | 0.877 | 1.3 | 1.918 | 2.554 | 2.452 | 2.301 | 1.956 | 1.069 | 0.512 | 0.454 |
| MÉRA | 0.339 | 0.668 | 0.796 | 1.274 | 1.84 | 2.354 | 2.24 | 2.301 | 2.077 | 1.027 | 0.407 | 0.407 |
| **Daily** | | | | | | | | | | | | |
| COSMO-CLM | 0.642 | 1.132 | 1.628 | 2.333 | 3.07 | 3.995 | 3.77 | 3.842 | 3.338 | 1.892 | 0.765 | 0.677 |
| WRF | 0.675 | 1.145 | 1.542 | 2.155 | 2.801 | 3.556 | 3.427 | 3.35 | 2.909 | 1.782 | 0.863 | 0.767 |
| MÉRA | 0.591 | 1.014 | 1.489 | 2.127 | 2.705 | 3.353 | 3.246 | 3.329 | 3.015 | 1.758 | 0.758 | 0.701 |

**The best and worst performers are colour coded green and red, respectively.**

**Table 4.13. Errors in daily values of SMD (mm) (moderately drained) at selected stations from 1981 to 2017 using an overall weighted average across 22 stations**

| Station | RMSE | | | Standard deviation | | | Correlation coefficient | | |
|---|---|---|---|---|---|---|---|---|---|
| | COSMO-CLM | WRF | MÉRA | COSMO-CLM | WRF | MÉRA | COSMO-CLM | WRF | MÉRA |
| Belmullet | 3.18 | 3.218 | 3.122 | 12.364 | 13.424 | 12.653 | 0.969 | 0.971 | 0.970 |
| Casement | 3.165 | 3.188 | 3.209 | 19.084 | 19.405 | 18.949 | 0.986 | 0.986 | 0.986 |
| Cork Airport | 3.822 | 3.404 | 3.373 | 15.406 | 16.168 | 16.194 | 0.977 | 0.980 | 0.980 |
| Dublin Airport | 3.457 | 3.311 | 3.180 | 18.101 | 18.247 | 18.528 | 0.983 | 0.985 | 0.986 |
| Malin Head | 3.21 | 2.996 | 3.033 | 12.195 | 13.220 | 12.830 | 0.972 | 0.974 | 0.974 |
| Mullingar | 3.115 | 2.904 | 2.943 | 12.862 | 13.188 | 13.444 | 0.976 | 0.978 | 0.977 |
| Shannon Airport | 3.545 | 3.459 | 3.467 | 17.309 | 18.266 | 17.543 | 0.982 | 0.982 | 0.982 |
| Valentia | 3.636 | 3.383 | 3.399 | 11.884 | 12.742 | 12.439 | 0.96 | 0.965 | 0.964 |
| All | 3.363 | 3.171 | 3.177 | 13.982 | 14.663 | 14.453 | 0.968 | 0.971 | 0.972 |

**The best and worst performers are colour coded green and red, respectively.**

**Table 4.14. RMSEs of monthly average SMD (moderately drained) and daily values for each month (1981–2016) using an overall weighted average across 22 stations**

| Model | Jan | Feb | Mar | Apr | May | Jun | Jul | Aug | Sep | Oct | Nov | Dec |
|---|---|---|---|---|---|---|---|---|---|---|---|---|
| **Monthly** | | | | | | | | | | | | |
| COSMO-CLM | 0.492 | 0.84 | 0.908 | 1.463 | 2.224 | 3.097 | 2.922 | 2.812 | 2.398 | 1.172 | 0.491 | 0.525 |
| WRF | 0.558 | 0.912 | 0.916 | 1.375 | 1.896 | 2.54 | 2.427 | 2.299 | 1.921 | 1.113 | 0.634 | 0.63 |
| MÉRA | 0.485 | 0.77 | 0.909 | 1.322 | 1.974 | 2.374 | 2.604 | 2.279 | 2.021 | 1.081 | 0.513 | 0.562 |
| **Daily** | | | | | | | | | | | | |
| COSMO-CLM | 2.619 | 2.517 | 2.543 | 2.932 | 3.447 | 4.367 | 4.100 | 4.391 | 3.897 | 3.149 | 2.544 | 2.62 |
| WRF | 2.649 | 2.552 | 2.509 | 2.814 | 3.179 | 3.855 | 3.745 | 3.975 | 3.554 | 3.08 | 2.606 | 2.674 |
| MÉRA | 2.607 | 2.47 | 2.488 | 2.764 | 3.235 | 3.689 | 4.084 | 3.94 | 3.612 | 3.119 | 2.548 | 2.62 |

**The best and worst performers are colour coded green and red, respectively.**

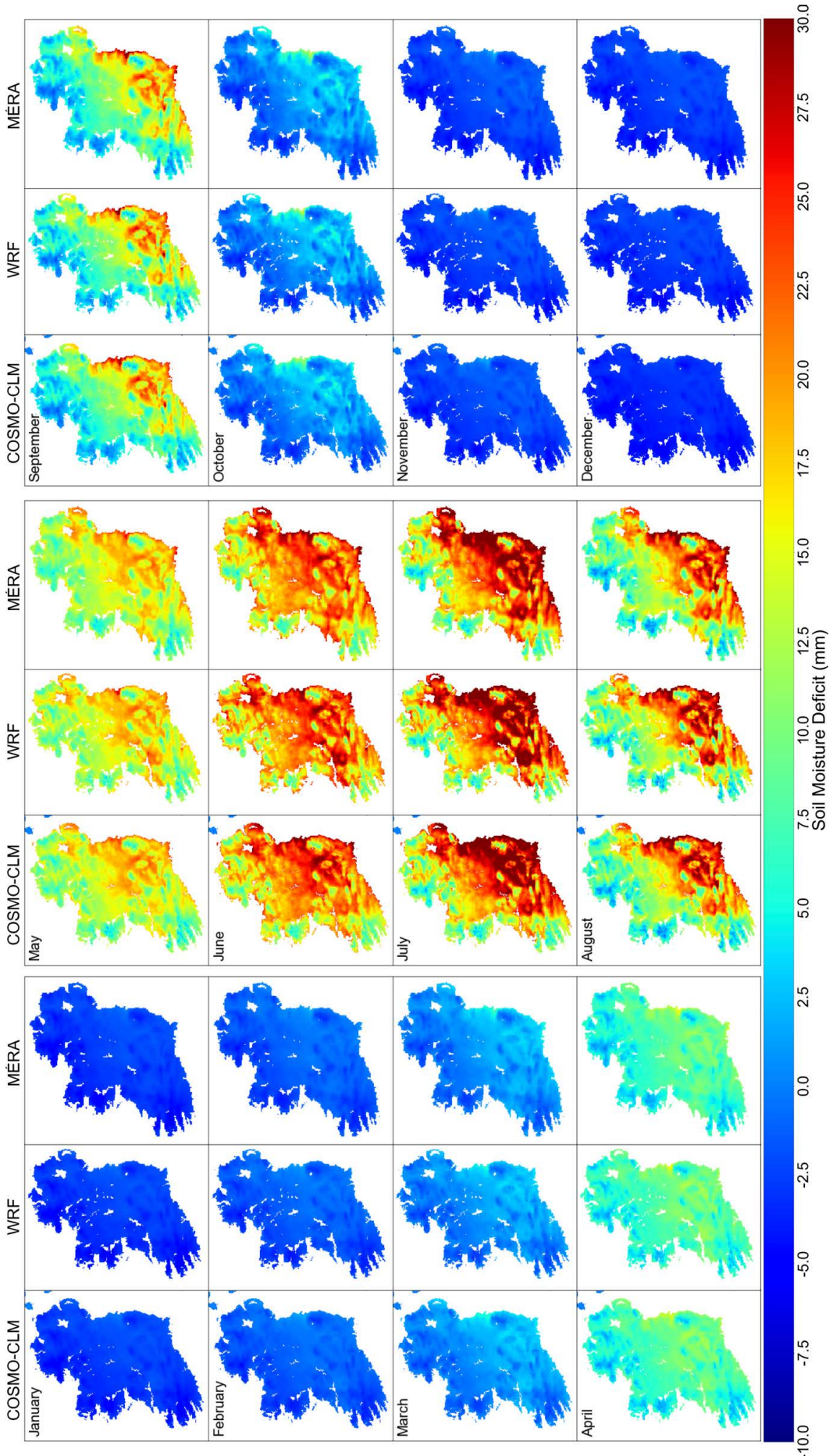


**Figure 4.22. Average monthly means of SMD for moderately drained soils using the COSMO-CLM, WRF and MÉRA models (1981–2016).**

that all models have performed well and there is only a small difference in model errors. The monthly maps in Figure 4.22 show very little difference between models for all months.

### *4.3.3 Poorly drained SMD*

For poorly drained soils, water surplus is drained at 0.5 mm/day, resulting in soils being at field capacity for larger portions of the year. Poorly drained soils are particularly common around Cavan, Leitrim, Limerick and Mayo. The change in water surplus and drainage rates results in a large difference between the model performance statistics. This is illustrated in the yearly averages shown in Figure 4.23, with the MÉRA model showing substantially lower SMDs than the WRF and COSMO-CLM models, particularly in the north and west. Table 4.15 shows that, in contrast to all previous analysis and tables, the MÉRA model is the worst performer because of having SMDs nearly consistently at field capacity during the winter months. To further emphasise the errors highlighted in Table 4.15, Figure 4.24 presents daily values of SMD for poorly drained soils at four locations. The scatter plots show large differences between the MÉRA model and the other two models, with the MÉRA model consistently underestimating the SMD. The poor performance of the MÉRA model for poorly drained soils may be attributed to the lower spatial resolution of the MÉRA data or the transformation of 1-km gridded precipitation to a 2.5-km grid.

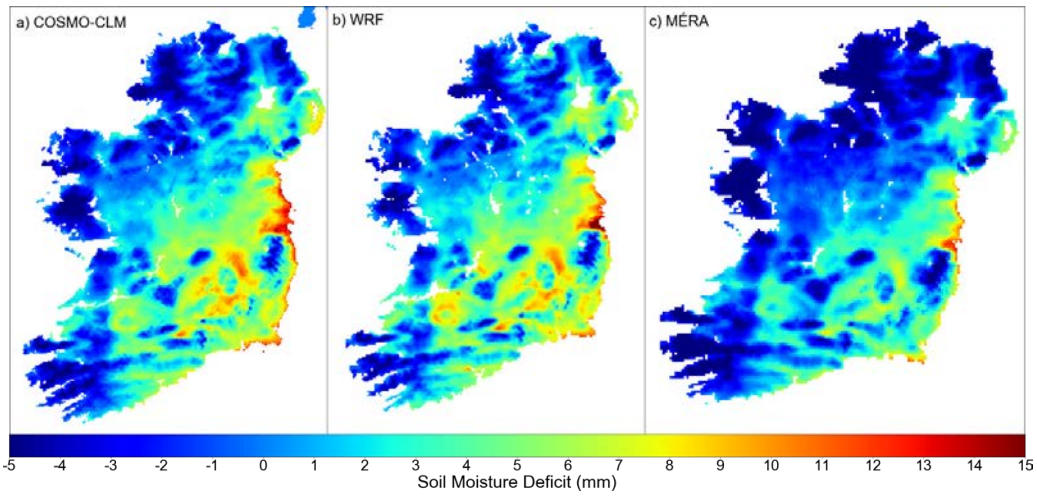


**Figure 4.23. Average annual mean SMD maps for poorly drained soils for the COSMO-CLM, WRF and MÉRA models (1981–2016).**

**Table 4.15. Errors in daily values of SMD (poorly drained) at selected stations from 1981 to 2016 using an overall weighted average across 22 stations**

| Station | RMSE | | | Standard deviation | | | Correlation coefficient | | |
|---|---|---|---|---|---|---|---|---|---|
| | COSMO-CLM | WRF | MÉRA | COSMO-CLM | WRF | MÉRA | COSMO-CLM | WRF | MÉRA |
| Belmullet | 2.752 | 2.93 | 3.945 | 14.774 | 16.038 | 14.69 | 0.983 | 0.985 | 0.974 |
| Casement | 3.111 | 3.115 | 5.205 | 23.031 | 23.353 | 23.263 | 0.991 | 0.991 | 0.983 |
| Cork Airport | 3.423 | 2.858 | 4.617 | 17.843 | 18.705 | 18.649 | 0.988 | 0.989 | 0.981 |
| Dublin Airport | 3.317 | 2.944 | 4.868 | 20.245 | 20.582 | 21.309 | 0.990 | 0.992 | 0.985 |
| Malin Head | 2.776 | 2.542 | 4.341 | 14.558 | 15.694 | 14.878 | 0.986 | 0.987 | 0.976 |
| Mullingar | 2.853 | 2.664 | 4.272 | 17.956 | 18.176 | 18.155 | 0.990 | 0.991 | 0.985 |
| Shannon Airport | 3.569 | 3.528 | 4.905 | 20.692 | 21.767 | 21.192 | 0.987 | 0.987 | 0.981 |
| Valentia | 2.896 | 2.493 | 3.754 | 13.121 | 14.209 | 13.426 | 0.981 | 0.985 | 0.976 |
| All | 3.149 | 2.886 | 4.470 | 16.864 | 17.671 | 17.297 | 0.985 | 0.987 | 0.977 |

**The best and worst performers are colour coded green and red, respectively.**

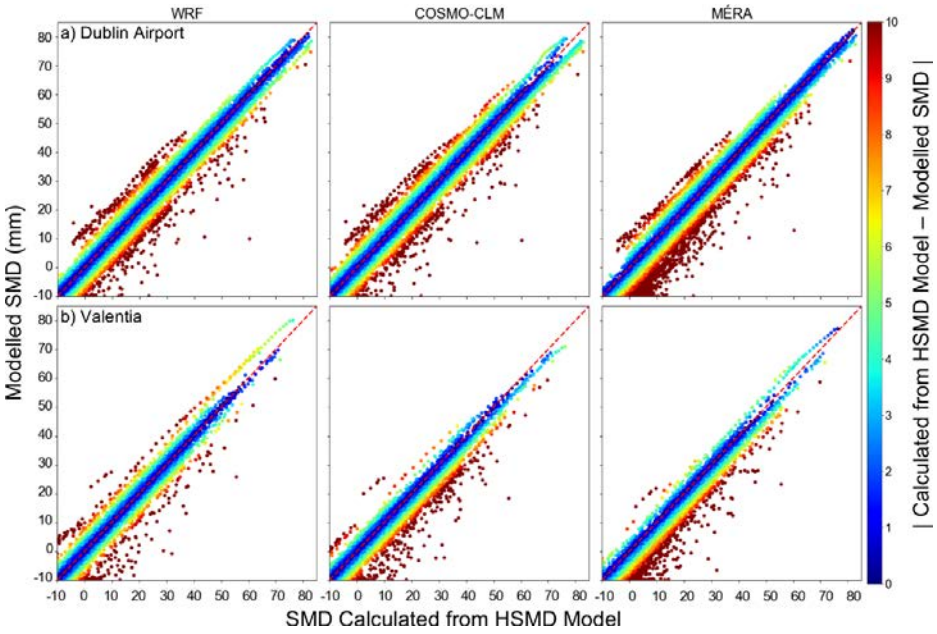


**Figure 4.24. Scatter plots of daily SMD values for poorly drained soils at Dublin Airport and Valentia Observatory for all models (1981–2016).**

Figure 4.25 highlights the negative bias of monthly MÉRA SMD values, with the largest underestimations noted for the winter months. Countrywide weighted averages for monthly and daily values are shown in Table 4.16, with errors in the MÉRA model consistently higher than those in the WRF and COSMO-CLM models. Despite this, as the MÉRA model is the best performer across all other drainage classes and

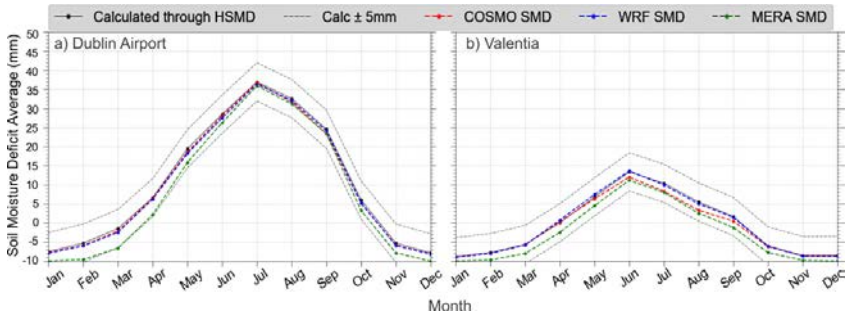


**Figure 4.25. Average monthly SMD means for poorly drained soils at Dublin Airport and Valentia Observatory (1981–2016).**

**Table 4.16 RMSEs of monthly average SMD (poorly drained) and daily values for each month (1981–2016) using an overall weighted average across 22 stations**

| Model | Jan | Feb | Mar | Apr | May | Jun | Jul | Aug | Sep | Oct | Nov | Dec |
|---|---|---|---|---|---|---|---|---|---|---|---|---|
| **Monthly** | | | | | | | | | | | | |
| COSMO-CLM | 0.577 | 0.713 | 1.001 | 1.731 | 2.599 | 3.561 | 3.468 | 3.574 | 3.159 | 1.529 | 0.454 | 0.383 |
| WRF | 0.635 | 0.765 | 0.957 | 1.616 | 2.343 | 3.15 | 2.995 | 2.91 | 2.586 | 1.381 | 0.558 | 0.486 |
| MÉRA | 2.017 | 3.318 | 4.28 | 4.557 | 4.204 | 3.92 | 3.902 | 3.904 | 3.865 | 3.54 | 2.083 | 2.012 |
| **Daily** | | | | | | | | | | | | |
| COSMO-CLM | 0.965 | 1.262 | 1.857 | 2.683 | 3.552 | 4.661 | 4.498 | 4.674 | 4.174 | 2.522 | 1.054 | 0.937 |
| WRF | 1.018 | 1.275 | 1.766 | 2.516 | 3.293 | 4.237 | 4.126 | 4.087 | 3.648 | 2.379 | 1.125 | 1.029 |
| MÉRA | 2.601 | 4.211 | 5.256 | 5.18 | 4.901 | 4.803 | 4.941 | 4.861 | 4.795 | 4.554 | 2.816 | 2.88 |

**The best and worst performers are colour coded green and red, respectively.**

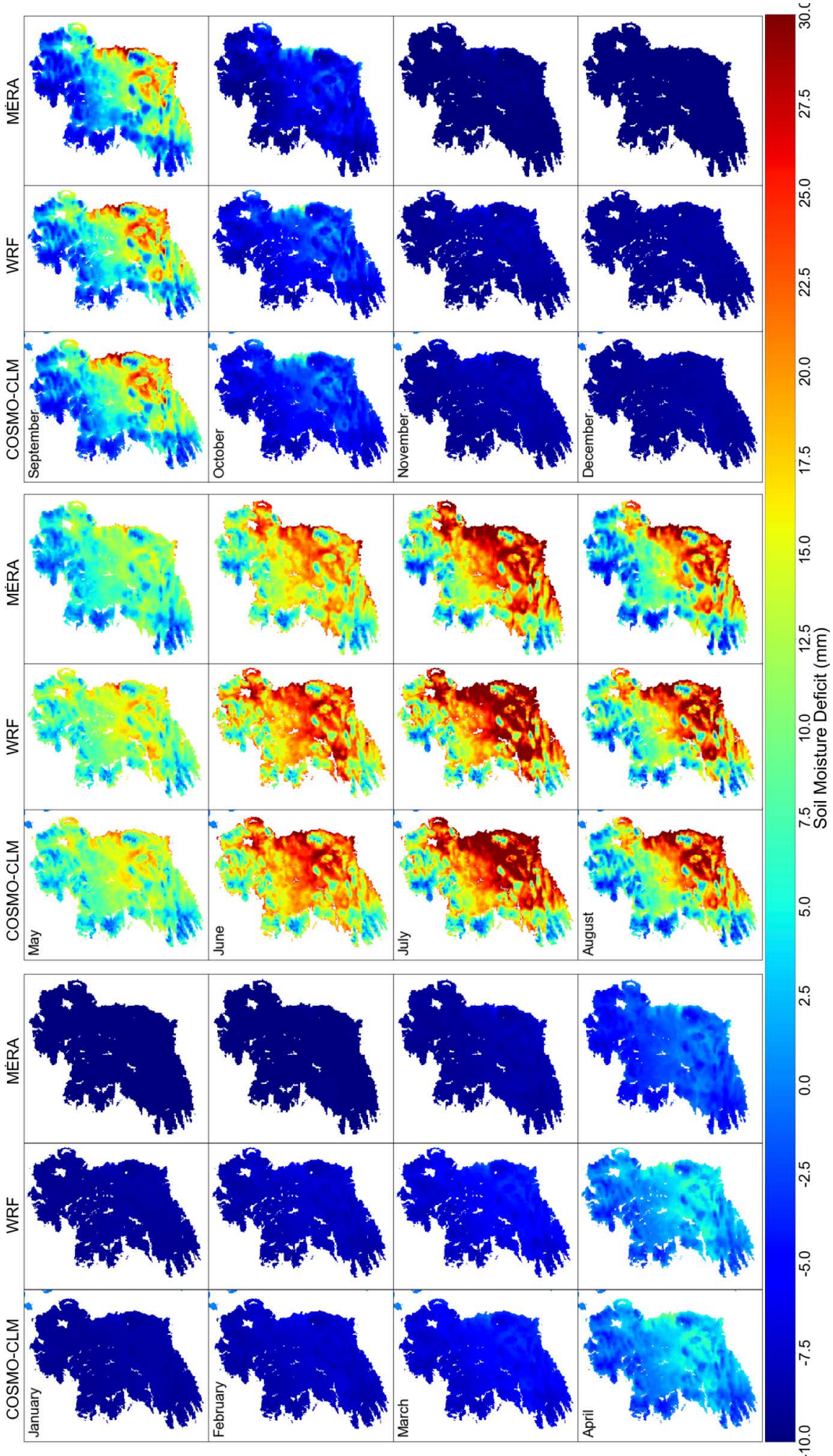


**Figure 4.26. Average monthly means of SMD for poorly drained soils using the COSMO-CLM, WRF and MÉRA models (1981–2016).**

demonstrates the highest skill in the representation of $ET_0$ and $ET_a$, the MÉRA dataset should still be considered as the definitive SMD dataset for Ireland. Figure 4.26 shows comparisons of monthly means of poorly drained SMDs across the whole country.

As discussed throughout this section, in contrast to well-drained and moderately drained soils, the MÉRA model has not performed as well for poorly drained soils. This is highlighted further in Figure 4.27, which shows daily SMDs for the three drainage classes analysed at Dublin Airport. The bottom right window of Figure 4.27 shows a greater proportion of underestimated values for the MÉRA model compared with the COSMO-CLM and WRF models. These errors should be taken into account when utilising the MÉRA poorly drained soils dataset, and in particular the indicative SMD dataset.

### *4.3.4 Excessively and imperfectly drained SMD*

Similarly to $ET_a$, excessively and imperfectly drained SMDs calculated from observed meteorological values are not currently available and it is therefore not possible to validate the models. Excessively drained soils have a SMD limit of 50 mm and are confined to a small area around Wexford. Imperfectly drained soils have a maximum drainage of 3 mm and are confined to areas in Wicklow, Laois and Westmeath. Figures 4.28 and 4.29 show annual average SMD maps for excessively and imperfectly drained soils, respectively.

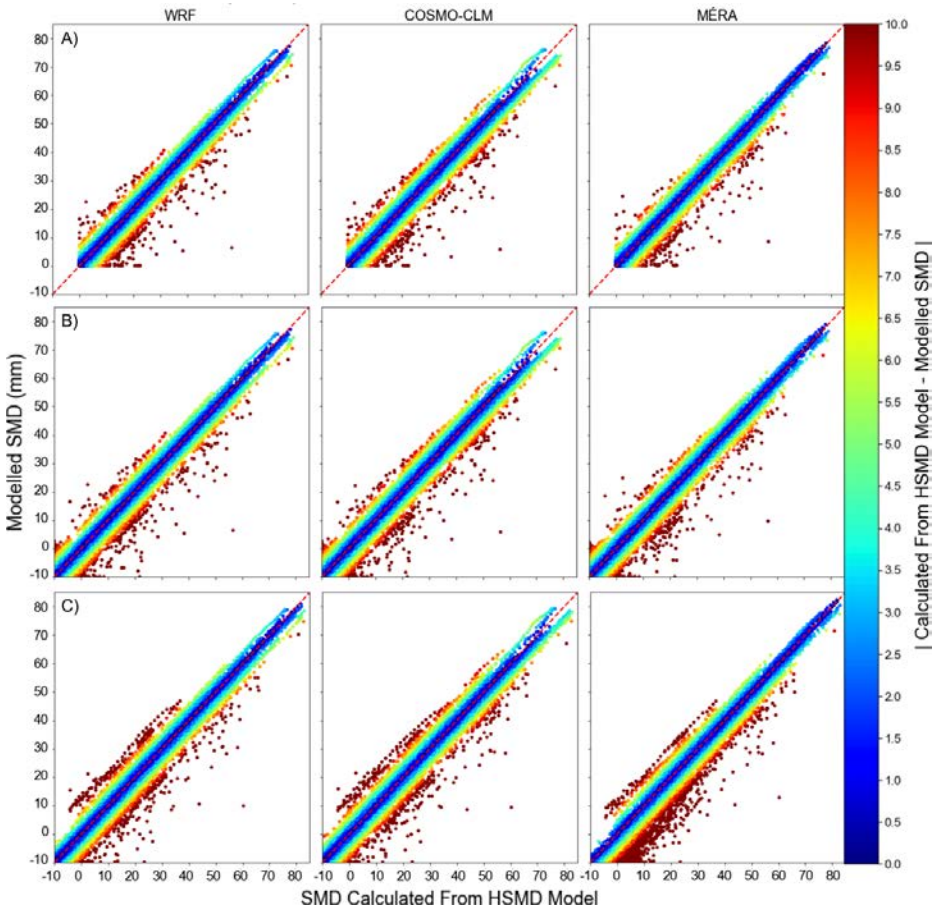


**Figure 4.27. Comparison of daily SMDs for (A) well-drained, (B) moderately drained and (C) poorly drained soils for Dublin Airport (1981–2016).**

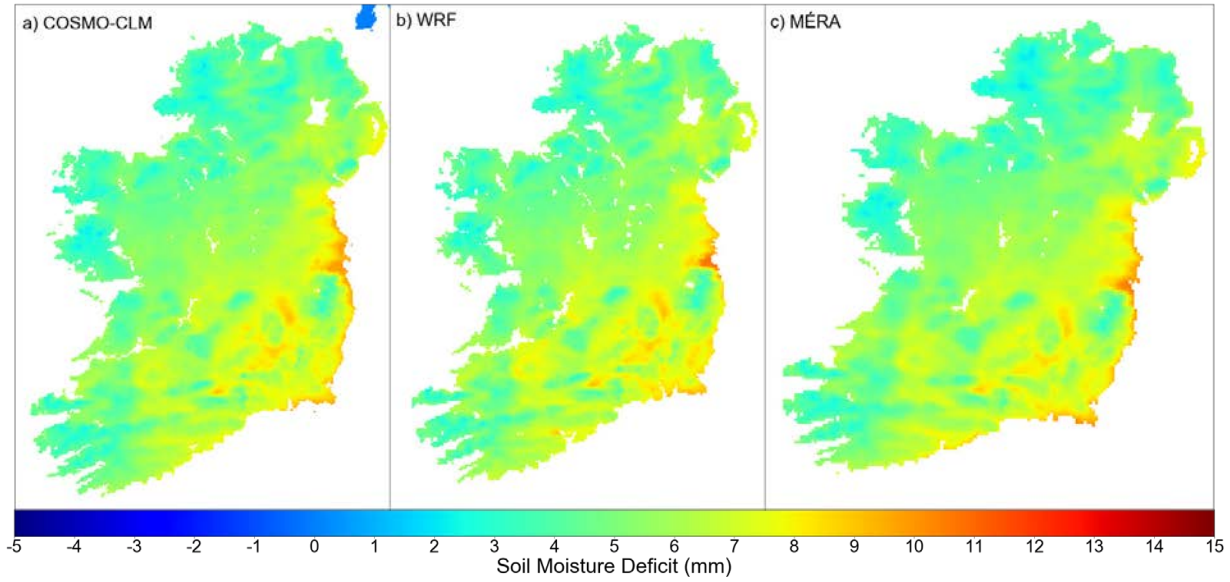


**Figure 4.28. Average annual mean SMD maps for excessively drained soils for the COSMO-CLM, WRF and MÉRA models (1981–2016).**

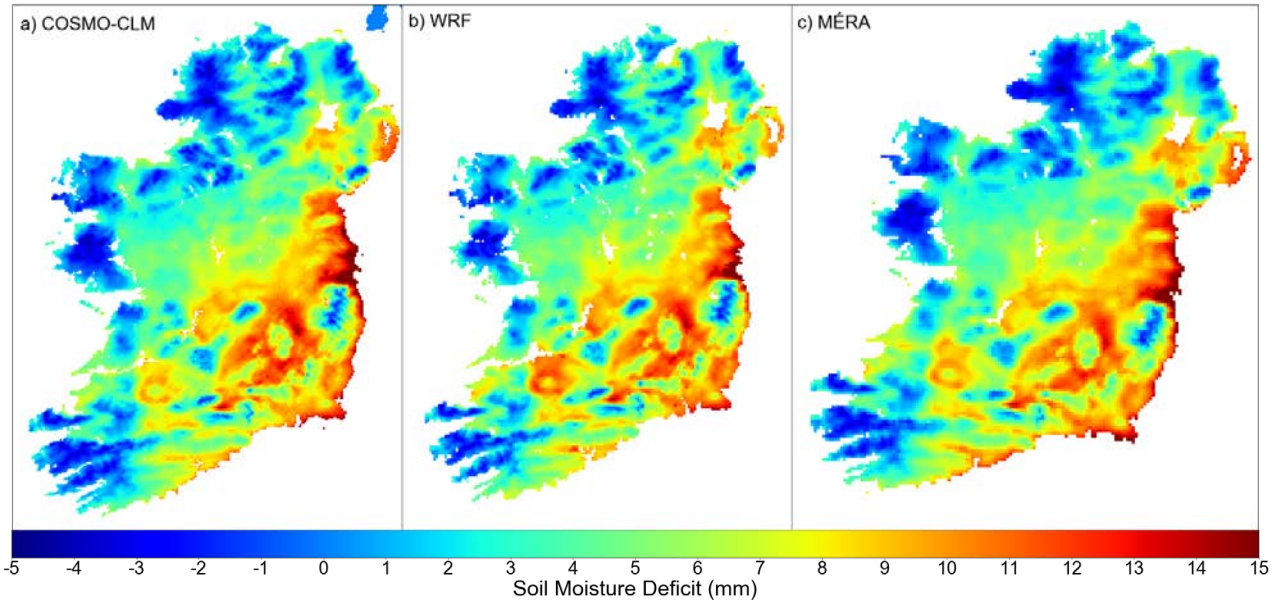


**Figure 4.29. Average annual mean SMD maps for imperfectly drained soils for the COSMO-CLM, WRF and MÉRA models (1981–2016).**

### *4.3.5. Indicative SMD maps*

As with $ET_a$, SMD datasets were derived using the Teagasc Indicative Soil Drainage Maps. Knowledge of the soil drainage class at the location of interest is required by the end user prior to utilising these datasets. Figure 4.30 shows indicative SMD maps for all drainage classes for each month.

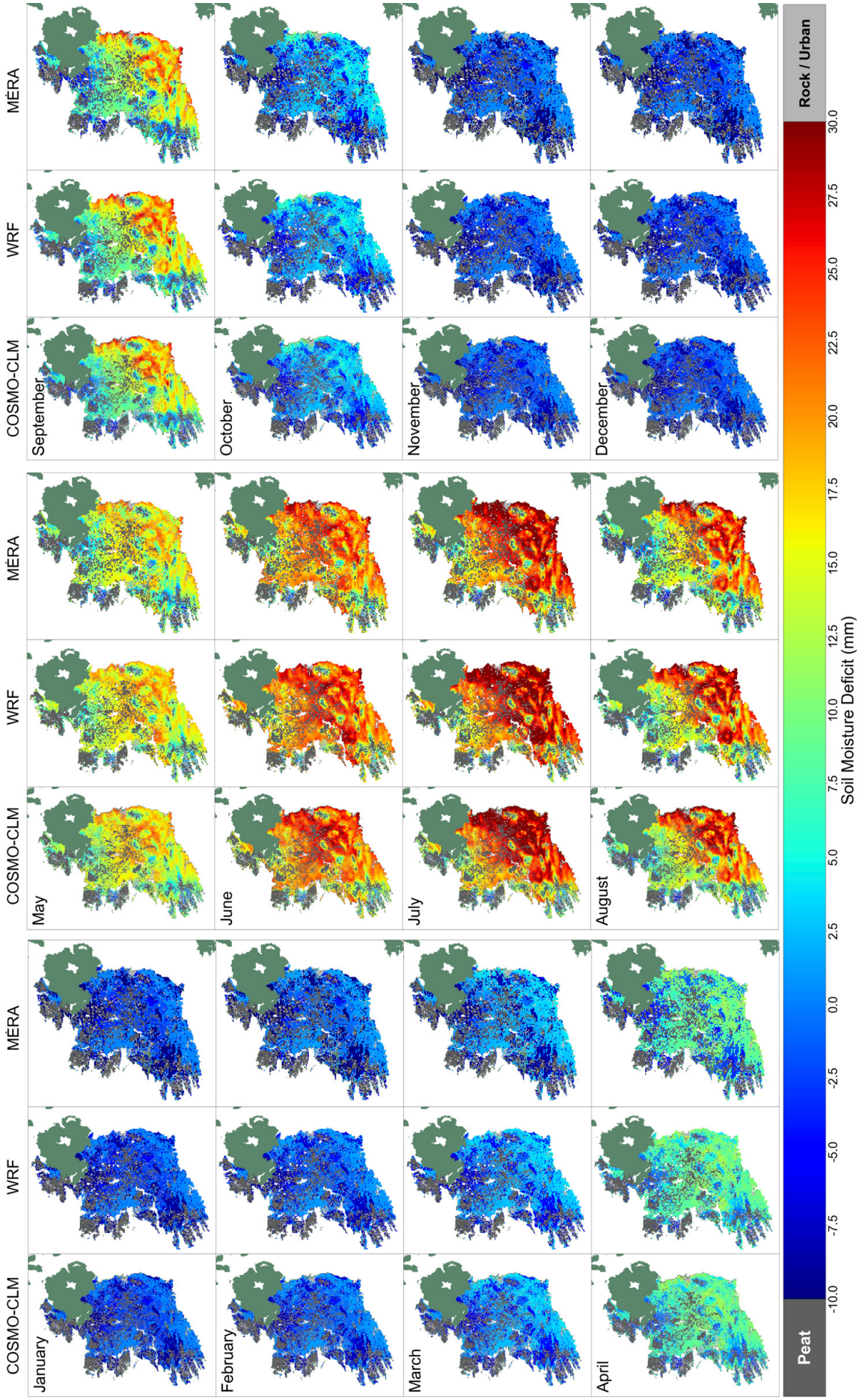


**Figure 4.30. Mean monthly SMD incorporating the Teagasc National Soil Map of soil drainage classes using the WRF, COSMO-CLM and MÉRA models (1981–2016).**

## 4.4 Standardised Precipitation Index

The SPI has been derived for Ireland using gridded observational datasets of precipitation.

Gridded datasets have been produced for the period 1981–2016 (an example of which is shown in Figure 4.31 for December 2016) at 1-, 2-, 3-, 6-, 12- and 24-month timescales.

Additionally, a script has been written allowing the end user to enter a latitude and longitude of interest and return the SPI values at that location for 1981–2016. An example of the output is provided in Figure 4.32. Additional station plots are presented in Appendix 2. The SPI script is shown in Appendix 3.

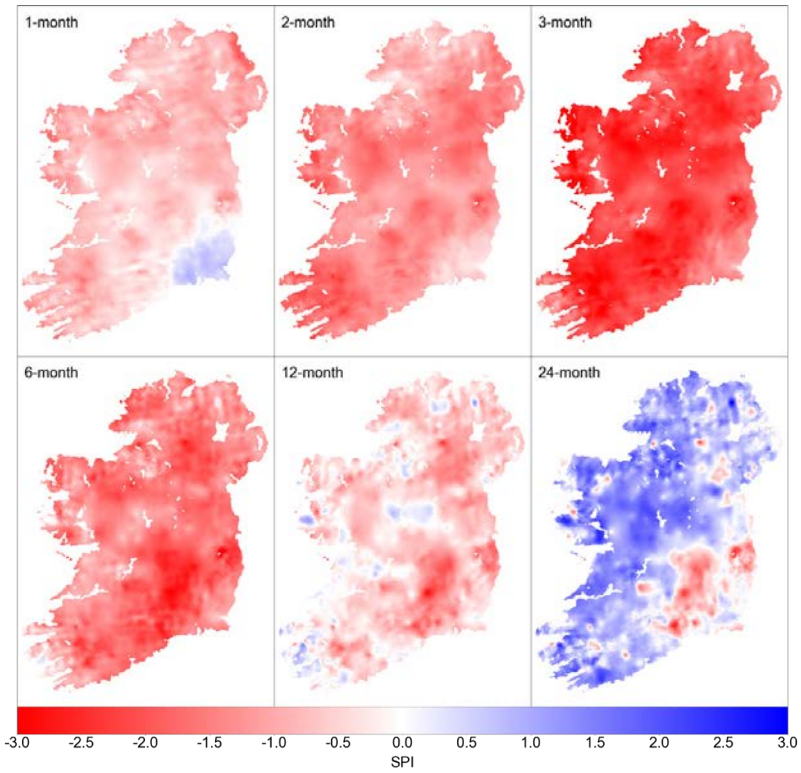


**Figure 4.31. Gridded SPI sample for December 2016 for six different timescales.**

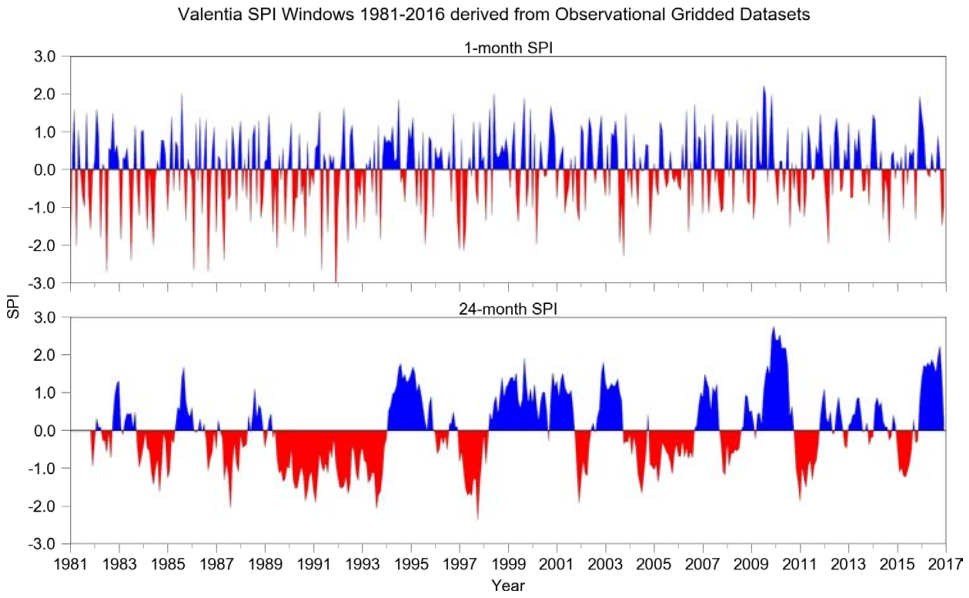


**Figure 4.32. SPI sample focused on Valentia Observatory for 1 month and 24 months.**

## 4.5 *Agroclimatic Atlas of Ireland*

In 1996, Collins and Cummins produced the *Agroclimatic Atlas of Ireland*, which included maps of Irish agricultural climatology and geomorphology. One of the project aims was to facilitate an update to these maps.

Met Éireann provided historical gridded datasets of precipitation and temperature at 1-km resolution from 1981 to 2016. For all agro-climatic variables, the 30-year period 1981–2010 is considered, corresponding to the current climate normals. The large network of temperature and precipitation observations allowed for the development of such high-resolution datasets. The agro-climatic variables that have been derived to facilitate an update of the *Agroclimatic Atlas of Ireland* are as follows:

1. mean annual precipitation;
2. mean monthly precipitation;
3. number of wet days per year (varying thresholds);
4. mean daily temperatures;
5. mean monthly temperatures;
6. maximum/minimum temperatures for specific months;
7. number of frost days;
8. $ET_0$;
9. $ET_a$;
10. SMDs;
11. number of field capacity days (derived from the MÉRA dataset);
12. growing season length and start and end dates;
13. SPI (varying thresholds).

Unless stated otherwise, all datasets were derived using the Met Éireann observed gridded rainfall and temperature datasets with 1-km grid spacings. For more detail and maps of the gridded datasets above, see Appendix 2.

# 5 Conclusions and Recommendations

High-resolution gridded datasets of $ET_0$, $ET_a$ and SMDs have been produced using inputs from three RCMs. $ET_0$ was calculated using RCM data as input to the FAO Penman–Monteith equation, in line with international best practice and the current $ET_0$ calculation method used by Met Éireann. The datasets were validated against Met Éireann synoptic station measurements and outputs of a SMD model at 22 locations across the country. Of the three RCM datasets analysed, COSMO-CLM5, WRF v3.7.1 and MÉRA, the MÉRA model has been shown to be the best performer across most categories. The advantage of the MÉRA model can largely be attributed to the inclusion of data assimilation during model simulation. It is recommended that the reference gridded national datasets for $ET_0$, $ET_a$ and SMD are those derived from the MÉRA dataset.

However, despite the WRF and COSMO-CLM models not performing as well as the MÉRA model, both datasets complement the MÉRA model well in estimating the hydro-climate variables and have the advantage of higher resolution (2 km and 1.5 km, respectively) than the MÉRA model (2.5 km). This advantage was highlighted when validating SMDs for poorly drained soils, with the MÉRA model underestimating SMDs for the winter months, resulting in higher errors. For climate studies and academic purposes, the WRF dataset is recommended as the next best option, having the next lowest errors and correlation coefficients. However, for a definitive dataset for each variable and to avoid internal inconsistencies, particularly with the combined maps and datasets, it is recommended that the MÉRA dataset should be used.

The research also facilitated an update of the *Agroclimatic Atlas of Ireland*, by preparing a number of additional datasets using Met Éireann gridded observational datasets of temperature and precipitation. The derived agro-climate datasets include the number of wet days at different thresholds (1, 5, 10, 15, 20, 30 mm), the number of frost days, growing season lengths and the SPI at varying time intervals.

The research described in this report is based solely on calculated values for evapotranspiration and does not include validation against direct observations. The lack of adequate observational infrastructure for evapotranspiration and soil moisture conditions has been recognised as a significant limitation and source of uncertainty in hydro-meteorological studies in Ireland. Developing such infrastructure would be of great benefit to future hydro-climate research in Ireland, as well as providing baseline data for the future assessment and development of the methodologies and datasets described in this report.

# References


Abatzoglou, J.T., 2013. Development of gridded surface meteorological data for ecological applications and modelling. *International Journal of Climatology* 33: 121–131.

Allen, R.G., Pereira, L.S., Raes, D. and Smith, M., 1998. *Crop Evapotranspiration. Guidelines for Computing Crop Water Requirements*. FAO irrigation and drainage paper 56. Food and Agriculture Organization of the United Nations, Rome.

Analitis, A., Katsouyanni, K., Biggeri, A., Baccini, M., Forsberg, B., Bisanti, L., Kirchmayer, U., Ballester, F., Cadum, E., Goodman, P.G. and Hojs, A., 2008. Effects of cold weather on mortality: results from 15 European cities within the PHEWE project. *American Journal of Epidemiology* 168: 1397–1408.

Aslyng, H.C., 1965. Evaporation, evapotranspiration and water balance investigations at Copenhagen 1955–64. *Acta Agriculturae Scandinavica* XV: 284–300.

Australia Bureau of Meteorology and Wang, Q.J., 2001. *Climatic Atlas of Australia: Evapotranspiration*. Bureau of Meteorology, Melbourne.

Bieniek, P.A., Bhatt, U.S., Walsh, J.E., Rupp, T.S., Zhang, J., Krieger, J.R. and Lader, R., 2016. Dynamical downscaling of ERA-interim temperature and precipitation for Alaska. *Journal of Applied Meteorology and Climatology* 55: 635–654.

Blaney, H.F. and Criddle, W.D., 1950. *Determining Water Requirements in Irrigated Areas from Climatological and Irrigation Data*. Soil Conservation Service technical paper 96. Soil Conservation Service. US Department of Agriculture, Washington, DC.

Bollmeyer, C., Keller, J.D., Ohlwein, C., Wahl, S., Crewell, S., Friederichs, P., Hense, A., Keune, J., Kneifel, S., Pscheidt, I. and Redl, S., 2015. Towards a high-resolution regional reanalysis for the European CORDEX domain. *Quarterly Journal of the Royal Meteorological Society* 141: 1–15.

Bouwer, L.M., 2011. Have disaster losses increased due to anthropogenic climate change? *Bulletin of the American Meteorological Society* 92: 39–46.

Brereton, A.J. and Keane, T., 1982. The effect of water on grassland productivity in Ireland. *Irish Journal of Agricultural Research* 21: 227–248.

Burke, W., 1962. Calculated potential evapotranspiration and soil moisture deficits for North County Dublin (1950–1961). *Irish Journal of Agricultural Research* 1: 329–333.

Burman, R. and Pochop, L.O., 1994. *Evaporation, Evapotranspiration and Climatic Data*. Elsevier, Amsterdam.

Bussay, A., Szinell, C. and Szentimery, T., 1999. *Investigation and Measurements of Droughts in Hungary*. Hungarian Meteorological Service, Budapest.

Carlson, T.N., Capehart, W.J. and Gillies, R.R., 1995. A new look at the simplified method for remote sensing of daily evapotranspiration. *Remote Sensing of Environment* 54: 161–167.

CFRAM (Catchment Flood Risk Assessment and Management), 2012. *The National Preliminary Flood Risk Assessment (PFRA). Overview Report*. Office of Public Works, Trim, Ireland.

Chen, D., Gao, G., Xu, C.Y., Guo, J. and Ren, G., 2005. Comparison of the Thornthwaite method and pan data with the standard Penman–Monteith estimates of reference evapotranspiration in China. *Climate Research* 28: 123–132.

Chiew, F., Wang, Q.J., McConachy, F., James, R., Wright, W. and deHoedt, G., 2002. Evapotranspiration maps for Australia. Hydrology and Water Resources Symposium, Melbourne, 20–23 May 2002, p. 167.

Collins, J.F. and Cummins, T., 1996. *Agroclimatic Atlas of Ireland*. Working Group on Applied Meteorology. University College Dublin, Dublin.

Creamer, R.E., Simo, I., O'Sullivan, L., Reidy, B., Schulte, R.P.O. and Fealy, R.M., 2016. *Irish Soil Information System: Soil Property Maps*. Environmental Protection Agency, Johnstown Castle, Ireland.

Dee, D.P., Uppala, S.M., Simmons, A.J., Berrisford, P., Poli, P., Kobayashi, S., Andrae, U., Balmaseda, M.A., Balsamo, G., Bauer, P. and Bechtold, P., 2011. The ERA-Interim reanalysis: configuration and performance of the data assimilation system. *Quarterly Journal of the Royal Meteorological Society* 137: 553–597.

Dee, D.P., Balmaseda, M., Balsamo, G., Engelen, R., Simmons, A.J. and Thépaut, J.N., 2014. Toward a consistent reanalysis of the climate system. *Bulletin of the American Meteorological Society* 95: 1235–1248.

Di Luca, A., de Elía, R. and Laprise, R., 2012. Potential for added value in precipitation simulated by high-resolution nested regional climate models and observations. *Climate Dynamics* 38: 1229–1247.

Di Luca, A., Argüeso, D., Evans, J.P., de Elía, R. and Laprise, R. 2016. Quantifying the overall added value of dynamical downscaling and the contribution from different spatial scales. *Journal of Geophysical Research Atmospheres* 121: 1575–1590.

D'Ippoliti, D., Michelozzi, P., Marino, C., De'Donato, F., Menne, B., Katsouyanni, K., Kirchmayer, U., Analitis, A., Medina-Ramón, M., Paldy, A. and Atkinson, R., 2010. The impact of heat waves on mortality in 9 European cities: results from the EuroHEAT project. *Environmental Health* 9: 37.

Doorenbos, J. and Pruitt, W.O., 1977. *Crop Water Requirements*. FAO irrigation and drainage paper No. 24. Food and Agriculture Organization of the United Nations, Rome.

Duethmann, D., Zimmer, J., Gafurov, A., Güntner, A., Kriegel, D., Merz, B. and Vorogushyn, S., 2013. Evaluation of areal precipitation estimates based on downscaled reanalysis and station data by hydrological modelling. *Hydrology and Earth System Sciences* 17: 2415–2434.

Edwards, D.C., 1997. *Characteristics of 20th Century Drought in the United States at Multiple Time Scales*. No. AFIT-97–051. Air Force Institute of Technology, Wright-Patterson Air Force Base, OH.

Elhag, M., Psilovikos, A., Manakos, I. and Perakis, K., 2011. Application of the SEBS water balance model in estimating daily evapotranspiration and evaporative fraction from remote sensing data over the Nile Delta. *Water Resources Management* 25: 2731–2742.

Feser, F., 2006. Enhanced detectability of added value in limited-area model results separated into different spatial scales. *Monthly Weather Review* 134: 2180–2190.

Feser, F. and Barcikowska, M., 2012. The influence of spectral nudging on typhoon formation in regional climate models. *Environmental Research Letters* 7: 014024.

Feser, F., Rockel, B., von Storch, H., Winterfeldt, J. and Zahn, M., 2011. Regional climate models add value to global model data: a review and selected examples. *Bulletin of the American Meteorological Society* 92: 1181–1192.

Flato, G., Marotzke, J., Abiodun, B., Braconnot, P., Chou, S.C., Collins, W., Cox, P., Driouech, F., Emori, S., Eyring, V., Forest, C., Gleckler, P., Guilyardi, E., Jakob, C., Kattsov, V., Reason, C. and Rummukainen, M., 2013. Evaluation of climate models. In Stocker, T.F., Qin, D., Plattner, G.-K., Tignor, M., Allen, S.K., Boschung, J., Nauels, A., Xia, Y., Bex, V. and Midgley, P.M. (eds), *Climate Change 2013: The Physical Science Basis.* Contribution of Working Group I to the Fifth Assessment Report of the Intergovernmental Panel on Climate Change. Cambridge University Press, Cambridge, pp. 741–883.

Gallagher, S., Tiron, R. and Dias, F., 2014. A long-term nearshore wave hindcast for Ireland: Atlantic and Irish Sea coasts (1979–2012). *Ocean Dynamics* 64: 1163–1180.

Gallagher, S., Tiron, R., Whelan, E., Gleeson, E., Dias, F. and McGrath, R., 2016. The nearshore wind and wave energy potential of Ireland: a high resolution assessment of availability and accessibility. *Renewable Energy* 88: 494–516.

Gao, Y., Long, D. and Li, Z.L., 2008. Estimation of daily actual evapotranspiration from remotely sensed data under complex terrain over the upper Chao river basin in North China. *International Journal of Remote Sensing* 29: 3295–3315.

Gardiner, M.J. and Radford, T., 1980. Soil associations of Ireland and their land use potential: explanatory bulletin to soil map of Ireland 1980. *Soil Survey Bulletin (An Foras Taluntais)* no. 36.

Gleeson, E., Whelan, E. and Hanley, J., 2017. Met Éireann high resolution reanalysis for Ireland. *Advances in Science and Research* 14: 49–61.

Glenn, E.P., Doody, T.M., Guerschman, J.P., Huete, A.R., King, E.A., McVicar, T.R., Van Dijk, A.I., Van Niel, T.G., Yebra, M. and Zhang, Y., 2011a. Actual evapotranspiration estimation by ground and remote sensing methods: the Australian experience. *Hydrological Processes* 25: 4103–4116.

Glenn, E.P., Neale, C.M., Hunsaker, D.J. and Nagler, P.L., 2011b. Vegetation index-based crop coefficients to estimate evapotranspiration by remote sensing in agricultural and natural ecosystems. *Hydrological Processes* 25: 4050–4062.

Grindley, J., 1969. *The Calculation of Actual Evaporation and Soil Moisture Deficit over Specified Catchment Areas*. Hydrological Memoir no. 38. Meteorological Office, Hydrological Services, Bracknell.

Hallett, S.H., Jones, R.J. and Keay, C.A., 1996. Environmental information systems developments for planning sustainable land use. *International Journal of Geographical Information Science* 10: 47–64.

Hallett, S., Carvalho, J. and Fealy, R.M, 2014. *Irish Soil Information System: User Guide for Systems Management*. Final Technical Report 17. Environmental Protection Agency, Johnstown Castle, Ireland.

Hargreaves, G.H. and Allen, R.G., 2003. History and evaluation of Hargreaves evapotranspiration equation. *Journal of Irrigation and Drainage Engineering* 129: 53–63.

Hargreaves, G.H. and Samani, Z.A., 1985. Reference crop evapotranspiration from temperature. *Applied Engineering in Agriculture* 1: 96–99.

Hawkins, E., Osborne, T.M., Ho, C.K. and Challinor, A.J., 2013. Calibration and bias correction of climate projections for crop modelling: an idealised case study over Europe. *Agricultural and Forest Meteorology* 170: 19–31.

Hay, L.E., Clark, M.P., Wilby, R.L., Gutowski Jr, W.J., Leavesley, G.H., Pan, Z., Arritt, R.W. and Takle, E.S., 2002. Use of regional climate model output for hydrologic simulations. *Journal of Hydrometeorology* 3: 571–590.

Holman, I.P., Rounsevell, M.D.A., Shackley, S., Harrison, P.A., Nicholls, R.J., Berry, P.M. and Audsley, E., 2005. A regional, multi-sectoral and integrated assessment of the impacts of climate and socio-economic change in the UK. *Climatic Change* 71: 9–41.

Hough, M.N. and Jones, R.J.A., 1997. The United Kingdom Meteorological Office rainfall and evaporation calculation system: MORECS version 2.0 – an overview. *Hydrology and Earth System Sciences Discussions* 1: 227–239.

Huisman, J.A., Hubbard, S.S., Redman, J.D. and Annan, A.P., 2003. Measuring soil water content with ground penetrating radar. *Vadose Zone Journal* 2: 476–491.

IPCC (Intergovernmental Panel on Climate Change), 2014. *Climate Change 2014 – Impacts, Adaptation and Vulnerability: Regional Aspects*. Cambridge University Press, Cambridge.

Jalee, L.A. and Farawn, M.A., 2014. Developing Rainfall intensity–duration–frequency relationship for Basrah City. *Kufa Journal of Engineering* 5: 105–112.

Jones, P.G. and Thornton, P.K., 2013. Generating downscaled weather data from a suite of climate models for agricultural modelling applications. *Agricultural Systems* 114: 1–5.

Kanada, S., Nakano, M., Hayashi, S., Kato, T., Nakamura, M., Kurihara, K. and Kitoh, A., 2008. Reproducibility of maximum daily precipitation amount over Japan by a high-resolution non-hydrostatic model. *Sola* 4: 105–108.

Karavitis, C.A., Alexandris, S., Tsesmelis, D.E. and Athanasopoulos, G., 2011. Application of the standardized precipitation index (SPI) in Greece. *Water* 3: 787–805.

Kendon, E.J., Roberts, N.M., Senior, C.A. and Roberts, M.J., 2012. Realism of rainfall in a very high-resolution regional climate model. *Journal of Climate* 25: 5791–5806.

Kendon, E.J., Roberts, N.M., Fowler, H.J., Roberts, M.J., Chan, S.C. and Senior, C.A., 2014. Heavier summer downpours with climate change revealed by weather forecast resolution model. *Nature Climate Change* 4: 570–576.

Keshta, N. and Elshorbagy, A., 2011. Utilizing North American regional reanalysis for modelling soil moisture and evapotranspiration in reconstructed watersheds. *Physics and Chemistry of the Earth, Parts A/B/C* 36: 31–41.

Kite, G.W. and Droogers, P., 2000. Comparing evapotranspiration estimates from satellites, hydrological models and field data. *Journal of Hydrology* 229: 3–18.

Kunkel, K.E., Pielke Jr, R.A. and Changnon, S.A., 1999. Temporal fluctuations in weather and climate extremes that cause economic and human health impacts: a review. *Bulletin of the American Meteorological Society* 80: 1077–1098.

Lana, X., Serra, C. and Burgueño, A., 2001. Patterns of monthly rainfall shortage and excess in terms of the standardized precipitation index for Catalonia (NE Spain). *International Journal of Climatology* 21: 1669–1691.

Lewis, G.L. and Holden, N.M., 2012. *The Modification of Soil Moisture Deficit Calculation Using Topographic Wetness Index to Account for the Effect of Slope and Landscape Position*. Dallas, TX, 29 July–1 August, 2012, p. 1. American Society of Agricultural and Biological Engineers, St Joseph, MI.

Liew, S.C., Raghavan, S.V. and Liong, S.Y., 2014. Development of intensity–duration–frequency curves at ungauged sites: risk management under changing climate. *Geoscience Letters* 1: 1–12.

Lockwood, J.G., Jones, C.A. and Smith, R.T., 1989. The estimation of soil moisture deficits using meteorological models at an upland moorland site in northern England. *Agricultural and Forest Meteorology* 46: 41–63.

Lucas-Picher, P., Wulff-Nielsen, M., Christensen, J,. Adalgeirsdottir, G., Mottram, R. and Simonsen, S., 2012. Very high resolution regional climate model simulations over Greenland: identifying added value. *Journal of Geophysical Research* 117: D02108.

McGrath, R. and Nolan, P., 2016. Regional climate modelling: impact of horizontal grid resolution on precipitation estimates over Ireland. *EGU General Assembly Conference Abstracts* 18: 15560.

McKee, T.B., Doesken, N.J. and Kleist, J., 1993. The relationship of drought frequency and duration to time scales. *Proceedings of the 8th Conference on Applied Climatology* 17: 179–183. American Meteorological Society, Boston, MA.

Mackenzie, N., Grainger, P., Cooper, J.D., Roberts, J. and Evans, B.M., 1991. *Assessment of Recharge to Groundwater Measured by the Soil Physics Method and the Grindley Method at Bicton College in East Devon*. University of Exeter, Earth Resources Centre, NRA South West Region, Exeter.

Mahringer, W., 1970. Verdunstungsstudien am Neusiedler See. *Theoretical and Applied Climatology* 18: 1–20.

Makkink, G.F., 1957. Testing the Penman formula by means of lysimeters. *Journal of the Institution of Water Engineers and Scientists* 11: 277–288.

Mecklenburg, S., Drusch, M., Kerr, Y.H., Font, J., Martin-Neira, M., Delwart, S., Buenadicha, G., Reul, N., Daganzo-Eusebio, E., Oliva, R. and Crapolicchio, R., 2012. ESA's soil moisture and ocean salinity mission: mission performance and operations. *IEEE Transactions on Geoscience and Remote Sensing* 50: 1354–1366.

Merz, B., Aerts, J.C.J.H., Arnbjerg-Nielsen, K., Baldi, M., Becker, A., Bichet, A., Blöschl, G., Bouwer, L.M., Brauer, A., Cioffi, F. and Delgado, J.M., 2014. Floods and climate: emerging perspectives for flood risk assessment and management. *Natural Hazards and Earth System Sciences* 14: 1921.

Mills, G., 2000. Modelling the water budget of Ireland – evapotranspiration and soil moisture. *Irish Geography* 33: 99–116.

Monteith, J.L. and Unsworth, M., 1990. *Principles of Environmental Physics*. Arnold, London.

Morton, F.I., 1983. Operational estimates of areal evapotranspiration and their significance to the science and practice of hydrology. *Journal of Hydrology* 66: 1–76.

Mu, Q., Zhao, M. and Running, S.W., 2013. *MODIS Global Terrestrial Evapotranspiration (ET) Product (NASA MOD16A2/3)*. Algorithm Theoretical Basis Document, Collection 5. NASA Headquarters, Washington, DC.

Narasimhan, B. and Srinivasan, R., 2005. Development and evaluation of Soil Moisture Deficit Index (SMDI) and Evapotranspiration Deficit Index (ETDI) for agricultural drought monitoring. *Agricultural and Forest Meteorology* 133: 69–88.

NIWA (National Institute of Water and Atmospheric Research), 2017. Virtual Climate Station Data and Products. Available online: https://www.niwa.co.nz/climate/our-services/virtual-climate-stations (accessed 17 December 2017).

Olesen, J.E., Carter, T.R., Diaz-Ambrona, C.H., Fronzek, S., Heidmann, T., Hickler, T., Holt, T., Minguez, M.I., Morales, P., Palutikof, J.P. and Quemada, M., 2007. Uncertainties in projected impacts of climate change on European agriculture and terrestrial ecosystems based on scenarios from regional climate models. *Climatic Change* 81: 123–143.

Palmer, W.C., 1965. *Meteorological Drought*. Volume 30. US Department of Commerce, Weather Bureau, Washington, DC.

Penman, H.L., 1948. Natural evaporation from open water, bare soil and grass. *Proceedings of the Royal Society of London A: Mathematical, Physical and Engineering Sciences* 193: 120–145.

Penman, H.L., 1963. Vegetation and hydrology. *Soil Science* 96: 357.

Pereira, A.R., Nova, N.A.V., Pereira, A.S. and Barbieri, V., 1995. A model for the class A pan coefficient. *Agricultural and Forest Meteorology* 76: 75–82.

Perry, M. and Hollis, D., 2005. The generation of monthly gridded datasets for a range of climatic variables over the UK. *International Journal of Climatology* 25: 1041–1054.

Priestley, C.H.B. and Taylor, R.J., 1972. On the assessment of surface heat flux and evaporation using large-scale parameters. *Monthly Weather Review* 100: 81–92.

Rácz, C., Nagy, J. and Dobos, A.C., 2013. Comparison of several methods for calculation of reference evapotranspiration. *Acta Silvatica et Lignaria Hungarica* 9: 9–24.

Ragg, J.M. and Proctor, M.E., 1983. *The Soil Survey Information System. Soil Survey of England and Wales: Report for 1982. P1: Rothamsted Reports: Rothamsted Experimental Station for 1982*. Harpenden, pp. 232–236.

Rajeevan, M. and Bhate, J., 2009. A high resolution daily gridded rainfall dataset (1971–2005) for mesoscale meteorological studies. *Current Science* 96: 558–562.

Rauscher, S.A., Coppola, E., Piani, C. and Giorgi, F., 2010. Resolution effects on regional climate model simulations of seasonal precipitation over Europe. *Climate Dynamics* 35: 685–711.

Rockel, B., Will, A. and Hense, A., 2008. The regional climate model COSMO-CLM (CCLM). *Meteorologische Zeitschrift* 17: 347–348.

Saha, S., Moorthi, S., Pan, H.L., Wu, X., Wang, J., Nadiga, S., Tripp, P., Kistler, R., Woollen, J., Behringer, D. and Liu, H., 2010. The NCEP climate forecast system reanalysis. *Bulletin of the American Meteorological Society* 91: 1015–1057.

Sanford, W.E. and Selnick, D.L., 2013. Estimation of evapotranspiration across the conterminous United States using a regression with climate and land-cover data. *Journal of the American Water Resources Association* 49: 217–230.

Schamm, K., Ziese, M., Becker, A., Finger, P., Meyer-Christoffer, A., Schneider, U., Schröder, M. and Stender, P., 2014. Global gridded precipitation over land: a description of the new GPCC First Guess Daily product. *Earth System Science Data* 6: 49–60.

Schulte, R.P.O., Diamond, J., Finkele, K., Holden, N.M. and Brereton, A.J., 2005. Predicting the soil moisture conditions of Irish grasslands. *Irish Journal of Agricultural and Food Research* 44: 95–110.

Schulte, R.P., Simo, I., Creamer, R.E. and Holden, N.M., 2015. A note on the hybrid soil moisture deficit model v2.0. *Irish Journal of Agricultural and Food Research* 54: 126–131.

SEAI (Sustainable Energy Authority of Ireland), 2016. *Wind Energy*. Available online: https://www.seai.ie/sustainable-solutions/renewable-energy/wind-energy/ (accessed 15 May 2018).

Seiler, R.A., Hayes, M. and Bressan, L., 2002. Using the standardized precipitation index for flood risk monitoring. *International Journal of Climatology* 22: 1365–1376.

Senay, G.B., Budde, M., Verdin, J.P. and Melesse, A.M., 2007. A coupled remote sensing and simplified surface energy balance approach to estimate actual evapotranspiration from irrigated fields. *Sensors* 7: 979–1000.

Seyyedi, H., Anagnostou, E.N., Beighley, E. and McCollum, J., 2014. Satellite-driven downscaling of global reanalysis precipitation products for hydrological applications. *Hydrology and Earth System Sciences* 18: 5077.

Shkol'nik, I., Meleshko, V., Efimov, S., Stafeeva, E., 2012. Changes in climate extremes on the territory of Siberia by the middle of the 21st century: an ensemble forecast based on the MGO regional climate model. *Russian Meteorology and Hydrol*ogy 37: 71–84.

Silvestrin, P., Berger, M., Kerr, Y. and Font, J., 2001. ESA's second earth explorer opportunity mission: the soil moisture and ocean salinity mission – SMOS. *IEEE Geoscience and Remote Sensing Newsletter* 118: 11–14.

Skamarock, W.C., Klemp, J., Dudhia, J., Gill, D.O., Barker, D., Wang, W. and Powers, J.G., 2008. *A Description of the Advanced Research WRF Version 3*. NCAR/TN–475+STR. National Center for Atmospheric Research, Boulder, CO.

Slater, A.G., 2016. Surface solar radiation in North America: a comparison of observations, reanalyses, satellite, and derived products. *Journal of Hydrometeorology* 17: 401–420.

Soer, G.J.R., 1980. Estimation of regional evapotranspiration and soil moisture conditions using remotely sensed crop surface temperatures. *Remote Sensing of Environment* 9: 27–45.

Stocker, T.F., Qin, D., Plattner, G.K., Tignor, M., Allen, S.K., Boschung, J., Nauels, A., Xia, Y., Bex, V. and Midgley, P.M. (eds), 2013. *Climate Change 2013: The Physical Science Basis*. Contribution of Working Group I to the Fifth Assessment Report of the Intergovernmental Panel on Climate Change. Cambridge University Press, Cambridge.

Szalai, S. and Szinell, C.S., 2000. Comparison of two drought indices for drought monitoring in Hungary – a case study. In Vogt, J.V. and Somma, F. (eds), *Drought and Drought Mitigation in Europe*. Springer, Dordrecht, the Netherlands, pp. 161–166.

Szász, G., 1973. A potenciális párolgás meghatározásának új módszere. [New method for calculating potential evapotranspiration.] *Hidrológiai Közlöny* 10: 435–442.

Tait, A. and Woods, R., 2007. Spatial interpolation of daily potential evapotranspiration for New Zealand using a spline model. *Journal of Hydrometeorology* 8: 430–438.

Tait, A., Henderson, R., Turner, R., Zheng, X.G., 2006. Thin plate smoothing spline interpolation of daily rainfall for New Zealand using a climatological rainfall surface. *International Journal of Climatology* 26: 2097–2115.

Teixeira, A.H.D.C., 2010. Determining regional actual evapotranspiration of irrigated crops and natural vegetation in the São Francisco River Basin (Brazil) using remote sensing and Penman–Monteith equation. *Remote Sensing* 2:1287–1319.

Thompson, N., Barrie, I.A. and Ayles, M., 1981. *The Meteorological Office Rainfall and Evaporation Calculation System: MORECS Meteorological Office*. Met O 8 (Hydrometeorological Services), London.

Thornthwaite, C.W., 1948. An approach toward a rational classification of climate. *Geographical Review* 38: 55–94.

Timmermans, W.J. and Meijerink, A.M.J., 1999. Remotely sensed actual evapotranspiration: implications for groundwater management in Botswana. *International Journal of Applied Earth Observation and Geoinformation* 1: 222–233.

Troen, I. and Petersen, E.L., 1989. *European Wind Atlas*. Risø National Laboratory, Roskilde, Denmark.

Ulaby, F., 1974. Radar measurement of soil moisture content. *IEEE Transactions on Antennas and Propagation* 22: 257–265.

Vautard, R., Gobiet, A., Jacob, D., Belda, M., Colette, A., Déqué, M., Fernández, J., García-Díez, M., Goergen, K., Güttler, I. and Halenka, T., 2013. The simulation of European heat waves from an ensemble of regional climate models within the EURO-CORDEX project. *Climate Dynamics* 41: 2555–2575.

Vicente-Serrano, S.M., Beguería, S. and López-Moreno, J.I., 2010. A multiscalar drought index sensitive to global warming: the standardized precipitation evapotranspiration index. *Journal of Climate* 23: 1696–1718.

Wagner, W., Naeimi, V., Scipal, K., de Jeu, R. and Martínez-Fernández, J., 2007. Soil moisture from operational meteorological satellites. *Hydrogeology Journal* 15: 121–131.

Walsh, S., 2012. *A Summary of Climate Averages for Ireland*. Met Éireann, Dublin.

WAMIS (World AgroMeteorological Information Service), 2012. *Standardised Precipitation Index User Guide*. Available online: http://www.wamis.org/agm/pubs/SPI/WMO_1090_EN.pdf (accessed 10 December 2017).

Westerhoff, R.S., 2015. Using uncertainty of Penman and Penman–Monteith methods in combined satellite and ground-based evapotranspiration estimates. *Remote Sensing of Environment* 169: 102–112.

Whelan, E., Gleeson, E., Gallagher, S. and McGrath, R., 2016. Met Éireann NWP highlights 2015. *ALADIN-HIRLAM Newsletter* 6: 76–78.

Williams, N.H., Misstear, B.D.R., Daly, D. and Lee, M., 2013. Development of a national groundwater recharge map for the Republic of Ireland. *Quarterly Journal of Engineering Geology and Hydrogeology* 46: 493–506.

WMO (World Metereological Organization), 1966. *Measurement and Estimation of Evaporation and Evapotranspiration: WMO – No. 201 Technical Paper 105 (CIMO-Rep.)*. World Meteorological Organization, Geneva.

Wu, W., Hall, C.A., Scatena, F.N. and Quackenbush, L.J., 2006. Spatial modelling of evapotranspiration in the Luquillo experimental forest of Puerto Rico using remotely-sensed data. *Journal of Hydrology* 328: 733–752.

Zotarelli, L., Dukes, M.D., Romero, C.C., Migliaccio, K.W. and Morgan, K.T., 2010. *Step by Step Calculation of the Penman–Monteith Evapotranspiration (FAO-56 Method)*. Institute of Food and Agricultural Sciences, University of Florida, Gainesville, FL.

# Abbreviations

| | |
|---|---|
| **CHESS** | Climate, Hydrological and Ecological research Support System |
| **$ET_0$** | Reference evapotranspiration |
| **$ET_a$** | Actual evapotranspiration |
| **FAO** | Food and Agriculture Organization of the United Nations |
| **HSMD** | Hybrid soil moisture deficit |
| **ICHEC** | Irish Centre for High-End Computing |
| **JULES** | Joint UK Land Environment Simulator |
| **MÉRA** | Met Éireann Re-Analysis |
| **MORECS** | Meteorological Office Rainfall and Evaporation Calculation System |
| **NWP** | Numerical weather prediction |
| **PFRA** | *Preliminary Flood Risk Assessment* |
| **RCM** | Regional climate NWP model |
| **RMSE** | Root mean square error |
| **RS** | Remote sensing |
| **SMD** | Soil moisture deficit |
| **SPEI** | Standardised Precipitation Evapotranspiration Index |
| **SPI** | Standardised Precipitation Index |
| **USGS** | US Geological Survey |
| **WRF** | Weather Research and Forecasting |

# Appendix 1 List of Archived Variables from Each Model

**Table A1.1. List of variables from the COSMO-CLM5 dataset produced by ICHEC researchers**

| Variable | Units | Variable | Units |
|---|---|---|---|
| Surface pressure | Pa | Surface lifted index | K |
| Mean sea level pressure | Pa | Showalter Index | K |
| Surface temperature | K | Surface net downward SW radiation | $W/m^2$ |
| 2-m temperature | K | Averaged surface net downward SW radiation | $W/m^2$ |
| 2-m dew point temperature | K | Direct surface downward SW radiation | $W/m^2$ |
| U-component of 10-m wind | m/s | Averaged direct surface downward SW radiation | $W/m^2$ |
| V-component of 10-m wind | m/s | Averaged surface diffuse downward SW radiation | $W/m^2$ |
| Surface roughness length | m | Averaged surface diffuse upward SW radiation | $W/m^2$ |
| Maximum 10-m wind speed | m/s | Averaged downward LW radiation at the surface | $W/m^2$ |
| Surface specific humidity | kg/kg | Averaged upward LW radiation at the surface | $W/m^2$ |
| 2-m specific humidity | kg/kg | Averaged surface net downward LW radiation | $W/m^2$ |
| 2-m relative humidity | % | Averaged surface photosynthetic active radiation | $W/m^2$ |
| Snow surface temperature | K | Surface albedo | 0–1 |
| Thickness of snow | m | Surface latent heat flux | $W/m^2$ |
| Height of freezing level | m | Surface sensible heat flux | $W/m^2$ |
| Precipitation rate | $kg/m^2/s$ | Surface evaporation | $kg/m^2$ |
| Large-scale rainfall | $kg/m^2$ | Total precipitation amount | $kg/m^2$ |
| Convective rainfall | $kg/m^2$ | Soil temperature (eight levels) | K |
| Large-scale snowfall | $kg/m^2$ | Soil water content (eight levels) | m |
| Convective snowfall | $kg/m^2$ | Daily average 2-m temperature | K |
| Large-scale graupel | $kg/m^2$ | Daily maximum 2-m temperature | K |
| Surface run-off | $kg/m^2$ | Daily minimum 2-m temperature | K |
| Subsurface run-off | $kg/m^2$ | Daily duration of sunshine | s |
| Vertical integrated water vapour | $kg/m^2$ | Daily relative duration of sunshine | s |
| Vertical integrated cloud ice | $kg/m^2$ | Below variables archived at 20, 40, … 200 m: | |
| Vertical integrated cloud water | $kg/m^2$ | U-component of wind | m/s |
| Total cloud cover | 0–1 | V-component of wind | m/s |
| Low cloud cover | 0–1 | Air density | $kg/m^3$ |
| Medium cloud cover | 0–1 | Wind speed | m/s |
| High cloud cover | 0–1 | Cube wind speed | $m^3/s^3$ |
| CAPE 3 km | J/kg | Wind direction | Degrees |

**CAPE, convective available potential energy; LW, long wave; SW, short wave.**

**Table A1.2. List of variables from the WRF dataset (v 3.7.1) produced by ICHEC researchers**

| Variable | Units | Variable | Units |
|---|---|---|---|
| Surface temperature | K | Air density at lowest model level | $kg/m^3$ |
| Surface pressure | Pa | U-component of wind (Earth) at 40, 60, 80, 100, 120 m | m/s |
| Sea level pressure | Pa | V-component of wind (Earth) at 40, 60, 80, 100, 120 m | m/s |
| Sea level pressure | Pa | SW flux downward at surface instant | $W/m^2$ |
| 2-m temperature | °C | SW flux downward at surface accumulated | $W/m^2$ |
| Total cloud fraction | 0–1 | Bucket SW flux downward at surface accumulated | $W/m^2$ |
| Time varying roughness height | m | Friction velocity | m/s |
| Water vapour mixing ratio at 2 m | kg/kg | Liquid path water | $kg/m^2$ |
| Relative humidity at 2 m | % | Ice path water | $kg/m^2$ |
| U-component of wind at 10 m | m/s | Ground heat flux | $W/m^2$ |
| V-component of wind at 10 m | m/s | Physical snow depth | m |
| Maximum 10-m wind speed previous output time | m/s | Water evaporation flux at surface | $kg/m^2$ |
| Total precipitation | mm | Soil temperature, at four levels | K |
| Accumulated snowfall | mm | Soil moisture, at four levels | $m^3/m^3$ |

**SW, short wave.**

**Table A1.3. List of variables from the MÉRA dataset produced by Met Éireann**

| Variable | Units | Variable | Units |
|---|---|---|---|
| Surface pressure | Pa | Cloud base | m |
| Mean sea level pressure | Pa | Cloud top | m |
| Surface temperature | K | Momentum flux, v-component | $N/m^2$ |
| 2-m temperature | K | Momentum flux, u-component | $N/m^2$ |
| 2-m relative humidity | % | Height of $T'_w = 0$ isotherm | m |
| U-component of 10-m wind | m/s | Height of 0° isotherm | m |
| V-component of 10-m wind | m/s | Total precipitation | $kg/m^2$ |
| Total cloud cover | 0–1 | Rain | $kg/m^2$ |
| High cloud cover | 0–1 | Graupel | $kg/m^2$ |
| Medium cloud cover | 0–1 | Snow | $kg/m^2$ |
| Low cloud cover | 0–1 | Sensible heat flux | $J/m^2$ |
| Mixed layer depth | m | Latent heat flux of evaporation | $J/m^2$ |
| Direct SW irradiance | $W/m^2$ | Latent heat flux of sublimation | J/kg |
| LW irradiance | $W/m^2$ | Water evaporation | $kg/m^2$ |
| Snow depth | $kg/m^2$ | Snow sublimation | $kg/m^2$ |
| Total cloud cover (fog) | 0–1 | Net SW irradiance | $J/m^2$ |
| Visibility | m | Net LW irradiance | $J/m^2$ |
| Icing index | – | Direct SW irradiance | $J/m^2$ |
| Precipitation type | – | LW irradiance | $J/m^2$ |
| Global irradiance | $J/m^2$ | U-component of wind | m/s |
| Direct normal irradiance | $J/m^2$ | V-component of wind | m/s |
| Lightning | $m^3$ | Vertical velocity | m/s |

**Table A1.3. Continued**

| Variable | Units | Variable | Units |
|---|---|---|---|
| Hail diagnostic | $kg/m^2$ | Relative humidity | % |
| Maximum temperature | K | Cloud ice | $kg/m^2$ |
| Minimum temperature | K | Cloud water | $kg/m^2$ |
| Gust, u-component | m/s | Cloud top temperature (infrared) | K |
| Gust, v-component | m/s | $T_b$ (water vapour) | K |
| Direct SW irradiance | $J/m^2$ | $T_b$ (water vapour) + cloud correction | K |
| Net SW irradiance | $J/m^2$ | Cloud water reflectivity (visible) | – |
| Net SW irradiance (accumulated) | $J/m^2$ | Precipitable water | $kg/m^2$ |
| Net LW irradiance | $J/m^2$ | Rain | $kg/m^2$ |
| Net LW irradiance (accumulated) | $J/m^2$ | Snow | $kg/m^2$ |
| Temperature | K | Graupel | $kg/m^2$ |
| U-component of wind | m/s | Cloud ice | $kg/m^2$ |
| V-component of wind | m/s | Cloud water | $kg/m^2$ |
| Relative humidity | % | Soil temperature (two levels) | $J/m^2$ |
| Geopotential | $m^2/s^2$ | Soil moisture content (three levels) | $J/m^2$ |
| Precipitation type | K | Surface soil ice (three levels) | $J/m^2$ |

**LW, long wave; SW, short wave.**

# Appendix 2 *Agroclimatic Atlas of Ireland*

The following agro-climate datasets were prepared for the *Agroclimatic Atlas of Ireland*:

1. mean annual precipitation;
2. mean monthly precipitation;
3. number of wet days per year (varying thresholds);
4. mean daily temperatures;
5. mean monthly temperatures;
6. maximum/minimum temperatures for specific months;
7. number of frost days;
8. $ET_0$;
9. $ET_a$;
10. SMDs;
11. number of field capacity days (derived from the MÉRA dataset);
12. growing season length and start and end dates;
13. SPI (varying thresholds).

For all agro-climate variables, the current climate normal period of 1981–2010 is considered. Unless stated otherwise, all datasets were derived using the Met Éireann observed gridded rainfall and temperature datasets, with 1-km grid spacings. First, for no. 7, it should be noted that the number of days of well-drained soils at field capacity is equal to that for excessively drained soils. Second, the field capacities have been taken to be 0.1 instead of 0 for well-drained soils and –9.9 for all other soil types. This is to accommodate regions where the soils are very nearly at field capacity, allowing for SMD = 0.001, for example, to be registered as a field capacity day. Example figures of agroclimate outputs are shown in Figures A2.1–A.2.12.

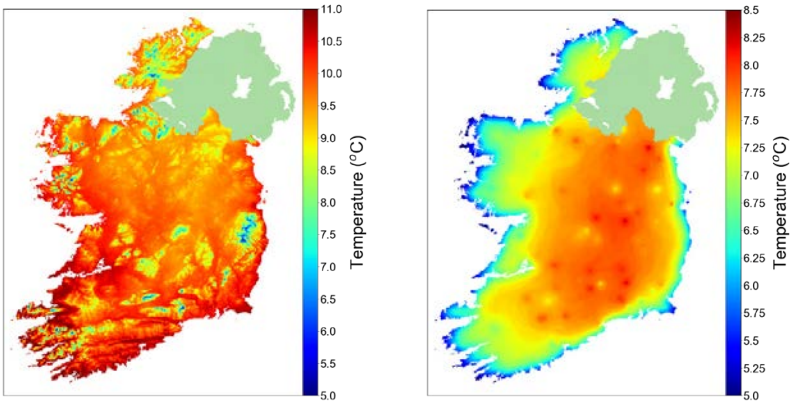


**Figure A2.1. Mean daily temperature (left) and mean daily temperature range (right) for 1981–2010.**

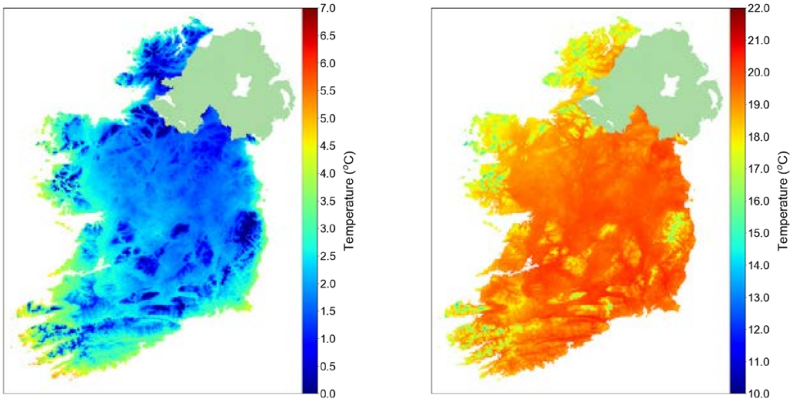


**Figure A2.2. Mean January minimum temperatures in 1981–2010 (left) and mean July maximum temperatures in 1981–2010 (right).**

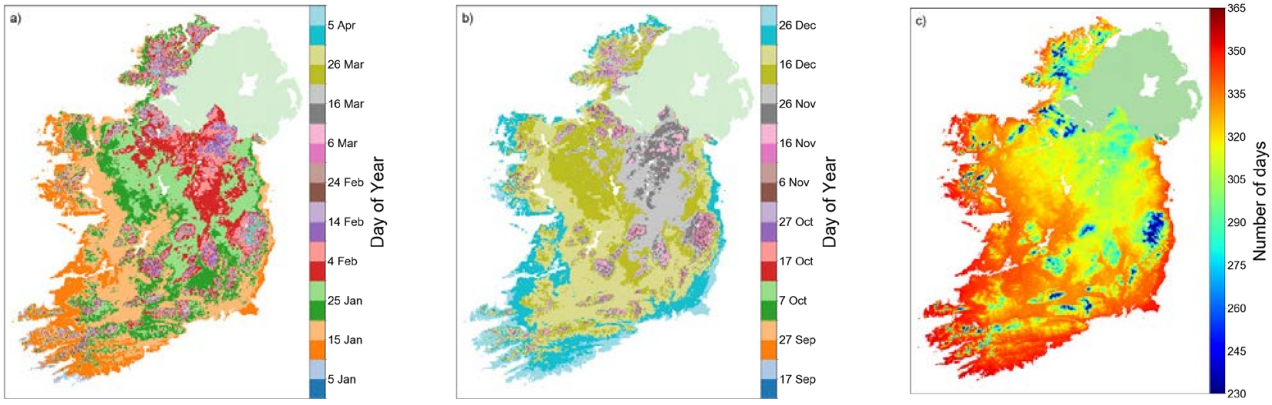


**Figure A2.3. Grass-growing season: (a) mean season start date, (b) mean season end date and (c) mean season length in days per year (1981–2010).**

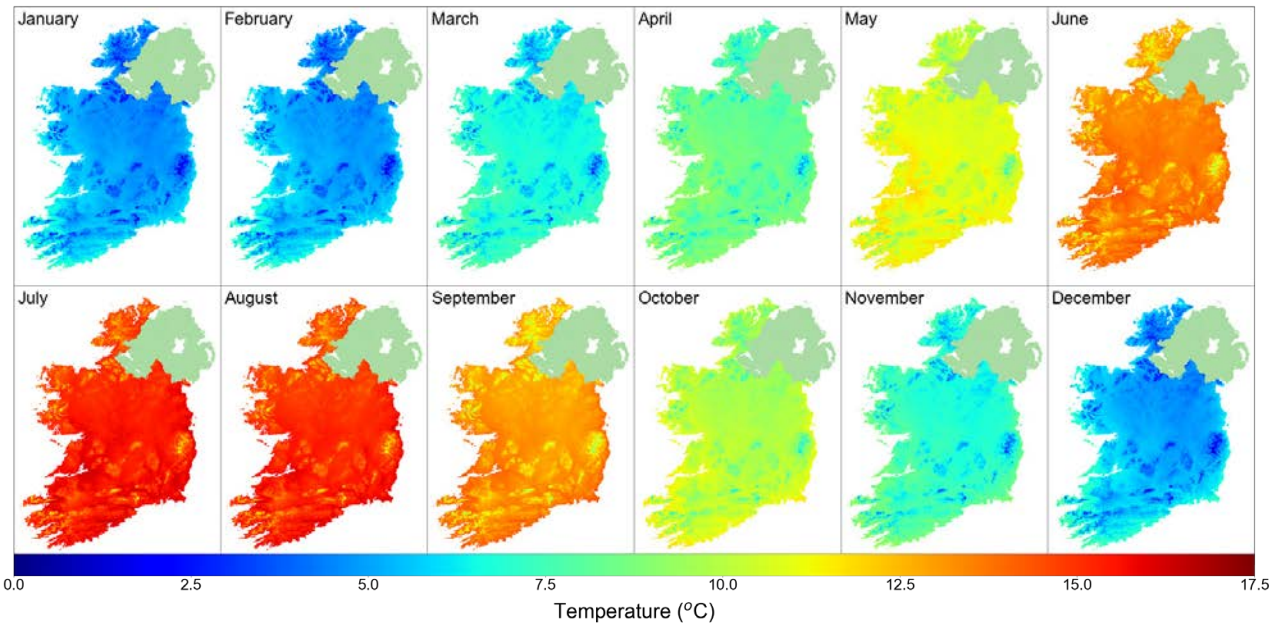


**Figure A2.4. Mean daily temperatures for individual months (1981–2010).**

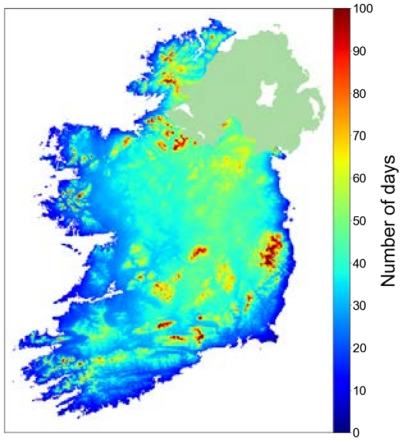


**Figure A2.5. Average number of frost days per year (1981–2010).**

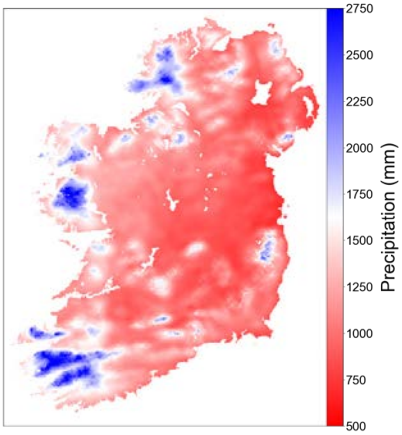


**Figure A2.6. Mean annual precipitation (mm/year) from Met Éireann gridded observational datasets (1981–2010).**

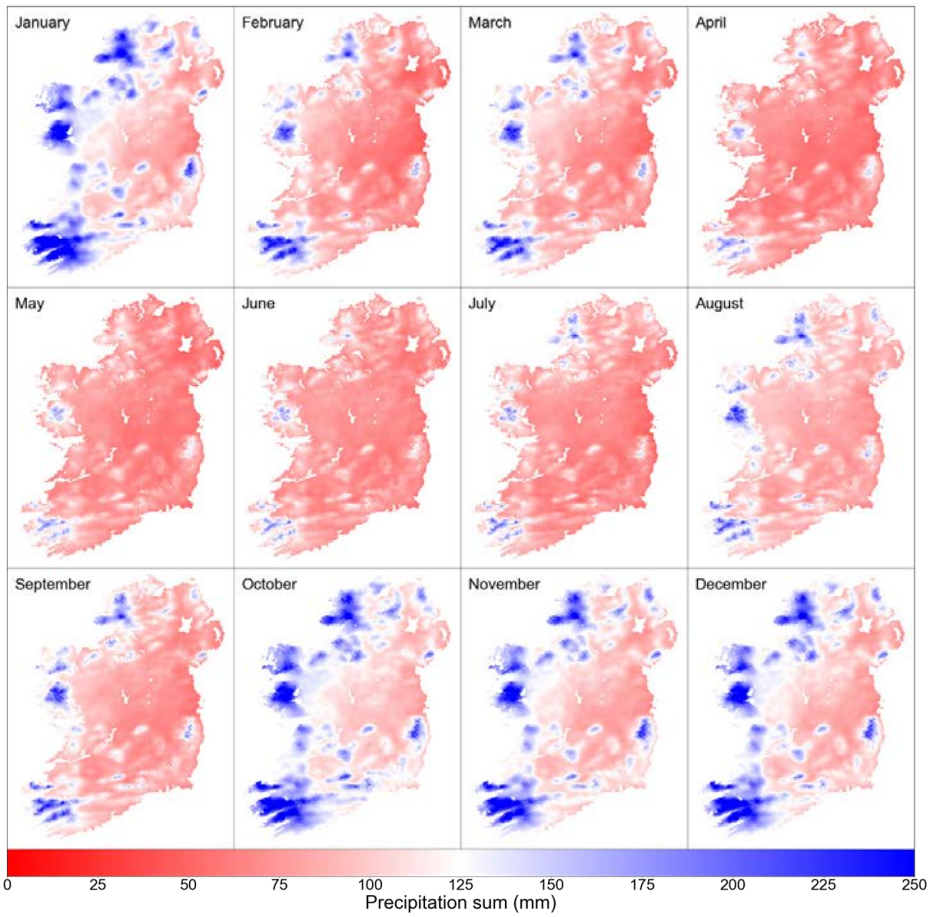


**Figure A2.7. Mean monthly precipitation (mm/month) from Met Éireann gridded observational datasets (1981–2010).**

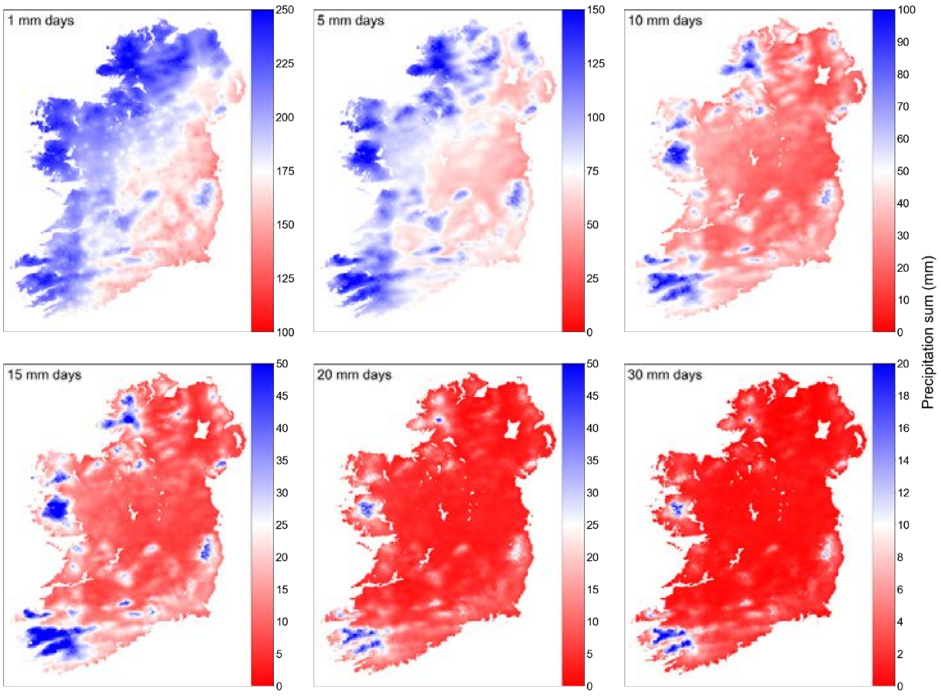


**Figure A2.8. Number of wet days at different thresholds: ≥1, ≥5, ≥10, ≥ 15, ≥20 and ≥30 mm (1981–2010).**

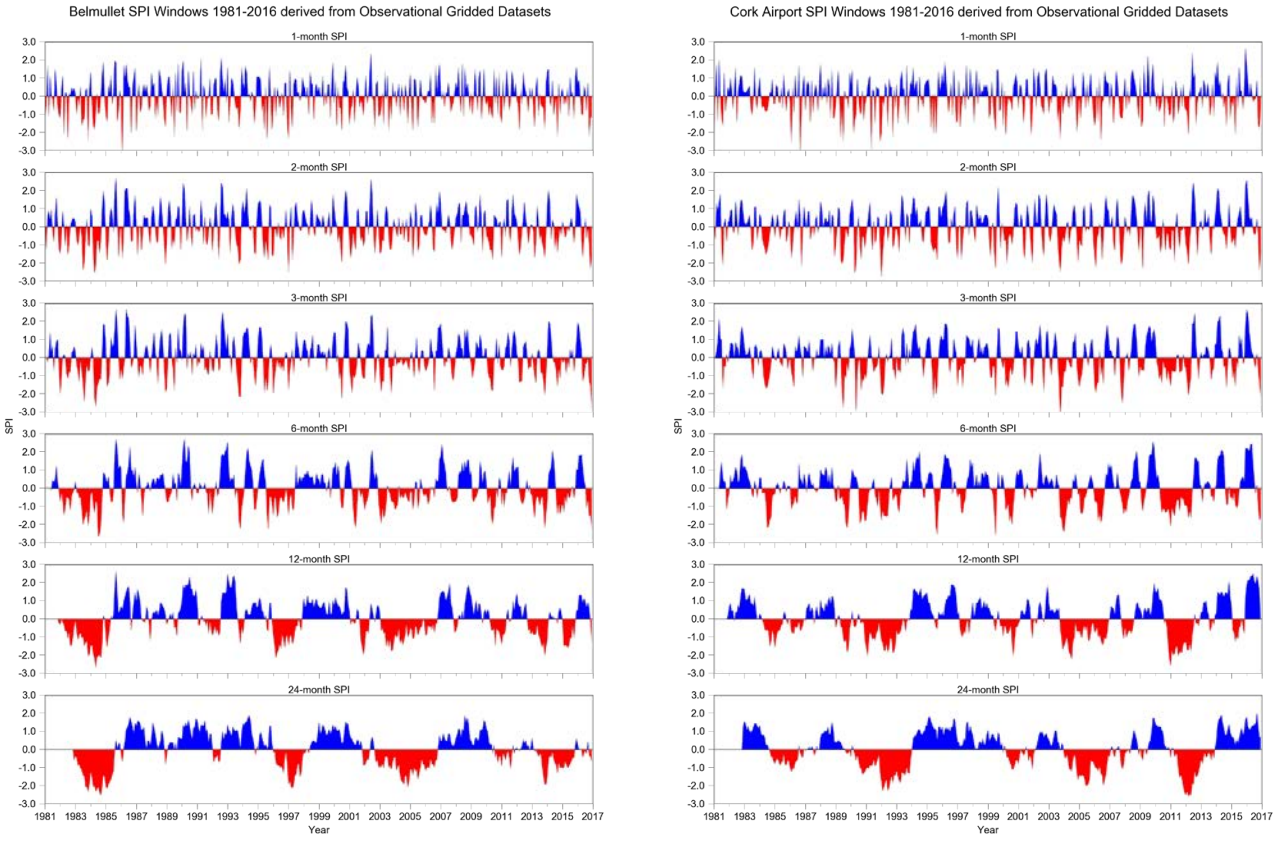


**Figure A2.9. SPI windows from 1981 to 2016 for Belmullet (left) and Cork Airport (right).**

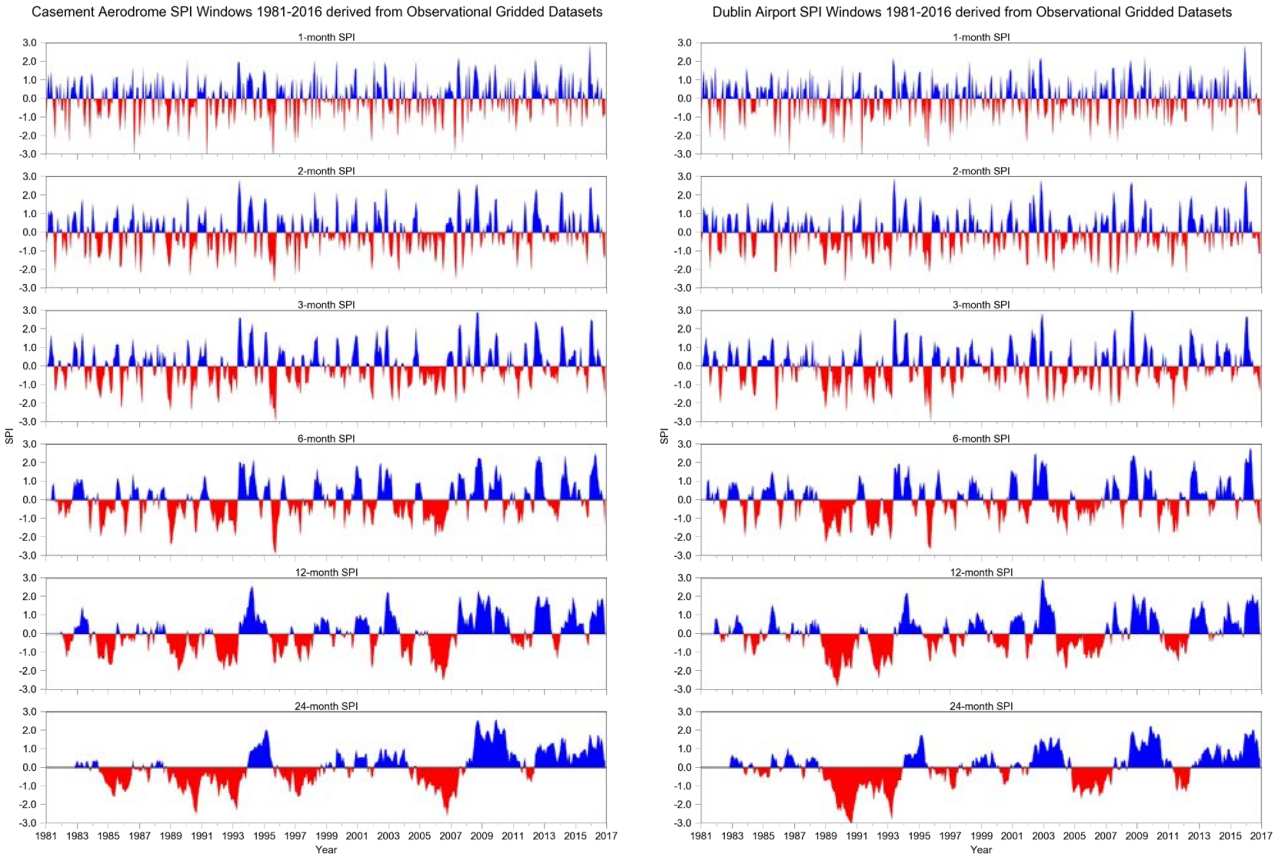


**Figure A2.10. SPI windows from 1981 to 2016 for Casement Aerodrome (left) and Dublin Airport (right).**

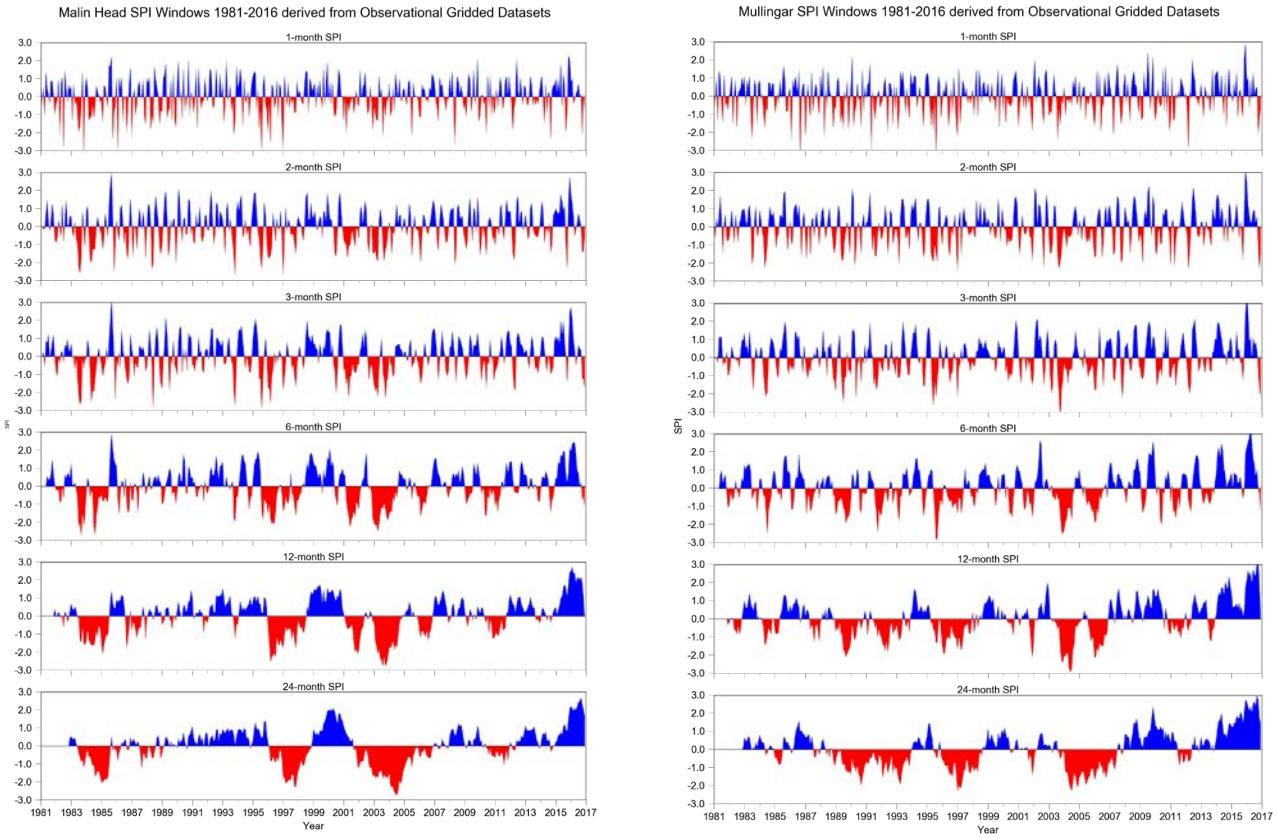


**Figure A2.11. SPI windows from 1981 to 2016 for Malin Head (left) and Mullingar (right).**

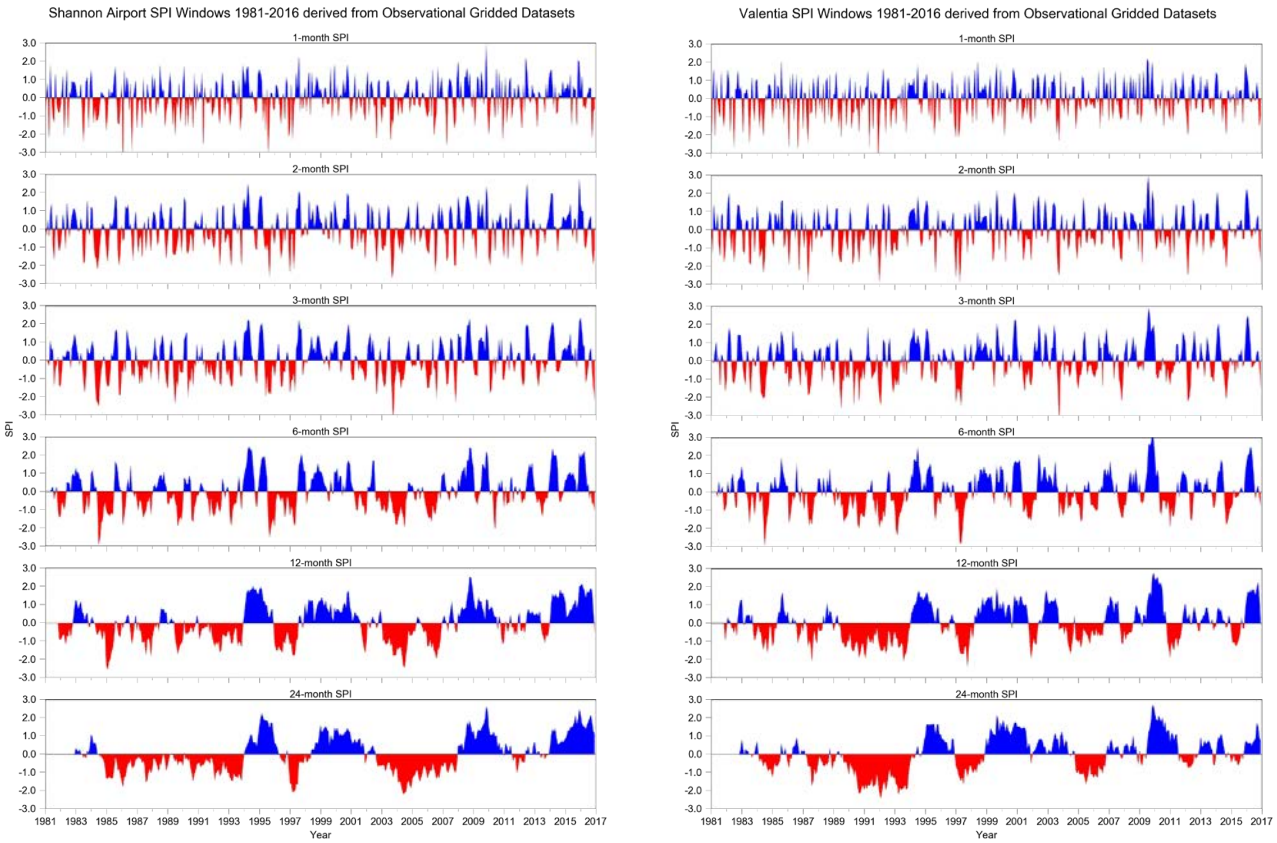


**Figure A2.12. SPI windows from 1981 to 2016 for Shannon Airport (left) and Valentia Observatory (right).**

# Appendix 3 Accessing the Datasets

The datasets are made available through the ICHEC ERRDAP server: https://erddap.ichec.ie/erddap/files/EPA_Hydroclimate/.

The data for all models are available over the island of Ireland. At present, the data are available in netCDF format only. The files available for download are outlined in Table A3.1 and the file structure on the ERDDAP server is outlined in Figure A3.1.

An SPI time series for any location can be extracted using the cdo (climate data operators) program and a simple script whereby the user specifies a longitude and latitude location and a time interval (1–48 months). The script is provided in Figure A3.2.

Queries on the datasets and applied usage should be made to christopher.werner@ichec.ie, paul.nolan@ichec.ie or naughto@tcd.ie. Queries regarding the ERDDAP server should be directed to alastair.mckinstry@ichec.ie.

For the $ET_a$ and SMD datasets, the folder and file notations for each of the soil drainage classes are as follows:

- ED = excessively drained;
- WD = well drained;
- MD = moderately drained;
- ID = imperfectly drained;
- PD = poorly drained.

**Table A3.1. List of variables available for download at ICHEC's ERDDAP server**

| File name | Description | Variables |
|---|---|---|
| (Model)_(variable)-daily.nc | Daily dataset from 1981 to 2016 | $ET_0$,[a] $ET_a$, SMD |
| (Model)_(variable)-monthlysums.nc | Monthly sums from 1981 to 2016 (432 time steps) | $ET_0$,[a] $ET_a$ |
| (Model)_(variable)-monthsumavg.nc | Average of monthly sums 1981 to 2016 (12 time steps) | $ET_0$,[a] $ET_a$ |
| (Model)_(variable)-seasonsum.nc | Seasonal sums from 1981 to 2016 (108 time steps) | $ET_0$,[a] $ET_a$ |
| (Model)_(variable)-seasonsumavg.nc | Average of seasonal sums 1981 to 2016 (4 time steps) | $ET_0$,[a] $ET_a$ |
| (Model)_(variable)-yearlysums.nc | Yearly sums from 1981 to 2016 (36 time steps) | $ET_0$,[a] $ET_a$ |
| (Model)_(variable)-yearlysumavg.nc | Average of yearly sums 1981 to 2016 (1 time step) | $ET_0$,[a] $ET_a$ |

[a]**Signifies data for COSMO-CLM and WRF available for 2017.**

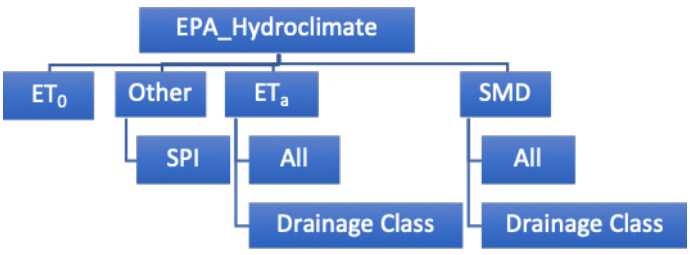


**Figure A3.1. Hierarchy of files in ICHEC's ERDDAP server.**

```
###            User Input            ###

RCM = OBS                            ## Dataset

lon =-7.36; lat=53.54;               ## Lat / Lon Location

len_month=48                         ## SPI run period

###         End of User Input         ###

cdo –s remapnn,lon=${lon}_lat=${lat} –selname,SPI_M${len_month} SPI_${RCM}_1981-2016.nc temp.nc

cdo –s infon temp.nc > a1

sed –i '/9.9692e+36/d' a1

awk '{print $1,$3,$9}' a1 > a2 && rm a1

sed 's/-/ /g' a2 > a3 && rm a2

tail –n +2 a3 > a4 && rm a3

echo "M${len_month}=[" > top

echo "];" > end

cat top a4 end > SPI_M${len_month}_${RCM}_lat${lat}_lon${lon}.m
```

**Figure A3.2. Script using cdo (climate data operators) to obtain the SPI at a user-specified location from the SPI dataset.**

**AN GHNÍOMHAIREACHT UM CHAOMHNÚ COMHSHAOIL**
Tá an Ghníomhaireacht um Chaomhnú Comhshaoil (GCC) freagrach as an gcomhshaol a chaomhnú agus a fheabhsú mar shócmhainn luachmhar do mhuintir na hÉireann. Táimid tiomanta do dhaoine agus don chomhshaol a chosaint ó éifeachtaí díobhálacha na radaíochta agus an truaillithe.

## Is féidir obair na Gníomhaireachta a roinnt ina trí phríomhréimse:

**Rialú:** *Déanaimid córais éifeachtacha rialaithe agus comhlíonta comhshaoil a chur i bhfeidhm chun torthaí maithe comhshaoil a sholáthar agus chun díriú orthu siúd nach gcloíonn leis na córais sin.*

**Eolas:** *Soláthraímid sonraí, faisnéis agus measúnú comhshaoil atá ar ardchaighdeán, spriocdhírithe agus tráthúil chun bonn eolais a chur faoin gcinnteoireacht ar gach leibhéal.*

**Tacaíocht:** *Bímid ag saothrú i gcomhar le grúpaí eile chun tacú le comhshaol atá glan, táirgiúil agus cosanta go maith, agus le hiompar a chuirfidh le comhshaol inbhuanaithe.*

## Ár bhFreagrachtaí

### Ceadúnú
Déanaimid na gníomhaíochtaí seo a leanas a rialú ionas nach ndéanann siad dochar do shláinte an phobail ná don chomhshaol:
- saoráidí dramhaíola *(m.sh. láithreáin líonta talún, loisceoirí, stáisiúin aistrithe dramhaíola)*;
- gníomhaíochtaí tionsclaíocha ar scála mór *(m.sh. déantúsaíocht cógaisíochta, déantúsaíocht stroighne, stáisiúin chumhachta)*;
- an diantalmhaíocht *(m.sh. muca, éanlaith)*;
- úsáid shrianta agus scaoileadh rialaithe Orgánach Géinmhodhnaithe *(OGM)*;
- foinsí radaíochta ianúcháin *(m.sh. trealamh x-gha agus radaiteiripe, foinsí tionsclaíocha)*;
- áiseanna móra stórála peitril;
- scardadh dramhuisce;
- gníomhaíochtaí dumpála ar farraige.

### Forfheidhmiú Náisiúnta i leith Cúrsaí Comhshaoil
- Clár náisiúnta iniúchtaí agus cigireachtaí a dhéanamh gach bliain ar shaoráidí a bhfuil ceadúnas ón nGníomhaireacht acu.
- Maoirseacht a dhéanamh ar fhreagrachtaí cosanta comhshaoil na n-údarás áitiúil.
- Caighdeán an uisce óil, arna sholáthar ag soláthraithe uisce phoiblí, a mhaoirsiú.
- Obair le húdaráis áitiúla agus le gníomhaireachtaí eile chun dul i ngleic le coireanna comhshaoil trí chomhordú a dhéanamh ar líonra forfheidhmiúcháin náisiúnta, trí dhíriú ar chiontóirí, agus trí mhaoirsiú a dhéanamh ar leasúchán.
- Cur i bhfeidhm rialachán ar nós na Rialachán um Dhramhthrealamh Leictreach agus Leictreonach (DTLL), um Shrian ar Shubstaintí Guaiseacha agus na Rialachán um rialú ar shubstaintí a ídíonn an ciseal ózóin.
- An dlí a chur orthu siúd a bhriseann dlí an chomhshaoil agus a dhéanann dochar don chomhshaol.

### Bainistíocht Uisce
- Monatóireacht agus tuairisciú a dhéanamh ar cháilíocht aibhneacha, lochanna, uiscí idirchriosacha agus cósta na hÉireann, agus screamhuiscí; leibhéil uisce agus sruthanna aibhneacha a thomhas.
- Comhordú náisiúnta agus maoirsiú a dhéanamh ar an gCreat-Treoir Uisce.
- Monatóireacht agus tuairisciú a dhéanamh ar Cháilíocht an Uisce Snámha.

### Monatóireacht, Anailís agus Tuairisciú ar an gComhshaol
- Monatóireacht a dhéanamh ar cháilíocht an aeir agus Treoir an AE maidir le hAer Glan don Eoraip (CAFÉ) a chur chun feidhme.
- Tuairisciú neamhspleách le cabhrú le cinnteoireacht an rialtais náisiúnta agus na n-údarás áitiúil *(m.sh. tuairisciú tréimhsiúil ar staid Chomhshaol na hÉireann agus Tuarascálacha ar Tháscairí)*.

### Rialú Astaíochtaí na nGás Ceaptha Teasa in Éirinn
- Fardail agus réamh-mheastacháin na hÉireann maidir le gáis cheaptha teasa a ullmhú.
- An Treoir maidir le Trádáil Astaíochtaí a chur chun feidhme i gcomhair breis agus 100 de na táirgeoirí dé-ocsaíde carbóin is mó in Éirinn.

### Taighde agus Forbairt Comhshaoil
- Taighde comhshaoil a chistiú chun brúnna a shainaithint, bonn eolais a chur faoi bheartais, agus réitigh a sholáthar i réimsí na haeráide, an uisce agus na hinbhuanaitheachta.

### Measúnacht Straitéiseach Timpeallachta
- Measúnacht a dhéanamh ar thionchar pleananna agus clár beartaithe ar an gcomhshaol in Éirinn *(m.sh. mórphleananna forbartha)*.

### Cosaint Raideolaíoch
- Monatóireacht a dhéanamh ar leibhéil radaíochta, measúnacht a dhéanamh ar nochtadh mhuintir na hÉireann don radaíocht ianúcháin.
- Cabhrú le pleananna náisiúnta a fhorbairt le haghaidh éigeandálaí ag eascairt as taismí núicléacha.
- Monatóireacht a dhéanamh ar fhorbairtí thar lear a bhaineann le saoráidí núicléacha agus leis an tsábháilteacht raideolaíochta.
- Sainseirbhísí cosanta ar an radaíocht a sholáthar, nó maoirsiú a dhéanamh ar sholáthar na seirbhísí sin.

### Treoir, Faisnéis Inrochtana agus Oideachas
- Comhairle agus treoir a chur ar fáil d'earnáil na tionsclaíochta agus don phobal maidir le hábhair a bhaineann le caomhnú an chomhshaoil agus leis an gcosaint raideolaíoch.
- Faisnéis thráthúil ar an gcomhshaol ar a bhfuil fáil éasca a chur ar fáil chun rannpháirtíocht an phobail a spreagadh sa chinnteoireacht i ndáil leis an gcomhshaol *(m.sh. Timpeall an Tí, léarscáileanna radóin)*.
- Comhairle a chur ar fáil don Rialtas maidir le hábhair a bhaineann leis an tsábháilteacht raideolaíoch agus le cúrsaí práinnfhreagartha.
- Plean Náisiúnta Bainistíochta Dramhaíola Guaisí a fhorbairt chun dramhaíl ghuaiseach a chosc agus a bhainistiú.

### Múscailt Feasachta agus Athrú Iompraíochta
- Feasacht chomhshaoil níos fearr a ghiniúint agus dul i bhfeidhm ar athrú iompraíochta dearfach trí thacú le gnóthais, le pobail agus le teaghlaigh a bheith níos éifeachtúla ar acmhainní.
- Tástáil le haghaidh radóin a chur chun cinn i dtithe agus in ionaid oibre, agus gníomhartha leasúcháin a spreagadh nuair is gá.

### Bainistíocht agus struchtúr na Gníomhaireachta um Chaomhnú Comhshaoil
Tá an ghníomhaíocht á bainistiú ag Bord lánaimseartha, ar a bhfuil Ard-Stiúrthóir agus cúigear Stiúrthóirí. Déantar an obair ar fud cúig cinn d'Oifigí:
- An Oifig um Inmharthanacht Comhshaoil
- An Oifig Forfheidhmithe i leith cúrsaí Comhshaoil
- An Oifig um Fianaise is Measúnú
- Oifig um Chosaint Radaíochta agus Monatóireachta Comhshaoil
- An Oifig Cumarsáide agus Seirbhísí Corparáideacha

Tá Coiste Comhairleach ag an nGníomhaireacht le cabhrú léi. Tá dáréag comhaltaí air agus tagann siad le chéile go rialta le plé a dhéanamh ar ábhair imní agus le comhairle a chur ar an mBord.

# EPA Research Report 267

## High-resolution gridded Datasets of Hydro-climate Indices for Ireland

Authors: Christopher Werner, Paul Nolan and Owen Naughton

## Identifying Pressures

Key stakeholders in water resource management, such as the Office of Public Works (OPW), Irish Water, the Environmental Protection Agency (EPA) and Geological Survey Ireland (GSI), share a common challenge in managing and protecting the aquatic environment, particularly in the face of climate variability, land use and demographic change, pollution and the demand for natural resources. These challenges are exacerbated by a warming climate, which is expected to result in an increase in drought and flooding events in Ireland. The EPA Research Programme specifically calls for support for development of the analysis of the fundamental processes that drive the rate and extent of climate change. Such analysis is necessary to provide the evidence base to inform relevant national policymakers, planners and stakeholders of potential climate-related issues and enable the development of pre-emptive mitigation strategies as called for under the National Climate Change Adaptation Framework (NCCAF). However, the datasets required for such research have not been available in Ireland.

## Informing Policy

Under the Water Framework Directive (WFD), the state is responsible for protecting and maintaining groundwater bodies and catchment areas and ensuring the long-term sustainability of water resources. Hydro-climate variables such as evapotranspiration and soil moisture conditions are crucial factors in ensuring water sustainability, understanding groundwater recharge, agronomic management and the management of flood and drought. The research and datasets resulting from this project will assist Ireland to meet its obligations under EU directives such as the WFD.

The knowledge gained, and hydro-climate datasets generated, through this research will contribute towards the long-term goal of mitigating and adapting to climate change and developing a climate-resilient Ireland by 2050, as set out in the EPA Climate Research Strategy 2014–2020. To facilitate climate change policy, a greater understanding of the primary processes driving energy and water exchanges within the hydrological cycle is required for hydro-climate trend analysis and prediction. This research will inform climate change policy through the provision of long-term high-resolution datasets of key hydro-climate meteorological variables – a fundamental foundation for the interpretation of climate change trends in Irish hydro-climatology.

## Developing Solutions

The research presents an important data resource for Irish researchers, policymakers and industry by providing, for the first time, high-resolution gridded datasets of hydro-climate variables. It is envisaged that the datasets will lead to a better understanding not only of the physical climate system but also of the interaction between climate and Irish society. In addition, it is envisaged that the datasets will be used as a basis for more-focused hydro-climate impact studies. To promote the use of the data and enhance climate research in Ireland, the datasets are made publicly available to researchers, policymakers, the general public and Irish industry through the Irish Centre for High-End Computing (ICHEC) ERDDAP server.

This study has produced high-resolution gridded datasets of hydro-climate variables, including:

- reference evapotranspiration;
- actual evapotranspiration (five drainage classes);
- soil moisture deficits (five drainage classes);
- Standardised Precipitation Index for various intervals.

In addition, the evapotranspiration and soil moisture deficit datasets were improved by incorporating the Teagasc Indicative Soil Drainage Map, resulting in a more accurate representation of actual soil conditions throughout the country.

**EPA Research:** McCumiskey House, Richiew, Clonskeagh, Dublin 14.

**Phone:** 01 268 0100
**Twitter:** @EPAResearchNews
**Email:** research@epa.ie

www.epa.ie

**EPA Research Webpages**
www.epa.ie/researchandeducation/research/